Assessment of Intrinsic Bioremediation at a PCE Contaminated Site

Heather Veith Rectanus

Thesis submitted to the Faculty of the
Virginia Polytechnic Institute and State University
in partial fulfillment of the requirements for the degree of

Master of Science
in
Civil Engineering

Dr. John Novak, Co-chair
Dr. Mark Widdowson, Co-chair
Dr. Duane Berry

August, 2000
Blacksburg, Virginia

Keywords: PCE, Natural Attenuation, Bioremediation, Microcosms, SEAM3D

Assessment of Intrinsic Bioremediation at a PCE Contaminated Site

Heather Veith Rectanus

The Charles E. Via Department of Civil Engineering

(ABSTRACT)

Groundwater parameter analysis, microcosm experiments, and microcosms modeling were undertaken to assess the potential of Monitored Natural Attenuation as a remediation strategy at Site 12 at the Naval Amphibious Base (NAB) Little Creek. Site 12 was contaminated with PCE waste disposed by a former dry cleaning facility. In the groundwater analysis, contaminant characteristics and redox indicators were evaluated to assess the reductive dechlorination potential of Site 12. The results of the groundwater analysis indicated that Site 12 exhibited sulfate-reducing and methanogenic conditions which provide the required environment for reductive dechlorination. However, Site 12 only demonstrated partial reductive dechlorination to *cis*-1,2-DCE and possible anaerobic oxidation of *cis*-1,2-DCE and VC to CO_2. Microcosms were designed to further evaluate the extent of microbial degradation of the chlorinated ethenes at Site 12 and to provide concentration versus time data for the estimation of chlorinated ethenes' biodegradation rates. The extent of degradation in the microcosms was consistent with the groundwater data. However, ethene production was not observed and the quantity of TCE measured for two of the microcosms differed substantially when compared to the groundwater data. The microcosm model used SEAM3D to simulate the results of the microcosm experiments (concentration versus time data) to estimate the biodegradation rates of PCE and its daughter products. The SEAM3D reductive dechlorination package, based on Monod kinetics, predicted for the MLS12-Shallow microcosm maximum specific utilization rates for PCE, TCE, *cis*-1,2-DCE and VC at 0.4, 0.42, 0.05, and 0.25 day^{-1}, respectively and half saturation coefficients for PCE, TCE, *cis*-1,2-DCE and VC at 0.41, 0.01, 0.07, and 0.02 mg/L, respectively. The results of this study suggest that while the groundwater environment provides the necessary conditions for reductive dechlorination, Site 12 is not an efficient system for reductive dechlorination. This lack of efficiency may stem from sparse microbial populations capable of reducing *cis*-1,2-DCE or the system may contain levels of PCE which inhibit the further reduction of *cis*-1,2-DCE. Based on the observed inhibitory relationship between PCE and *cis*-1,2-DCE and VC production, source removal would reduce the PCE levels and encourage further reductive dechlorination at Site 12. Therefore, the recommended first step for a monitered natural attenuation-based remediation strategy at Site 12 should be source removal.

Acknowledgments

I would like to thank my co-advisors, Dr. John Novak and Dr. Mark Widdowson, for their support throughout my studies as a master's student and the opportunity to contribute towards the understanding of this research project. I truly enjoyed the field, laboratory and modeling aspects of the project. I would also like to thank Dr. Duane Berry for his time and support over the last two years. Our conversions helped immensely in grasping the microbial concepts in this project.

I would like to thank my husband, Brian, for his patience, support and computer prowess. Without his aid, this thesis would not be a reality.

I would especially like to recognize and thank the financial support of National Science Foundation and Charles E. Via Fellowship throughout my masters studies at Virginia Tech.

Contents

1 Introduction **1**

2 Literature Review **4**

3 Site Characterization **10**

3.1 Site History 10

3.2 Hydrogeology 12

3.2.1 Hydrostratigraphic Units 12

3.2.2 Hydraulic Conductivity 12

3.2.3 Groundwater Flow 13

3.3 Groundwater Parameters 15

3.3.1 Contaminant Distribution 20

3.3.2 Redox Indicators 31

4 Experimental Microcosm Design **47**

4.1 Introduction 47

4.2 Chlorinated Ethene Properties 48

4.3 Aquifer Sediment Sample Collection 51

4.4 Continuous Microcosm Construction 51

4.5 Continuous Microcosm Sampling Method 55
4.6 Analytical Methods 55
4.6.1 Gases 55
4.6.2 Chlorinated Ethenes 56

5 Microcosm Model **57**

5.1 Conceptual Model 58
5.2 Mathematical Model 58
5.2.1 Reductive Dechlorination Equations 58
5.2.2 Reductive Dechlorination Parameters 63

6 Results and Discussion **71**

6.1 Groundwater Parameter Assessment 71
6.1.1 Contaminant Distribution 71
6.1.2 Redox Indicators 80
6.2 Microcosm Study 83
6.3 Microcosm Model 96

7 Conclusions **103**

8 Recommendations **107**

A Groundwater Data **111**

B Microcosm Data **119**

C Model Data **132**

List of Figures

3.1 Location of Site 12 on Naval Amphibious Base Little Creek, Virginia Beach, Virginia. Source: CH2MHill 2000 11

3.2 Potentiometric Surface of Site12 on July 27, 1998. Source: CH2MHill, 2000. 14

3.3 Locations of monitoring wells and multi-level sampling wells installed Site 12. Source: CH2MHill, 2000. 17

3.4 Multi-level sampler design that allows seven discrete groundwater samples. 18

3.5 Presumed PCE isopleth at Site 12 based on monitoring well data collected in August 1995. Source: CH2MHill, 2000. 19

3.6 The groundwater concentrations of PCE, TCE, and *cis*-1,2-DCE at all ports of MLS11 for the 1998, 1999, and 2000 sampling rounds. 23

3.7 The groundwater concentrations of ethene and chloride at all ports of MLS11 for the 1998, 1999, and 2000 sampling rounds. 24

3.8 The groundwater concentrations of PCE, TCE, and *cis*-1,2-DCE at all ports of MLS12 for the 1998, 1999, and 2000 sampling rounds. 25

3.9 The groundwater concentrations of VC, ethene, and chloride at all ports of MLS12 for the 1998, 1999, and 2000 sampling rounds. 26

3.10 The groundwater concentrations of PCE, TCE, and *cis*-1,2-DCE at all ports of MLS20 for the 1998, 1999, and 2000 sampling rounds. 27

3.11 The groundwater concentrations of VC, ethene, and chloride at all ports of MLS20 for the 1998, 1999, and 2000 sampling rounds. 28

3.12 The groundwater concentrations of PCE, TCE, and *cis*-1,2-DCE at all ports of MLS22 for the 1999 and 2000 sampling rounds. 29

3.13 The groundwater concentrations of ethene and chloride at all ports of MLS22 for the 1999 and 2000 sampling rounds. 30

3.14 The groundwater concentrations of sulfate for the 1998, 1999, and 2000 sampling rounds at MLS10, MLS11 and MLS12. 34

3.15 The groundwater concentrations of sulfate for the 1998, 1999, and 2000 sampling rounds at MLS20 and MLS22. 35

3.16 The groundwater concentrations of CO_2 for the 1998 and 1999 sampling rounds at MLS10, MLS11, and MLS12. 36

3.17 The groundwater concentrations of CO_2 for the 1999 sampling rounds at MLS20 and MLS22. 37

3.18 The groundwater concentrations of H_2 for the 1998, 1999, and 2000 sampling rounds at MLS10, MLS11, and MLS12. 38

3.19 The groundwater concentrations of H_2 for the 1998 sampling round at MLS13, MLS14, and MLS15. 39

3.20 The groundwater concentrations of H_2 for the 1999 and 2000 sampling rounds at MLS20 and MLS22. 40

3.21 The groundwater concentrations of ferrous iron for the 1998, and 2000 sampling rounds at MLS10, MLS11, and MLS12. 41

3.22 The groundwater concentrations of ferrous iron for the 1998 and 2000 sampling rounds at MLS20 and MLS22. 42

3.23 The groundwater concentrations of sulfide for the 1999 and 2000 sampling rounds at MLS10, MLS11, and MLS12. 43

3.24 The groundwater concentrations of sulfide for the 1999 and 2000 sampling rounds at MLS20 and MLS22. 44

3.25 The groundwater concentrations of methane for the 1998 and 1999 sampling rounds at MLS10, MLS11, and MLS12. 45

3.26 The groundwater concentrations of methane for the 1999 sampling rounds at MLS20 and MLS22. 46

4.1 The molecular structures of PCE, TCE, *cis*-1,2-DCE and VC. 50

4.2 Retrofitted microcosm flask 54

6.1 The measured concentrations of the chlorinated ethenes in the control microcosm MLS12-Shallow, MLS22-Shallow and MLS22-Deep experiments. 89

6.2 The measured concentrations of the chlorinated ethenes in MLS12-Shallow microcosm experiment amended with PCE. 90

6.3 The measured concentrations of the chlorinated ethenes in MLS12-Shallow microcosm experiment amended with TCE. 91

6.4 The measured concentrations of the chlorinated ethenes in MLS22-Shallow microcosm experiment amended with PCE. 92

6.5 The measured concentrations of the chlorinated ethenes in MLS22-Shallow microcosm experiment amended with TCE. 93

6.6 The measured concentrations of the chlorinated ethenes in MLS22-Deep microcosm experiment amended with PCE. 94

6.7 The measured concentrations of the chlorinated ethenes in MLS22-Deep microcosm experiment amended with TCE. 95

6.8 A comparison between measured (symbols) and predicted (lines) concentrations of the chlorinated ethenes in the MLS12-Shallow microcosm. 98

6.9 A comparison between measured (symbols) and predicted (lines) concentrations of the chlorinated ethenes in the MLS22-Shallow microcosm 99

6.10 A comparison between measured (symbols) and predicted (lines) concentrations of the chlorinated ethenes in the MLS22-Deep microcosm 100

6.11 A comparison between measured (symbols) and predicted (lines) concentrations of the chlorinated ethenes in the MLS22-Shallow microcosm where TCE degradation rates were calculated based on the TCE amended microcosm. 101

6.12 A comparison between measured (symbols) and predicted (lines) concentrations of the chlorinated ethenes in the MLS22-Deep microcosm where TCE degradation rates were calculated based on the TCE amended microcosm. 102

List of Tables

2.1 Ranges of Hydrogen Concentrations for TEAPS 7

4.1 Chemical and Physical Properties of the Chlorinated Ethenes 49

4.2 Microcosm Experimental Setup Matrix 53

5.1 Maximum specific utilization rate of the chlorinated ethenes (CE) (ν_{CE}^{max}, day^{-1}) for the three microcosm models. 65

5.2 Half saturation coefficients (K_{CE}, mg/L) of the chlorinated ethenes for the three microcosm models. 66

5.3 Inhibition Coefficients (mg/L) of one chlorinated ethene on the degradation of another chlorinated ethene for the three microcosm models. 67

5.4 The production coefficient (ξ) of one chlorinated ethene generated by the degradation of another chlorinated ethene. 68

5.5 The initial concentrations ($\mu g/L$)o f the PCE spike used by the model. 69

5.6 The initial microbial population M_2 (g), yield coefficient Y_{DCE} (g g^{-1}), and microbial death rate k_d (day^{-1}) for the *cis*-1,2-DCE degrading microbial population (M_2) in the MLS22 microcosms. 70

6.1 Sequential chlorinated ethene ratios for MLS11 76

6.2 Sequential chlorinated ethene ratios at MLS12 77

6.3 Sequential chlorinated ethene ratios at MLS20 78

6.4 Sequential chlorinated ethene ratios for MLS22 79

6.5 Zero order decay rates (ppm day^{-1}) for the continuous microcosm experiments . . . 88

A.1 Chlorinated ethene groundwater data for the 1998 sampling round 112

A.2 TEAP parameters for the 1998 sampling round-Part A 113

A.3 TEAP parameters for the 1998 sampling round-Part B 114

A.4 Chlorinated ethene groundwater data for the 1999 sampling round 115

A.5 TEAP parameters for the 1999 sampling round 116

A.6 Chlorinated ethene groundwater data for the 2000 sampling round 117

A.7 TEAP parameters for the 2000 sampling round 118

B.1 Concentration (μM) versus time data for MLS12-Shallow PCE amended microcosm 120

B.2 Concentration (μM) versus time data for Controls of MLS12-Shallow PCE amended microcosm 121

B.3 Concentration (μM) versus time data for MLS12-Shallow TCE amended microcosm 122

B.4 Concentration (μM) versus time data for Controls of MLS12-Shallow TCE amended microcosm 123

B.5 Concentration (μM) versus time data for MLS22-Shallow PCE amended microcosm 124

B.6 Concentration (μM) versus time data for Controls of MLS22-Shallow PCE amended microcosm 125

B.7 Concentration (μM) versus time data for MLS22-Shallow TCE amended microcosm 126

B.8 Concentration (μM) versus time data for Controls of MLS22-Shallow TCE amended microcosm 127

B.9 Concentration (μM) versus time data for MLS22-Deep PCE amended microcosm . . 128

B.10 Concentration (μM) versus time data for Controls of MLS22-Deep PCE amended microcosm 129

B.11 Concentration (μM) versus time data for MLS22-Deep TCE amended microcosm . . 130

B.12 Concentration (μM) versus time data for Controls of MLS22-Deep TCE amended microcosm 131

Chapter 1

Introduction

The widespread use of tetrachloroethene (PCE) in dry cleaning and industrial processes has led to PCE as a ubiquitous groundwater contaminant (Bradley, 2000; EPA., 1998; Harkness et al., 1999). While recalcitrant in aerobic environments, PCE has been shown to degrade by indigenous microorganisms under anaerobic conditions via reductive dechlorination (deBruin et al., 1992; Fetzner, 1998; Hollinger and Schumacher, 1994; Magnuson et al., 1998; Wu et al., 1998). However, PCE is observed often to partially dechlorinate. This leads to an accumulation of its daughter products, *cis*-1,2-DCE and/or VC, in the environment (Harkness et al., 1999; EPA., 1998). Because PCE, TCE, and *cis*-1,2-DCE are suspected carcinogens and VC is a known carcinogen, the fate of PCE and its daughter products in the environment is of concern (Bradley, 2000). Nevertheless, the ability of microorganisms to intrinsically biodegrade PCE has prompted the consideration of Monitored Natural Attenuation (MNA) as a remediation strategy at PCE contaminated sites. Therefore, it is important to fully assess the long-term reductive dechlorination potential of a site to support MNA.

Monitored Natural Attenuation is a remediation option that utilizes the in situ capabilities, such as dispersion, sorption, volatilization, and biodegradation, to reduce the contaminant concentration (Chapelle and Bradley, 1998). To determine if a site is suited for MNA, the OSWER Directive 9200.4-17 proposed three lines of evidence in which to investigate the site (EPA., 1998). The first line of evidence addresses the historical aspects of the groundwater and soil data at the contaminated site. This data should indicate the reduction of contaminant mass/concentration via natural attenuation processes such as biodegradation opposed to the effects of dilution of the contami-

nant by downstream migration of the plume. The second line of evidence includes evaluation of pertinent 'hydrogeologic and geochemical data' (EPA., 1998). Characterization of the subsurface environment through this data will aid in determining which MNA process affects the reduction in contamination at the site. The final line of evidence for MNA is the evaluation of field measurements and/or the construction of microcosms to demonstrate the potential of indigenous microbiota to degrade the contaminants. Through the evaluation of each line of evidence, the ability of the site to support MNA as a viable remediation option can be assessed relative to remediation objectives associated with regulatory compliance.

Objectives and Scope

This thesis evaluates the potential of MNA as a remediation strategy at a PCE contaminated site. The site was contaminated by improper disposal of PCE laden dry cleaning wastes. Previous investigations at the site by consulting firms confirmed the presence and source of contamination but failed to establish the fate of the contamination. Since biodegradation usually is the major contributing mechanism in the reduction of the contamination, this study focuses on understanding the predominant microbiological processes and their affect on contamination at the site. Through investigations of the subsurface environment, the potential of the indigenous microorganisms to reduce the contamination at the site was assessed. This evaluation process was divided into three main objectives:

- To evaluate the groundwater contaminant characteristics and geochemistry,
- To estimate the biodegradation rates of PCE and its daughter products,
- To determine the efficiency of the reductive dechlorination activity at the site.

The objectives of this study were separated into four phases of work. In the first phase of this study, the groundwater parameters such as the concentrations of redox indicators and contaminants were analyzed. These groundwater parameters were derived from depth-discrete samples collected using multi-level sampling monitoring wells. This type of well provides a vertical distribution of the groundwater characteristics by allowing seven discrete depths to be sampled at one well location.

In the second phase, laboratory microcosms were constructed with aquifer sediment collected from the site. The sampling locations were based on the concentrations of PCE and its daughter products determined by the groundwater analysis. In the third phase, the microcosm results were fit to a Monod kinetic model using the SEAM3D (Sequential Electron Acceptor Model, 3 Dimensional) Reductive Dechlorination package (beta v2.0) to estimate the biodegradation rates of PCE and its daughter products. In the final phase of this study, the results of the groundwater analysis, the microcosms, and the microcosm model were used to determine efficiency of the natural system at the site in reducing the levels of contamination where an efficient system has a strong potential for MNA as a remediation strategy at the site.

Chapter 2

Literature Review

The chlorinated solvents, tetrachloroethene (PCE) and trichloroethene (TCE), are commonly used in dry cleaning processes and as degreasers in military and industrial applications. Through improper handling and disposal techniques, these chlorinated ethenes have become ubiquitous groundwater contaminants such that PCE and TCE have been observed at over 50% of the national priorities list site (Butler and Hayes, 1999). The lessor chlorinated ethenes, such as *cis*-1,2-DCE, *trans*-1,2-DCE, and VC, are also commonly detected in groundwater. These chlorinated ethenes usually are the resultant daughter products of PCE and TCE degradation. The most important of these daughter products is VC. VC is listed as a known carcinogen and recognized as a priority pollutant by the US EPA while PCE, TCE and the DCE isomers are considered as probable carcinogens (Bradley and Chapelle, 1996). Therefore, the fate of VC and its parent compounds in the environment is on concern.

The remediation strategy for PCE and TCE was originally based on the presumption that PCE and TCE could not be biodegraded (Bradley, 2000). Pump and treat strategies were applied to contaminated sites. However, PCE and TCE are dense non-aqueous phase liquids (DNAPL). As PCE and TCE migrate down through the aquifer, parts of the DNAPL hang up on aquifer sediment and dissolve into the groundwater while the remaining portion of the DNAPL pools on the aquifer's confining unit. The DNAPL portion of the contamination throughout the aquifer serves as a source for continuous dissolution of PCE or TCE into the groundwater. Therefore, pump and treat remediation attempts were met with little success due to the effects of the residual PCE or TCE. Research in the 1980's began documenting the presence of lessor chlorinated compounds such as *cis*-

12-DCE and VC at PCE and/or TCE contaminated sites. The pathways for the production of these chlorinated ethenes were investigated (Bradley, 2000). Based on these investigations, microbially mediated reductive dechlorination is accepted as a biodegradation mechanism. Moreover, in situ reductive dechlorination introduced the possibility of intrinsic bioremediation as a remediation strategy for chlorinated ethene contaminated sites.

Intrinsic bioremediation, also known as Monitored Natural Attenuation (MNA), is a remediation strategy that relies on biotic and abiotic processes to reduce the levels of contamination to meet goals prescribed for a specific site. Most importantly, MNA must reach the remediation goals for the particular site within a reasonable time frame. The mechanisms used by MNA can be compared by whether the mechanism is destructive or non-destructive. A destructive mechanism reduces the mass of the contamination. The main destructive mechanism in MNA is biodegradation; however, abiotic processes such as hydrolysis can contribute to destructive mechanisms (EPA., 1998). Conversely, non-destructive mechanisms included in MNA are abiotic processes such as sorption, volatilization and dispersion. These processes reduce the concentration of the contamination in the groundwater but do not degrade the contamination.

To determine if a site is suited for MNA, the OSWER Directive 9200.4-17 proposed three lines of evidence in which to investigate (EPA., 1998). The first line of evidence addresses the historical aspects of the groundwater and soil data at the contaminated site. This data should indicate the reduction of contaminant mass/concentration via natural attenuation processes such biodegradation as opposed to pure dilution of the contaminant by down stream movement of the plume. The second line of evidence includes evaluation of pertinent 'hydrogeologic and geochemical data' (EPA., 1998). Characterization of the subsurface environment through this data will aid in determining which MNA process affects the reduction in contamination at the site, among other things. The final line of evidence for MNA is the evaluation of field measurements or the construction of microcosms to demonstrate the potential of indigenous microbiota to degrade the contaminants. Through the evaluation of each line of evidence, the ability of the site to support MNA as a viable remediation option can be assessed relative to remediation objectives associated with regulatory compliance.

If MNA is deemed a viable remediation option upon completion of the OSWER Directive's three lines of evidence, the next step is to develop a remediation plan, which includes MNA, for the

contaminated site. In the plan, the remediation goals and methodologies are described. Usually, MNA is recommended in conjunction with other remediation strategies such as source removal (EPA., 1998). In the case of source removal, the source material is removed at the beginning of the remediation efforts. MNA is used as a final step in reducing the contaminant concentrations. The long term monitoring of the site by MNA is recommended to chart the remediation progress and then to ensure compliance with the established remediation goals.

Geochemical Parameters

The geochemical parameters or redox indicators are used to characterize the subsurface environment that contributes to predicting the bioremediation potential of a site. Through investigations of petroleum hydrocarbon contamination, research has shown that the terminal electron accepting precess/es (TEAP) occurring the aquifer are the primary factor in determining the efficacy of biodegradation (Chapelle et al., 1995; Bradley and Chapelle, 1998b). Therefore, when analyzing the geochemical parameters of a site, groundwater samples are analyzed for indicators of microbially-mediated redox processes. These redox indicators consist of possible electron acceptors (oxygen, nitrate/nitrite, sulfate and CO_2), intermediate products (hydrogen), and the end products (Fe(II), sulfide, and methane).

For a particular groundwater sample, the concentrations of the electron acceptors and end products are indicative of the predominate TEAP in the aquifer. Based on energy gained by the microorganisms, the electron acceptors are depleted in order of oxygen, nitrate, Fe(II), sulfate and CO_2. As the electron acceptor is utilized by the microorganisms, the electron acceptor is converted to its end product. Thus, the depletion of a possible electron acceptor indicates that the microbial population is utilizing or has utilized this particular electron acceptor. Conversely, the accumulation of a microbial end product indicates that the microbial population is utilizing or has utilized the electron acceptor precursor for the associated end product. Therefore, the production of end products concurrent with the depletion of electron acceptors is an indicator of the TEAP.

Hydrogen is a short lived intermediate product of fermentation whose measurements can indicate the predominate TEAP at location sampled without possible bias from upstream flow of groundwater constituents. Based on work by Chapelle et al. (1995), the relationship between the hydrogen

concentrations and the TEAP is listed in Table 2.1. Table 2.1 illustrates the relative ability of microorganisms to utilize hydrogen as an electron donor. As the predominate microbial population is less efficient in using H_2 as an electron donor, the measurable concentration of H_2 increases.

Table 2.1: Ranges of Hydrogen Concentrations for TEAPS

Hydrogen Concentration (nM)	TEAP
<0.1	Denitrification
0.2 to 0.8	Iron (III) Reduction
1 to 4	Sulfate Reduction
5 to 20	Methanogenesis

Table adapted from Chapelle et al., 1995

Anaerobic Biodegradation Pathways

It has been well established that chlorinated ethenes can be reductively dechlorinated under anaerobic conditions (Bradley, 2000; Wu et al., 1998; deBruin et al., 1992). Through reductive dechlorination, PCE can be degraded to TCE, *cis*-1,2-DCE, VC, and ethene. While all isomers of DCE may also be produced, the *cis*-1,2-DCE isomer is predominately generated by reductive dechlorination (EPA., 1998). The mechanisms for the reduction of the chlorinated ethenes can be separated into two categories based on whether microorganisms derive energy from the reduction process. The first mechanism is based on cometabolism where chlorinated ethenes are reduced through a fortuitous reaction with an enzyme cofactor. The microorganisms producing the enzyme do not derive energy from this process. The other mechanism for reductive dechlorination is based on dehalorespiration where the microorganisms derives metabolic energy by utilizing the chlorinated ethene as an electron acceptor. A comparison of the degradation rates for the two reductive dechlorination pathways shows that dehalorespiration degrades chlorinated ethenes at rates several orders of magnitude greater than cometabolism (Fetzner, 1998; Cabirol et al., 1996, 1998). Therefore, cometabolism is often not an integral part of reductive dechlorination at a site due to the slower rates of reductive dechlorination (EPA., 1998).

In dehalorespiration, the chlorinated ethene is used as the electron acceptor for generation of metabolic energy. In this reaction, a chlorine atom is removed from the chlorinated ethene and is replaced by a hydrogen atom. This degradation pathway requires an electron donor. Research has

shown the electron donor for dehalogenation is H_2 (Smatlak et al., 1996; Yang and McCarty, 1998). The hydrogen can be produced via acetogenic fermentation by utilizing a variety of carbon sources (Fennell and Gossett, 1997; Gao et al., 1997). For reductive dechlorination, it has been shown that H_2 concentrations of 1 nM or greater are required (EPA., 1998). However, research by Smatlak et al. (1996) showed that high concentrations of H_2 favor methanogens and ultimately can suppress reductive dechlorination. Furthermore, research showed that dechlorinators are better scavengers for H_2 and most efficient under a steady supply of H_2 at 2 nM (Yang and McCarty, 1998).

When either the election donor or carbon source is limited partial reductive dechlorination is often times observed. This is marked by accumulation of chlorinated ethenes such as *cis*-1,2-DCE and VC. Furthermore, the extent of reductive dechlorination has been shown to be affected by the predominant TEAP (EPA., 1998; Bradley, 2000). As the chlorinated ethene becomes more reduced, it requires a more reduced environment in which to be dechlorinated. The highly oxidized nature of PCE enables degradation to TCE under all anaerobic conditions whereas TCE degradation requires at least Fe(III)-reducing conditions. The more reduced daughter products, *cis*-1,2-DCE and VC, have been shown to require sulfate-reducing or methanogenic conditions for efficient reductive dechlorination (EPA., 1998; Bradley, 2000).

As PCE is reduced, the resultant daughter products become more susceptible to oxidation reactions. It has been shown that vinyl chloride can oxidized readily to CO_2 under anaerobic (Bradley and Chapelle, 1996, 1997; Bradley et al., 1998; Bradley and Chapelle, 1998b) and aerobic conditions (Bradley and Chapelle, 1998a, 2000). Bradley and Chapelle have demonstrated that VC can be mineralized under Fe(III) reducing conditions (Bradley and Chapelle, 1996, 1997; Bradley et al., 1998; Bradley and Chapelle, 1998b), sulfate reducing conditions (Bradley and Chapelle, 1998b), and methanogenic conditions (Bradley and Chapelle, 1997; Bradley et al., 1998; Bradley and Chapelle, 1998b). The observation of VC oxidation led researchers to investigate the ability of *cis*-1,2-DCE to undergo anaerobic oxidation. Under Fe(III)-reducing, sulfate-reducing, and methanogenic conditions, *cis*-1,2-DCE has been mineralized to CO_2 at slower rates in comparison to VC direct oxidation (Bradley and Chapelle, 1997, 1998b). However, VC and ethene were also observed during the course of the experiments. This observation suggests that *cis*-1,2-DCE is reductively dechlorinated to VC in a rate limiting step, then VC is oxidized to CO_2. In the presence

of humic acids, serving as electron donors, Bradley et al. (1998) showed anaerobic oxidation of *cis*-1,2-DCE without the detection of VC and ethene. Therefore, the presence of an effective electron donor is required for efficient anaerobic oxidation.

Aerobic Biodegradation Pathways

Due to the highly oxidized nature of PCE, it has not demonstrated aerobic degradation. However, the lessor chlorinated ethenes have been shown to aerobically degrade through cometabolic processes to innocuous end products. The cometabolic process oxidizes the chlorinated ethene through a fortuitous reaction with an oxygenase enzyme. These non-specific enzymes are produced by aerobic microorganisms such as methanotrophs (Cabirol et al., 1998) and a variety of hydrocarbon oxidizers (EPA., 1998). Moreover, the microbes do not derive energy from the degradation of chlorinated ethenes. In some cases, cometabolic reactions can be detrimental to the microorganisms responsible for the generation of the enzyme (Fetzner, 1998). Aerobic cometabolic degradation not only depends on the presence of the non-specific oxygenase but also on the presence of a substrate and oxygen to support the oxygenase generating microorganism. The lessor chlorinated ethenes can also be aerobically oxidized without the presence of an oxygenase. Numerous researchers haven shown that VC can readily oxidize under aerobic conditions (Bradley et al., 1998; Bradley and Chapelle, 1998a). Furthermore, VC has been shown to support microbial growth (EPA., 1998) and has been shown to mineralize to CO_2 (Bradley et al., 1998). The mechanisms for *cis*-1,2-DCE oxidation is still on the forefront of research. Recently, *cis*-1,2-DCE was shown to provide metabolic energy for microorganisms but failed to be used as a carbon source for growth (Bradley and Chapelle, 2000).

Chapter 3

Site Characterization

3.1 Site History

The Naval Amphibious Base Little Creek (NABLC) Site 12 is located in Virginia Beach, VA (Figure 3.1). The site under investigation is located at the intersection of 3rd and B streets which was home to a former laundry/dry cleaning facility. From 1973 to 1978 the dry cleaning facility disposed of dry cleaning waste containing PCE and other organic byproducts through a manhole that fed into a storm sewer catch drain. An estimated volume of 200 gallons of PCE and 1100 gallons of soaps, sizing and dyes was discharged into the storm sewer (CH2MHill, 2000). In preparation for the construction of a new base commissary, the main portion of the storm sewer was removed in 1987. In 1992, the remaining parts of the storm sewer were removed as part of recommendations given in a Site Characterization Report for the Commissary Construction Project (CH2MHill, 2000). The site is currently nearing the end of Phase II of a Supplemental Remedial Investigation (SRI) and a Baseline Human Health Risk Assessment.

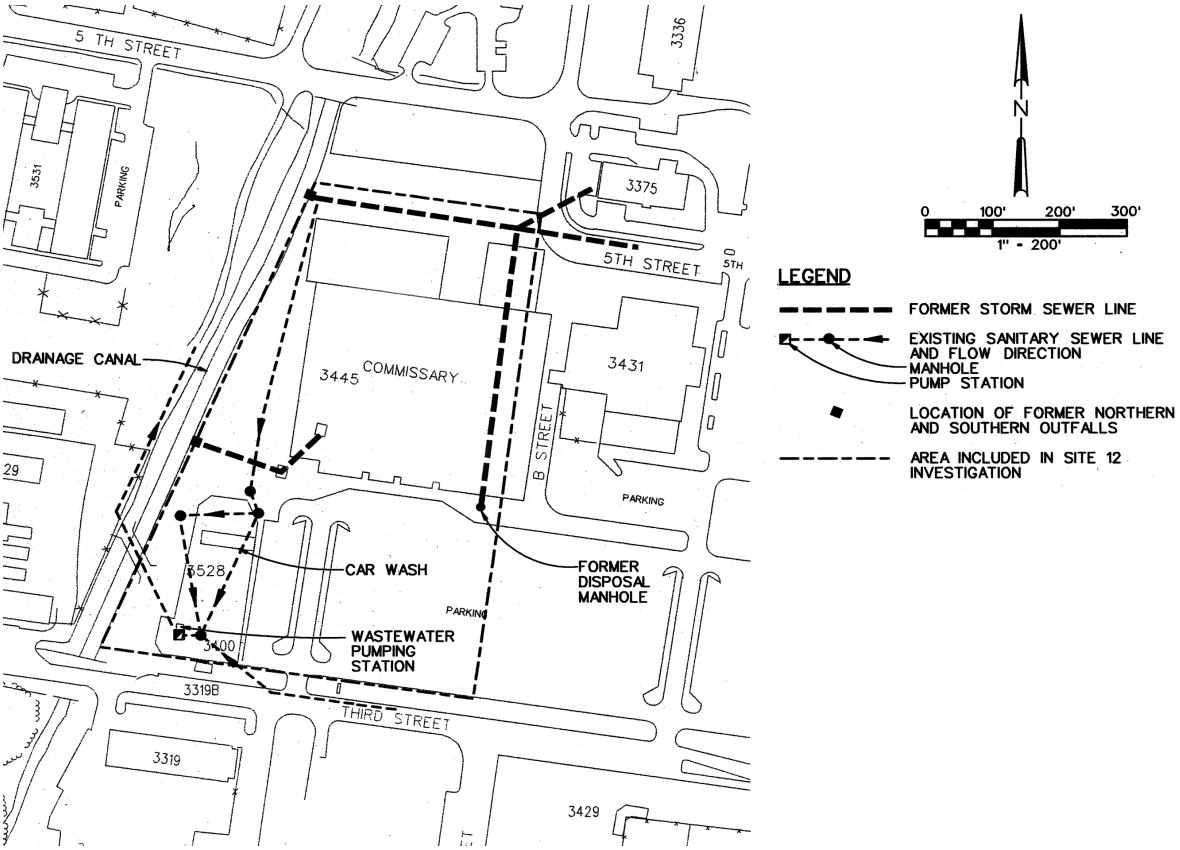

Figure 3.1: Location of Site 12 on Naval Amphibious Base Little Creek, Virginia Beach, Virginia. Source: CH2MHill 2000

3.2 Hydrogeology

3.2.1 Hydrostratigraphic Units

All work on the lithography of the site was completed by CH2MHill and reported in the Supplemental Remedial Investigation Report (CH2MHill, 2000). The following is a brief summary of the three main hydrostratigraphic units that the chlorinated ethene contamination impacts at Site 12. The upper unit is the Columbia Aquifer, which is an unconfined, coastal plain aquifer. The aquifer is approximately 20-25 feet thick at the site and is comprised of Pleistocene deposits that are characterized as well sorted to coarse beach-like sand. Below the Columbia Aquifer is the Yorktown confining unit which separates the Columbia from the Yorktown-Eastover Aquifer. The Yorktown confining unit is approximately 30 to 40 feet thick and is comprised of gray clay, silt and fine sand. The isolation of the Columbia and Yorktown-Eastover Aquifers is of utmost importance because the Yorktown-Eastover Aquifer is a source of potable water. Below NAB Little Creek Site 12, the Yorktown-Eastover Aquifer is approximately 280 feet thick and is comprised of silty and clayey fine sand with shell fragments.

3.2.2 Hydraulic Conductivity

To further the understanding of the groundwater and contaminant movement, slug and pumping tests were performed to determine the phreatic aquifer's hydraulic conductivity. Both a slug test and a pumping test were performed by Foster Wheeler Environmental Services (FWES) in September 1995 as part of Phase I of the SRI (CH2MHill, 2000). The results of the two tests differed considerably. The slug test produced an average hydraulic conductivity of 30 ft/day while the pumping test produced an average hydraulic conductivity of 109 ft/day. Based on previous experience dealing with coastal plain aquifers, FWES concluded that the slug test underestimated the hydraulic conductivity of the Columbia aquifer (CH2MHill, 2000). Therefore, the value of hydraulic conductivity based on the pumping test was used for the groundwater flow calculation in this study.

3.2.3 Groundwater Flow

Since most of the site is covered by bituminous concrete, recharge due to precipitation is restricted to grass-covered areas in the parking lot's medians and adjacent to the car wash (Figure 3.1). Groundwater inflow for the site comes from groundwater upgradient in the aquifer. Groundwater elevations recorded by CH2MHill in July 1998, November 1998, and February 1999 showed similar flow patterns between years. Figure 3.2 is a representative potentiometric surface from July 1998. The equipotential lines formed a radial pattern which surrounded a portion of a sanitary sewer line. Upon investigation, CH2MHill confirmed groundwater seepage into the sanitary sewer line at an estimated infiltration rate of 16 to 17 gpm (CH2MHill, 2000). Therefore, the groundwater flow pattern at Site 12 is controlled by a leaky sanitary sewer line that runs through the site.

The groundwater elevations were used to calculate the hydraulic gradient at the site. The hydraulic gradient at the site ranged from 0.001 ft/ft to 0.002 ft/ft between years with groundwater elevations differing by roughly one foot over time. Under the assumption that the Columbia Aquifer is homogeneous and isotropic, the average linear groundwater velocity for the site can be calculated using Darcy's Law

$$\nu = \frac{K}{\eta}\frac{dh}{dl} = 0.5 ft/day \tag{3.1}$$

where K is the hydraulic conductivity (109 ft/day), η is the effective porosity (0.35), and $\frac{dh}{dl}$ is the hydraulic gradient (0.0015 ft/ft).

During a site characterization by CH2MHill the vertical hydraulic gradient over the Yorktown Confining Unit was determined to be 0.03 ft/ft. Based on the vertical hydraulic gradient, CH2MHill concluded that the confining unit provides sufficient separation between the Columbia and Yorktown-Eastover Aquifer. The direction of groundwater flow for the Yorktown-Eastover Aquifer was determined via groundwater elevations taken in July 1998, November 1998, and February 1999 (CH2MHill, 2000). The potentiometric surface of the Yorktown-Eastover Aquifer showed groundwater flow north towards the Chesapeake Bay.

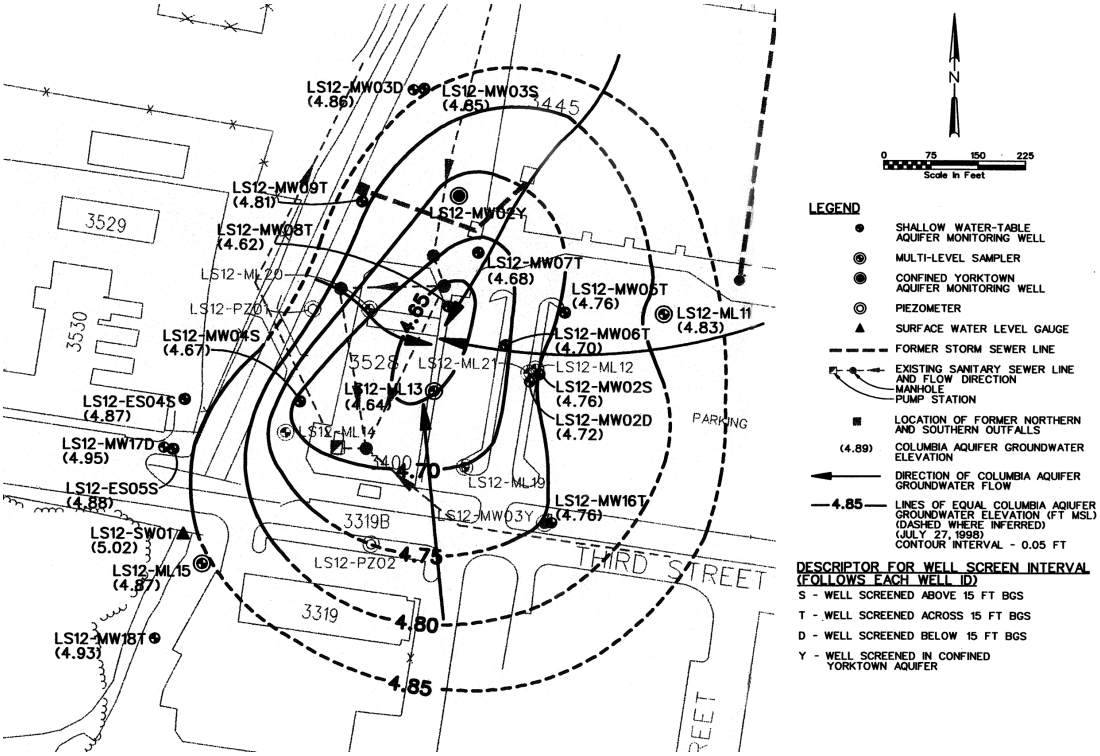

Figure 3.2: Potentiometric Surface of Site12 on July 27, 1998. Source: CH2MHill, 2000.

3.3 Groundwater Parameters

Groundwater parameters at Site 12 were measured using 19 monitoring wells and 10 multi-level sampling wells (MLS) (Figure 3.3). Monitoring wells were installed using one of three screening intervals: total (across the Columbia Aquifer), shallow (2.0 to 12 ft bgs) and deep (18 to 20 ft bgs). However, the monitoring wells produced an average groundwater constituent concentration over the depth of the screen. In order to produce an accurate vertical distribution of a constituent, MLS were installed. The multi-level sampling wells were designed to collect the groundwater at seven discrete depths for each well (Figure 3.4). The ports were numbered from one to seven with one being in the deepest part of the aquifer and seven being close to or at the water table. Furthermore, the placement of the MLS was designed to determine the concentration of the groundwater parameters along the flow path through the plume. In June of 1998 a line of MLS were installed along what was believed to be the longitudinal axis of the chlorinated ethene plume based on Figure 3.5. The plume was based on the depth-averaged chlorinated ethene concentrations taken in 1995 from monitoring wells located through Site 12, for a complete description see (CH2MHill, 2000). MLS20 and MLS22 were installed in September of 1998 and June of 1999, respectively to further evaluate the extent of the plume.

The groundwater was sampled in July 1998 and June 1999 through a combined effort of CH2MHill and Virginia Tech. Virginia Tech aided CH2MHill in the field by providing pumps and personnel for collecting groundwater samples for analysis by the outside laboratory. Groundwater parameters identified as relevant to the site such as chlorinated ethenes (PCE, TCE, *cis*-1,2-DCE, *trans*-1,2-DCE, and VC), redox indicators (dissolved oxygen, nitrate/nitrite, sulfate, CO_2, dissolved hydrogen, ferrous iron, sulfide, and methane) and dissolved ethene and ethane were analyzed. Groundwater was also collected and analyzed for other general parameters such as ammonium, calcium, potassium, TOC, temperature, pH, chloride, and alkalinity. The groundwater data for 1998 and 1999 are located in Appendix A. While each port of the MLS was attempted to be sampled, the level of the groundwater table did not always permit samples from the upper most ports. CH2MHill employed an outside laboratory to analyze the collected samples (For complete methods and procedures, see SRI CH2MHill, 2000).

The April 2000 sampling round was completed solely by Virginia Tech. MLS10, MLS11, MLS12, MLS20, and MLS22 were the only MLS sampled. All samples were collected in 40 mL VOA vials with the exception of the hydrogen gas sample. Chlorinated ethene samples were collected and analyzed using the method described in 4.6.2. The cations and anions were analyzed using ion chromatography. Dissolved hydrogen gas was analyzed using the method described in 4.6.1. No measurements of CO_2, methane, ethene and ethane were attempted in the field. Parameters, such as dissolved oxygen, sulfide, and ferrous iron, were analyzed in the field using Hach methods and instrumentation. Dissolved oxygen was analyzed with a modified Winkler titration method (Hach Method 8215). Sulfide measurements were taken using the methylene blue colorimetric method (Hach Method 8131 equivalent to US EPA Method 376.2) and ferrous iron was analyzed with phenanthroline colorimetric method (Hach Method 8146).

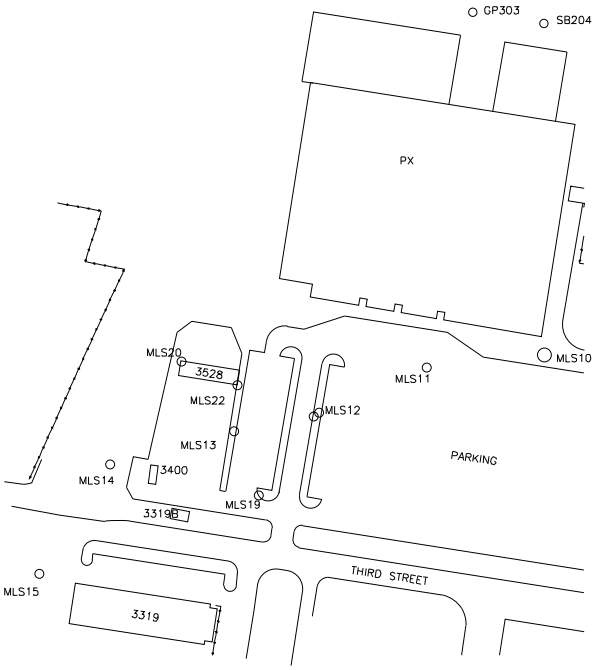

Figure 3.3: Locations of monitoring wells and multi-level sampling wells installed Site 12. Source: CH2MHill, 2000.

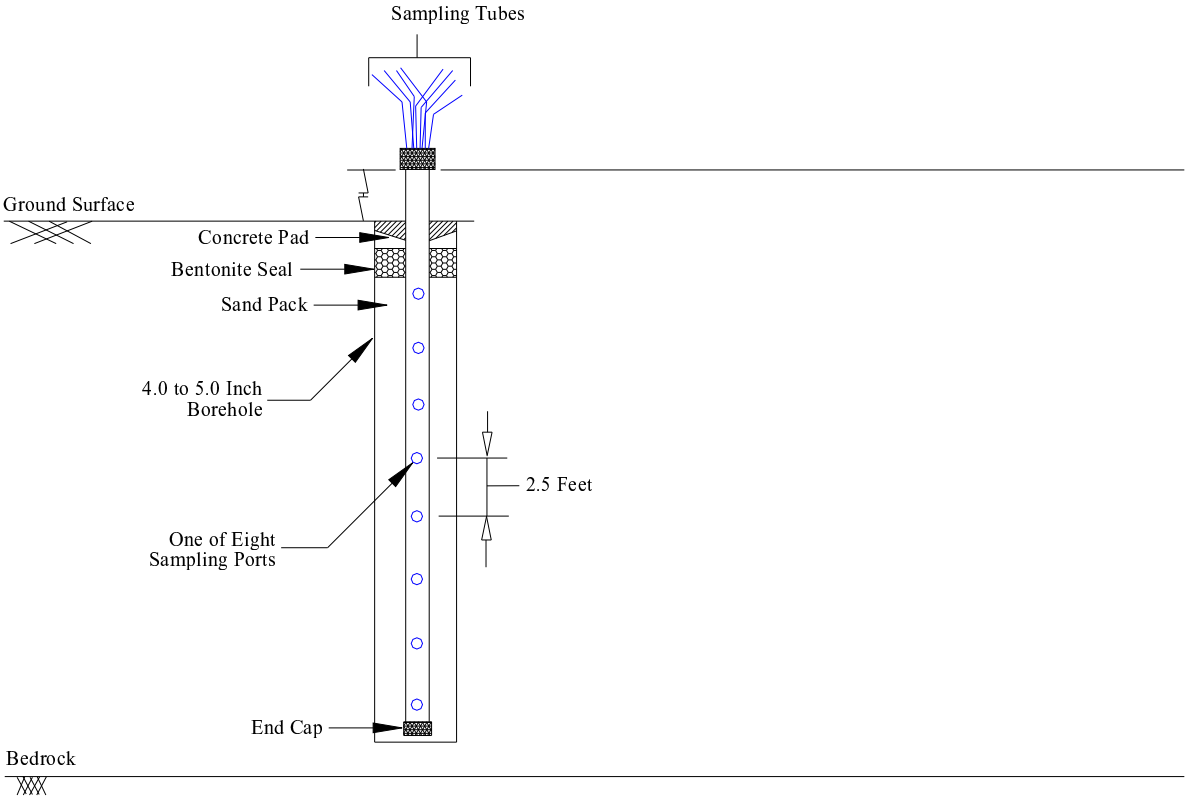

Figure 3.4: Multi-level sampler design that allows seven discrete groundwater samples.

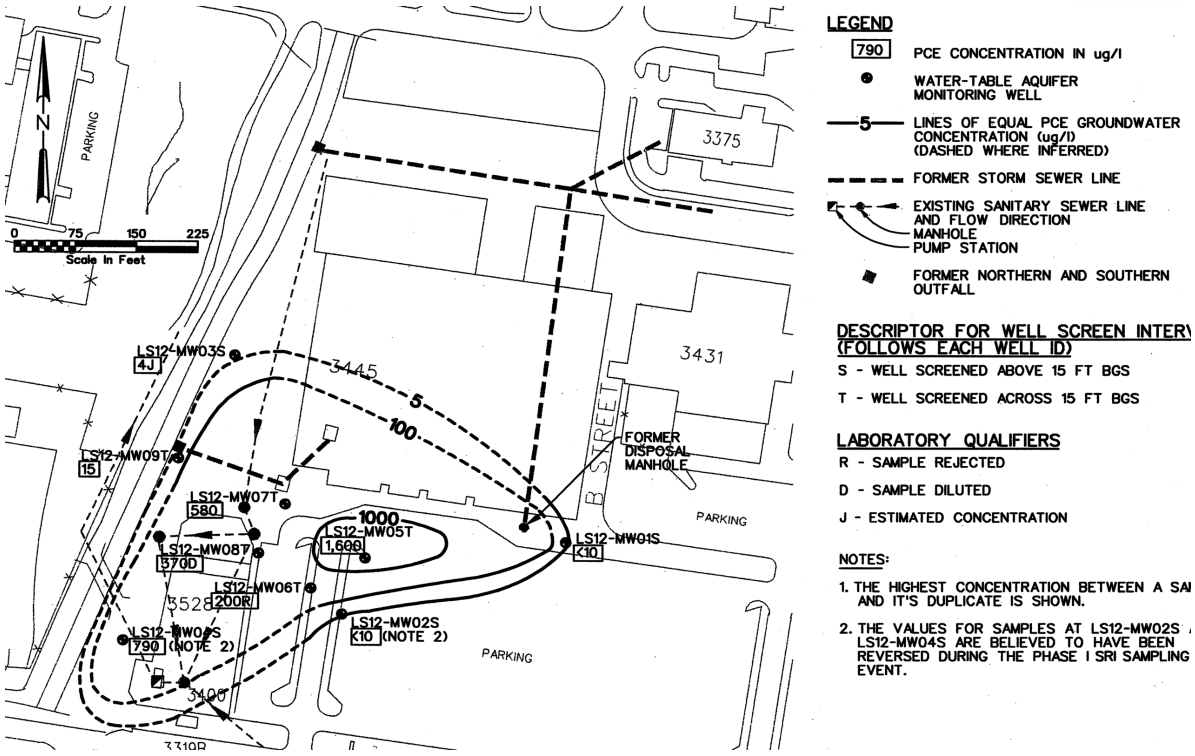

Figure 3.5: Presumed PCE isopleth at Site 12 based on monitoring well data collected in August 1995. Source: CH2MHill, 2000.

3.3.1 Contaminant Distribution

Groundwater was analyzed in the 1998, 1999, and 2000 sampling rounds for the presence of PCE and its daughter products-TCE, *cis*-1,2-DCE, VC and ethene. These analyses aided in understanding the extent of the PCE contamination and in identifying the highest zones of contamination in the aquifer. Furthermore, the detection of PCE's daughter products helped to assess the site's potential to reductively dechlorinate the PCE laden dry cleaning waste. The results of the analysis for each MLS are described in depth versus concentration profiles.

MLS11

The upper three ports in the aquifer (6-14 ft bgs) contained the highest levels of contamination at MLS11 (Figure 3.6). While the TCE contamination levels were a factor of 100 less than the PCE contamination levels, both the PCE and TCE followed the basic trend of higher levels of contamination in the upper ports and lower levels of contamination in the lower ports as can be seen in Figure 3.6. Between 1998 and 1999 the PCE concentration in the upper portion of the aquifer remained relatively constant at 11,000 μg/L, but in the 2000 sampling round the PCE concentration dropped to 4400 μg/L. The TCE levels at 7, 9, and 13 ft bgs were between 45-65 μg/L in 1998, decreased to 20 μg/L in 1999, and increased to 70 μg/L in 2000. The TCE concentration at 15 to 22 ft bgs were below 20 μg/L in 1998 and 1999. In 2000, the TCE concentration at 15 to 19 ft bgs increased to 30 and 20 μg/L, respectively. The *cis*-1,2-DCE contamination also decreased with increased depth in 1998. In 1999 and 2000, no *cis*-1,2-DCE was detected. VC was not detected in any of sampling rounds. In 1998, ethene levels were between 40 to 100 ng/L in all ports. Ethene levels dropped in 1999 as seen in Figure 3.7. The levels of chloride stayed between 24 and 40 mg/L during all three sampling rounds (Figure 3.7).

MLS12

The highest PCE concentration was consistently detected in MLS12 at a depth of 22 ft bgs. As shown in Figure 3.8, the PCE concentrations were highest at depths of 8-12 ft bgs and and 18-22 ft bgs. At a depth of 13-17 ft bgs the PCE contaminant levels were relatively low. The highest levels of TCE contamination were also at a depth of 8-12 ft bgs and 18-22 ft bgs with the middle

2 ports (13-17 ft bgs) at lower levels. *Cis*-1,2-DCE followed the same depth versus concentration profile trend as the PCE and TCE (Figure 3.8).

The PCE contamination levels at a depth of 22 ft bgs decreased between each sampling round (1998, 1999, and 2000) from 23,000 μg/L to 12,000 μg/L to 6000 μg/L while the TCE and *cis*-1,2-DCE concentrations remained constant throughout 1998-2000 at 1300 μg/L and 200 μg/L, respectively. Decreases of 4000 μg/L and 700 μg/L in PCE and TCE concentrations can be seen at a depth of of 8-12 ft bgs between 1998 and 1999. However, the TCE concentration at a depth of 22 ft bgs between 1999 and 2000 remained constant at 300 μg/L . At a depth of 18 ft bgs, the PCE and TCE concentrations decreased by 100 μg/L between 1999 and 2000. Concentrations of *cis*-1,2-DCE decreased by 100 μg/L at a depth of 22 ft bgs and 300 μg/L at a depth of 18 ft bgs between 1998 and 1999 while the *cis*-1,2-DCE levels remained constant between 1999 and 2000.

In 1998 and 1999, VC and ethene were detected at a depth of 8-12 ft bgs as seen in Figure 3.9. The concentrations of VC and ethene decreased between 1998 and 1999. In 2000 no VC was detected and ethene was not analyzed. Chloride's maximum concentration was 74 mg/L and lowest concentration was 25 mg/L (Figure 3.9).

MLS20

The PCE, TCE, and *cis*-1,2-DCE contamination exhibited increased contaminant concentration with depth as seen in Figure 3.10. In 1998, the highest levels of contamination were at a depth of 19 ft bgs with a concentration of 2800 μg/L while the highest TCE and *cis*-1,2-DCE levels were at a depth of 22 ft bgs with concentrations of 600 μg/L ppb and 100 μg/L , respectively. In 1999, the concentrations of PCE and TCE increased at a depth of 19 ft bgs and decreased at a depth of 22 ft bgs. In 2000, the PCE concentration decreased by 200 μg/L at a depth of 19 ft bgs and 1500 μg/L at a depth of 22 ft bgs. The TCE concentrations remained constant at a depth of 19 ft bgs and decreased to non-detect at a depth 22 ft bgs while the *cis*-1,2-DCE concentrations increased by 2500 μg/L at a depth of 19 ft bgs.

Low levels of VC and ethene were detected in 1998 and no VC was detected in 1999 as shown in Figure 3.11. In 2000, VC was detected at a depth of 19 ft bgs with a concentration of 230 μg/L while VC was not detected at any other depth (Figure 3.11). The ethene concentrations in 1999

were in the range of 0.2 - 0.5 μg/L in the lower ports. Ethene was not analyzed in 1998 and 2000.

MLS22

The depth versus concentration profile for MLS22 is similar to the profile at MLS20 where the highest levels of contamination are located at a depth 19 ft bgs and the upper ports of the well have lower levels of contamination (Figure 3.12). The PCE and *cis*-1,2-DCE concentrations did not decrease substantially between 1999 and 2000. However, the TCE concentration increased by 2000 μg/L between the two years in the lower ports.

No VC was detected at MLS22 during the 1999 and 2000 sampling rounds. However, ethene was detected in all ports in 1999 as seen in Figure 3.13. The highest levels of ethene were at 2400 μg/L at a depth of 19 ft bgs. The chloride levels were similar between 1999 and 200 with concentrations in the range of 20-36 mg/L (Figure 3.13).

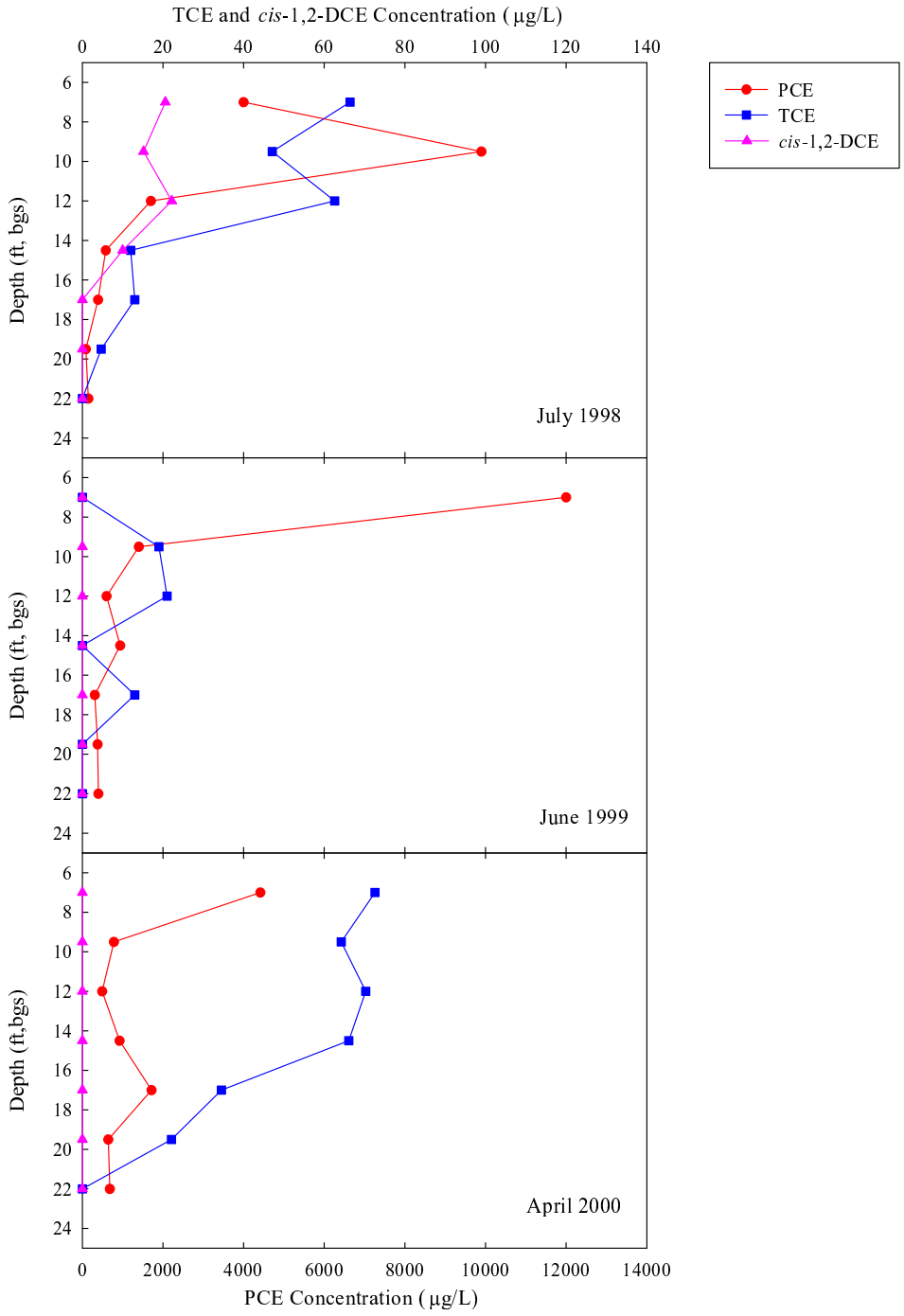

Figure 3.6: The groundwater concentrations of PCE, TCE, and *cis*-1,2-DCE at all ports of MLS11 for the 1998, 1999, and 2000 sampling rounds.

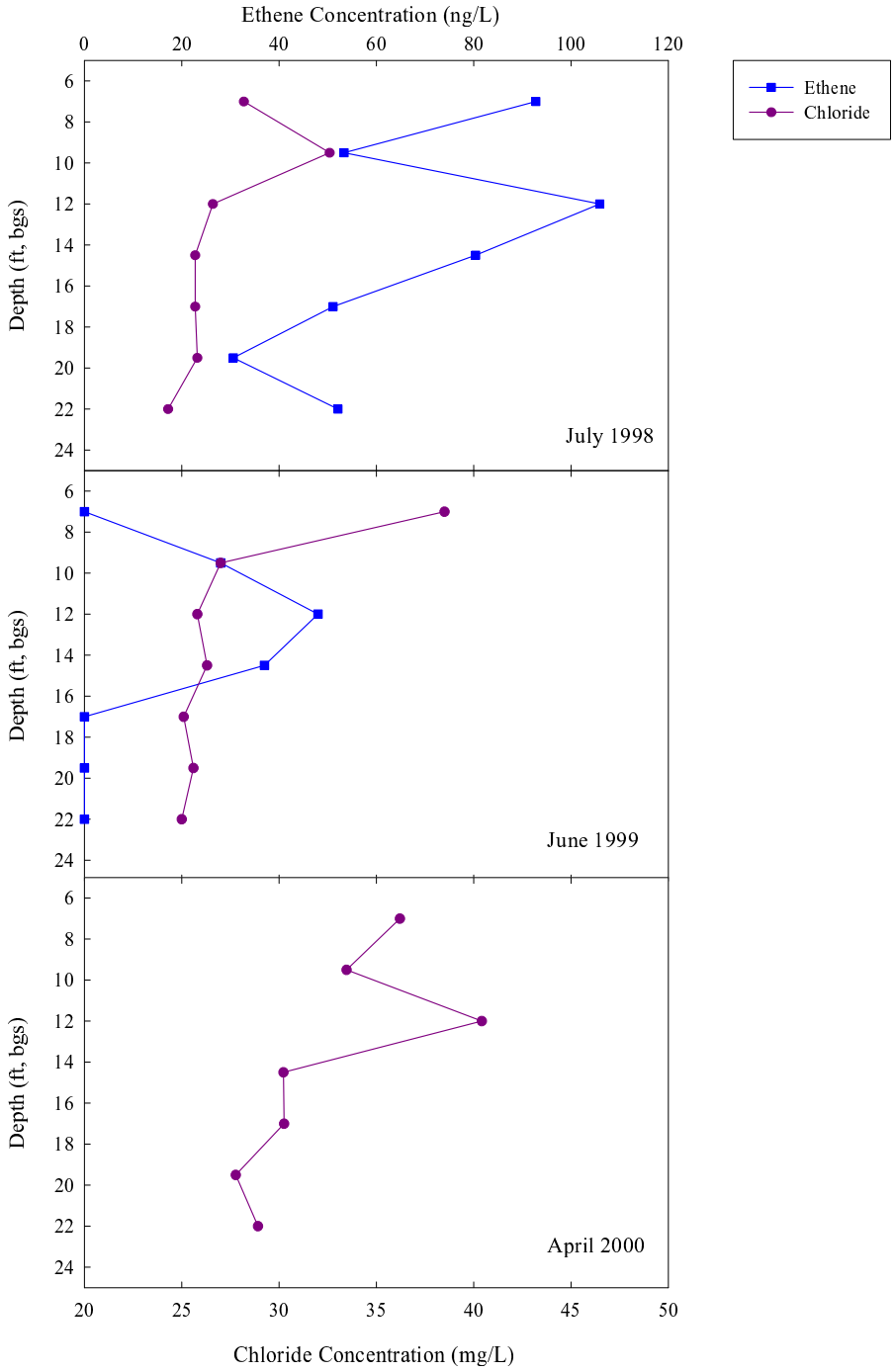

Figure 3.7: The groundwater concentrations of ethene and chloride at all ports of MLS11 for the 1998, 1999, and 2000 sampling rounds.

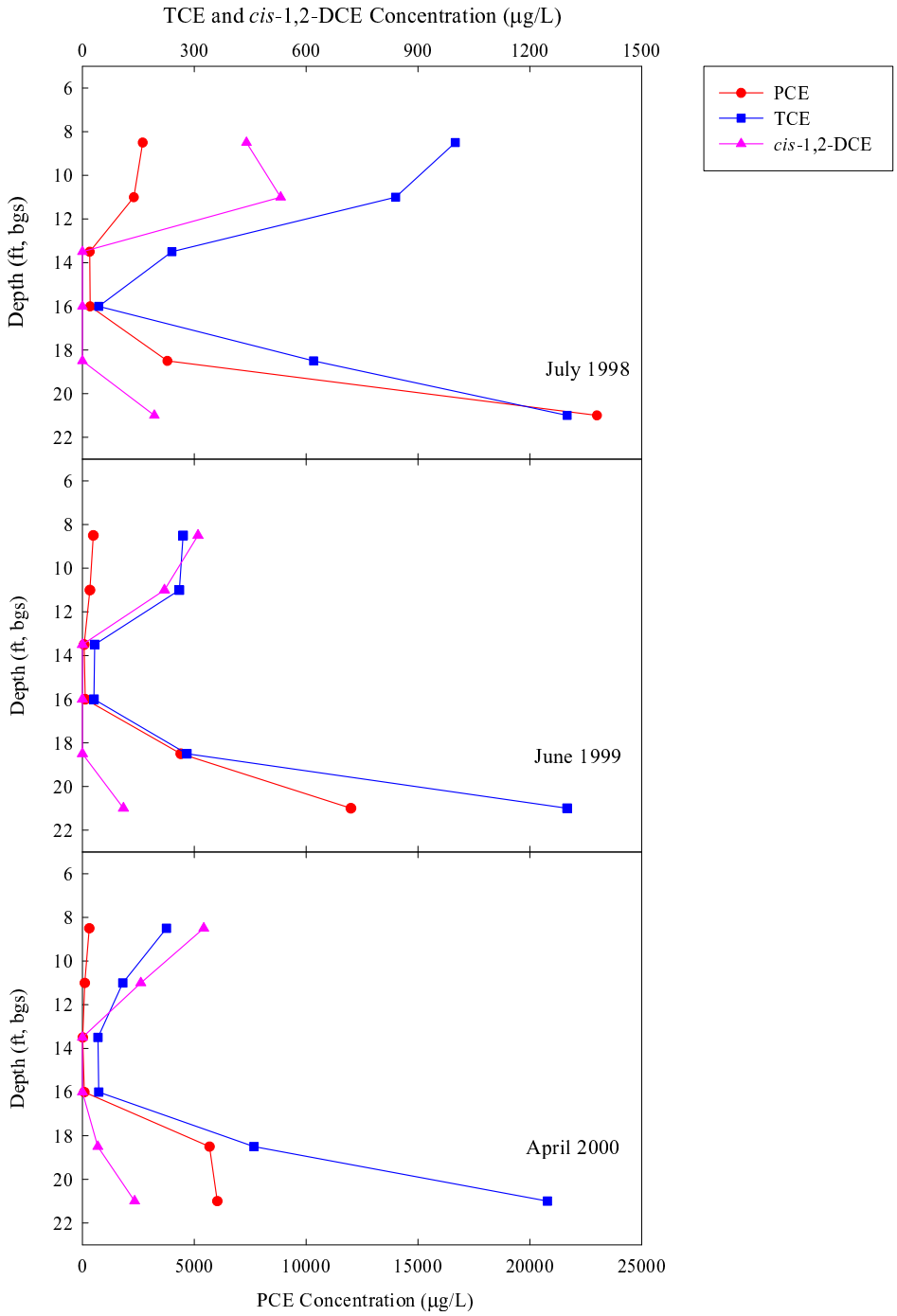

Figure 3.8: The groundwater concentrations of PCE, TCE, and *cis*-1,2-DCE at all ports of MLS12 for the 1998, 1999, and 2000 sampling rounds.

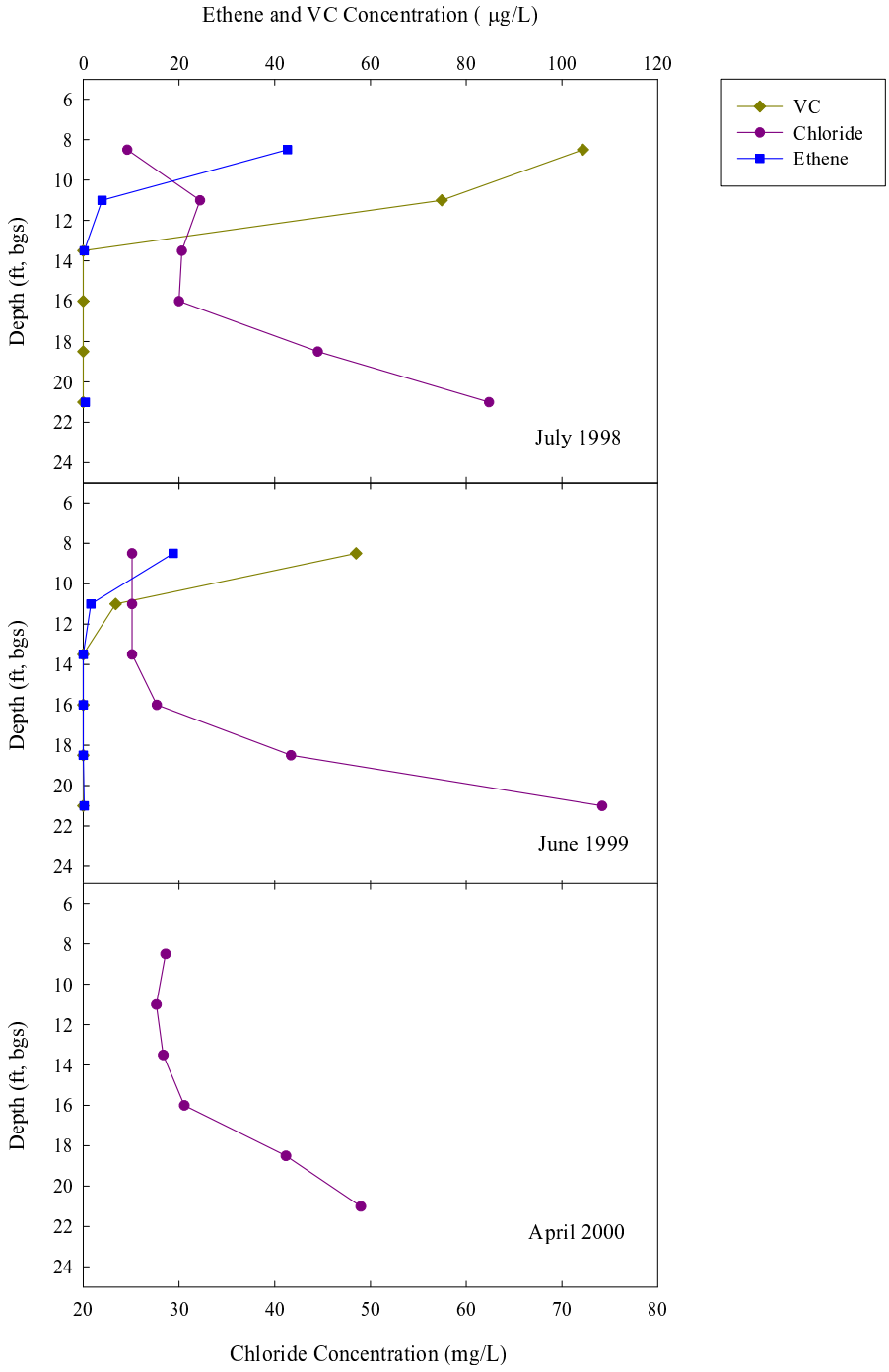

Figure 3.9: The groundwater concentrations of VC, ethene, and chloride at all ports of MLS12 for the 1998, 1999, and 2000 sampling rounds.

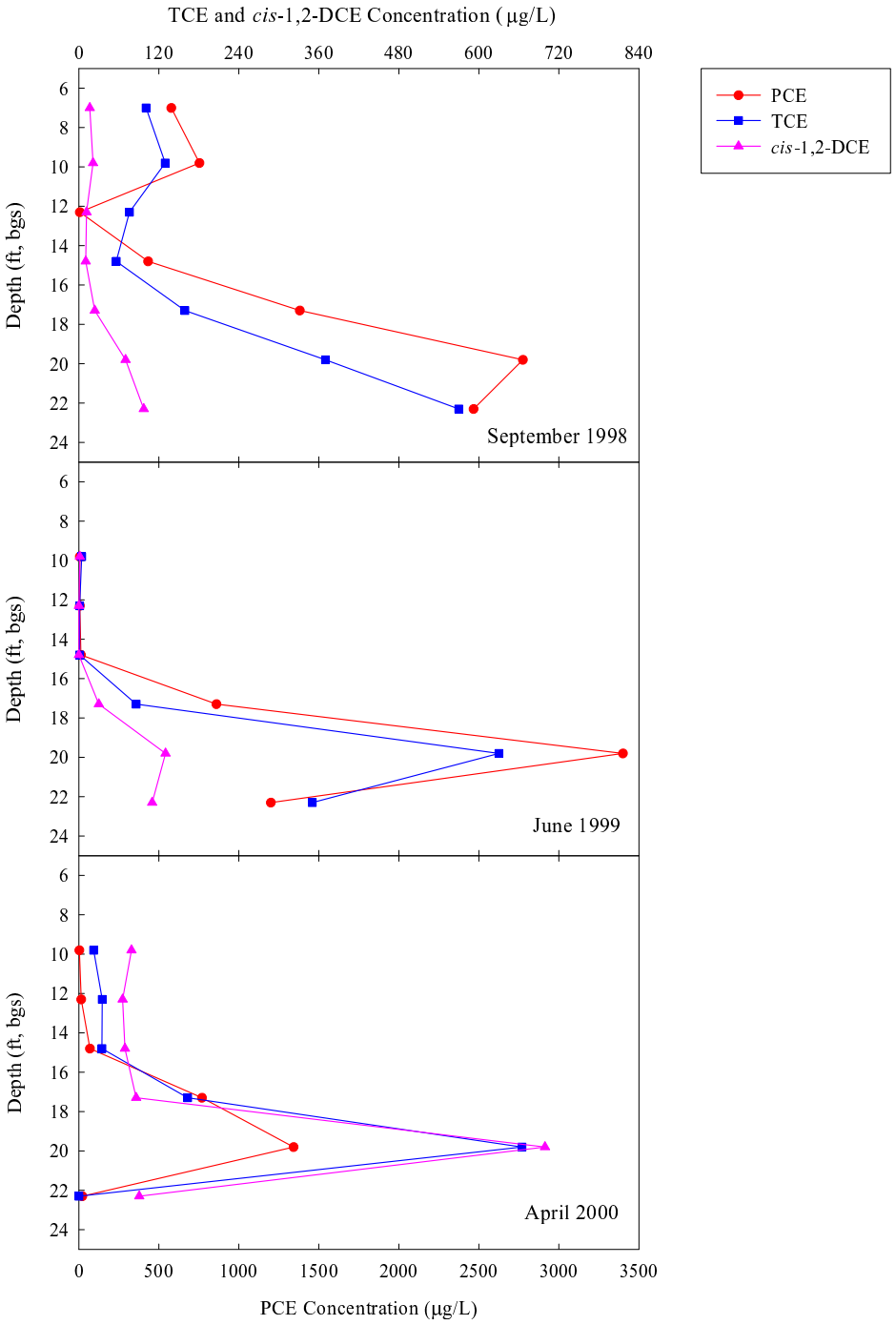

Figure 3.10: The groundwater concentrations of PCE, TCE, and *cis*-1,2-DCE at all ports of MLS20 for the 1998, 1999, and 2000 sampling rounds.

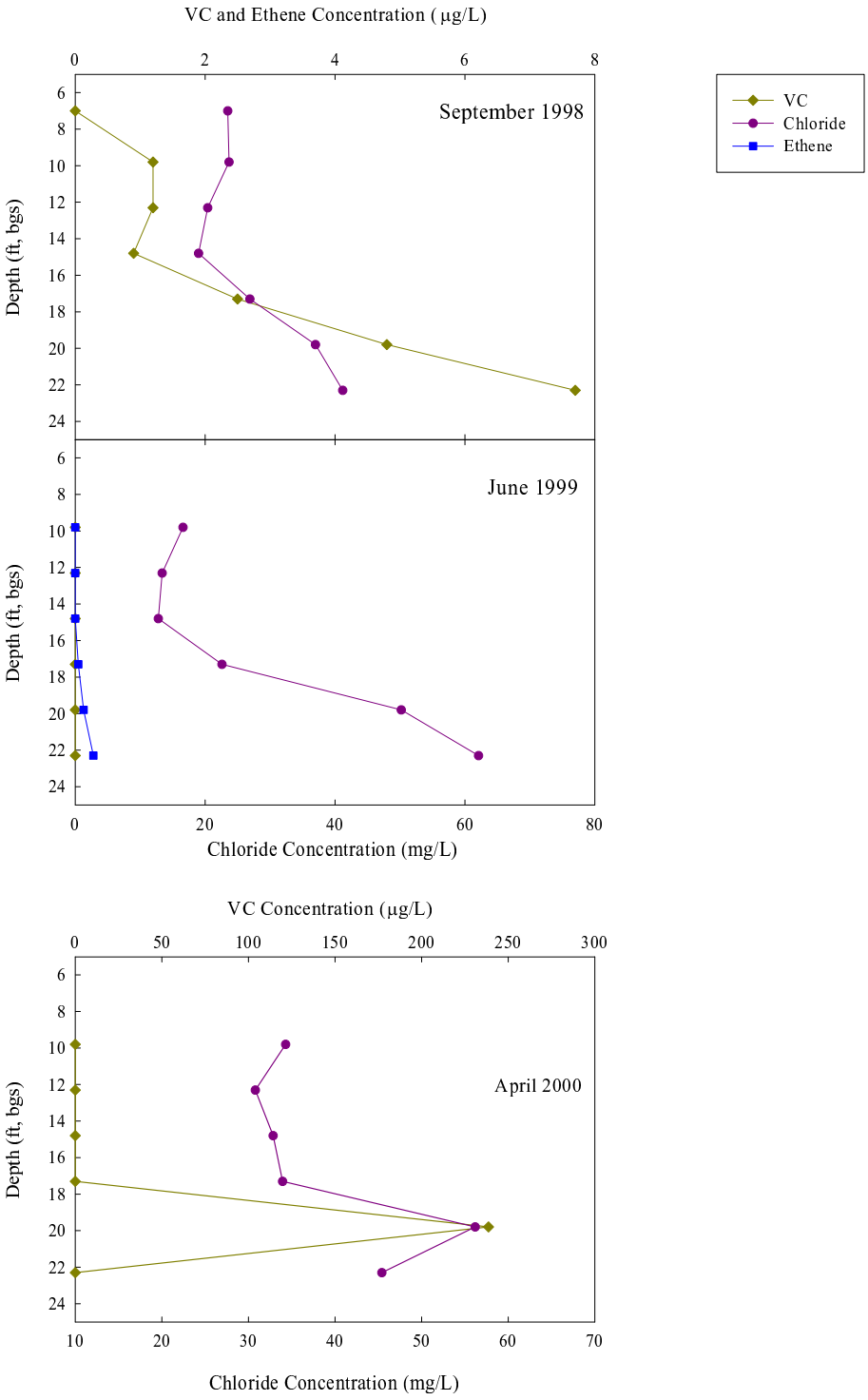

Figure 3.11: The groundwater concentrations of VC, ethene, and chloride at all ports of MLS20 for the 1998, 1999, and 2000 sampling rounds.

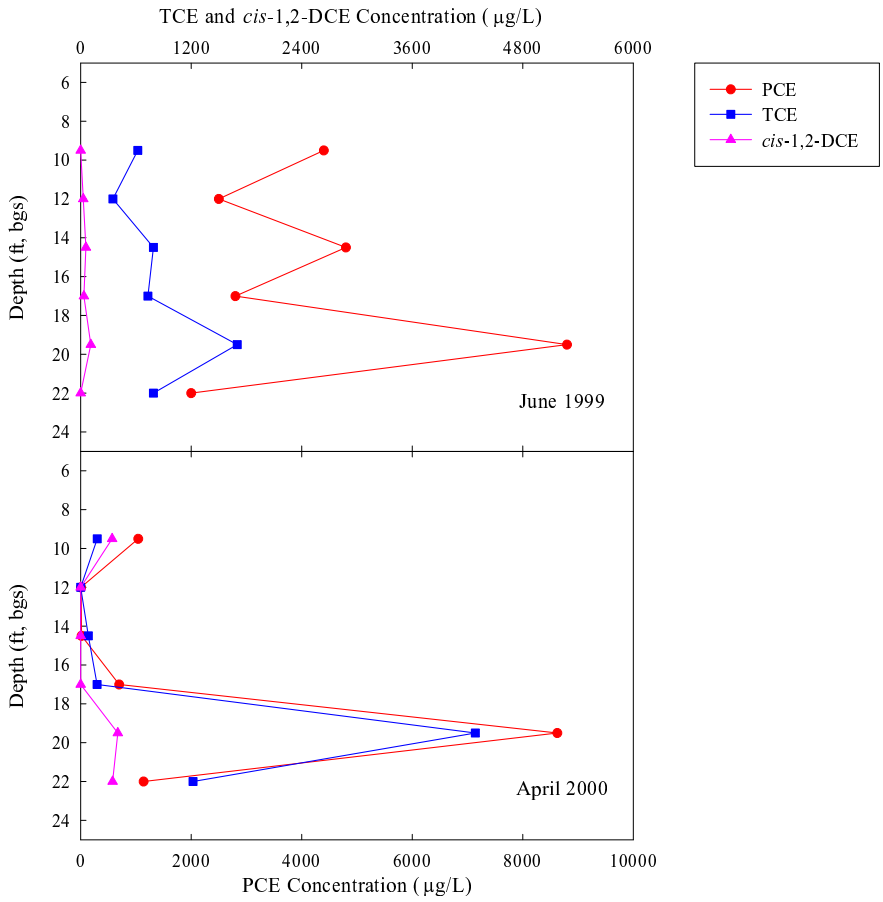

Figure 3.12: The groundwater concentrations of PCE, TCE, and *cis*-1,2-DCE at all ports of MLS22 for the 1999 and 2000 sampling rounds.

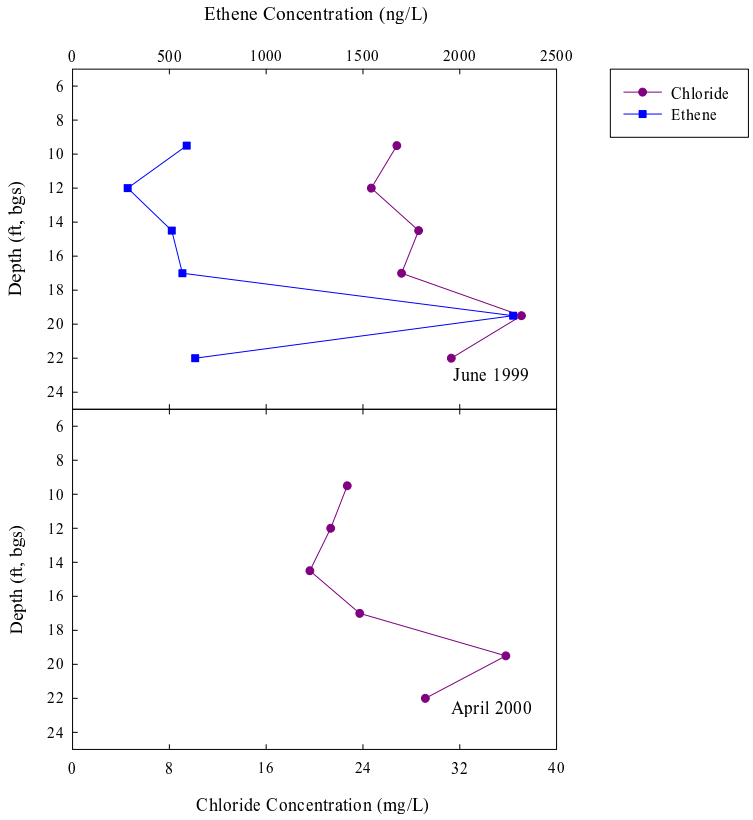

Figure 3.13: The groundwater concentrations of ethene and chloride at all ports of MLS22 for the 1999 and 2000 sampling rounds.

3.3.2 Redox Indicators

Groundwater samples were analyzed for indicators of microbially-mediated redox processes. These redox indicators consisted of potential electron acceptors (nitrate/nitrite, sulfate and CO_2), intermediate products (hydrogen), and the end products (Fe(II), sulfide, and methane). Since the redox indicators were used in deducing the prevalent terminal electron acceptor process/es occurring in the aquifer, each groundwater constituent is discussed with respect to all of the multi-level samplers. This approach allowed redox trends throughout the aquifer to be described for the 1998, 1999 and 2000 sampling rounds.

Nitrate/Nitrite

The levels of nitrate and nitrite at MLS12, MLS11 and MLS20 were below the detection limit of 0.5 mg/L for both compounds during all three sampling rounds. The low levels of these electron acceptors in the areas with the highest concentrations of chlorinated ethenes indicates that reducing conditions exist within the plume. At the upstream edge of the plume, nitrate concentrations of 0.9 mg/L are seen in the lower ports of MLS10. Conversely, the upper ports of MLS10, which have trace quantities (10 ppb) of PCE and TCE, also exhibited non-detectable levels of nitrate and nitrite.

Sulfate

Sulfate levels decrease in concentration with increased depth as seen in Figures 3.14 and 3.15. The lower portion of the aquifer exhibited sulfate concentrations in the range of 20-40 mg/L while the average sulfate concentrations in the upper portion of the aquifer (6-14 ft bgs) ranged between 40-100 mg/L in the 1998, 1999, and 2000 sampling rounds. Within the range of 40-100 mg/L, the levels sulfate varied in the upper portion of the aquifer between 1998, 1999, and 2000. For example, MLS 12 sulfate concentrations were between 60-80 mg/L in 1998, then increased to 100 mg/L in 1999 and decreased back to 60-80 mg/L in 2000 (Figure 3.14). The background levels of sulfate upgradient from the plume at MLS10 were similar to the levels within the plume.

Carbon Dioxide

Dissolved carbon dioxide concentrations were measured in 1998 and 1999 as shown in Figures 3.16 and 3.17. In general, the levels of CO_2 decreased with increased depth and exhibited concentrations of CO_2 between 100-160 mg/L in the upper four ports and between 40-100 mg/L in the lower two ports. MLS20 demonstrated the opposite trend, where the lowest levels were in the upper ports and the highest concentrations were in the lower ports. Moreover, the concentrations in the lower portions of the aquifer for MLS20 were in the same range (40-100 mg/L) as observed throughout the aquifer. The upper ports of MLS20 produced substantially lower concentrations of CO_2 between 20-40 mg/L. The background levels of CO_2 were similar to the general trend in the aquifer with high levels of CO_2 in the upper portion and low levels in the lower portion.

Hydrogen

The hydrogen levels were measured at Site 12 for each sampling round 1998, 1999, 2000. In 1998, the hydrogen concentrations in the upper portion of the aquifer (Figures 3.18- 3.20) were between 1 and 5 nM with exceptions at MLS11, MLS12 and MLS15. These exceptions all had at least one port with a hydrogen concentration higher than 8 nM. The lower portion of the aquifer had hydrogen concentrations of 5 nM or greater with the exception of MLS14. It had hydrogen levels of 0.4 to 0.8 nM. In 1999, fewer wells were sampled for hydrogen. Samples from MLS12 and MLS20 produced hydrogen levels between 1 and 4.5 nM. The lowest levels of hydrogen were detected in the middle portion of the aquifer. In 2000, the aquifer produced hydrogen levels of 5 nM or greater throughout the aquifer with the exception of the four port at MLS22 where the hydrogen concentration was 3 nM.

Ferrous Iron

In 1998 and 2000, the ferrous iron concentration ranged in MLS11, MLS12, and MLS20 between 2-15 mg/L with no apparent trend as shown in Figure 3.21 and 3.22. The levels of ferrous iron within the extent of the plume were comparable to the ferrous iron up gradient at MLS10. In 2000, the ferrous iron concentrations were considerably higher at MLS20. The levels increased by approximately 25 mg/L. The groundwater was not analyzed for ferrous iron in the 1999 sampling

round.

Sulfide

The levels of sulfide in 1998 were below detection limit of 0.06 mg/L for all of the multi-samplers (MLS10, MLS11, MLS12, MLS13, MLS14, MLS15, and MLS20) (See Figure 3.3 for locations of MLS). In 1999, the levels of sulfide were between 0.08-0.20 mg/L as shown in Figure 3.23 and 3.24. In 2000, sulfide was measured by Virginia Tech with the Hach Module 61.01. This method produced a detection limit of 0.01 mg/L. The levels of sulfide were between 0.01-0.04 mg/L for MLS11, MLS12, and MLS22. MLS20 showed a concentration of 0.15 mg/L at a depth of 10 ft bgs while ports 1-5 had levels between 0.01-0.04 mg/L.

Methane

Methane was detected in 1998 and 1999. In 1998, the lowest levels of methane were at a depth of 15-17 ft bgs with a concentration of 0.001 mg/L as shown in Figures 3.25 and 3.26. The highest levels (0.01 - 0.1 mg/L) of methane were at a depth of 19-21 ft bgs, while at a depth of 7-13 ft bgs concentrations were between 0.001 mg/L and 0.01 mg/L. However, the upper portion of the aquifer at MLS12 exhibited higher concentrations of methane (0.01 to 0.1 mg/L). In 1999, the methane concentrations exhibited no discernible trends across the aquifer.

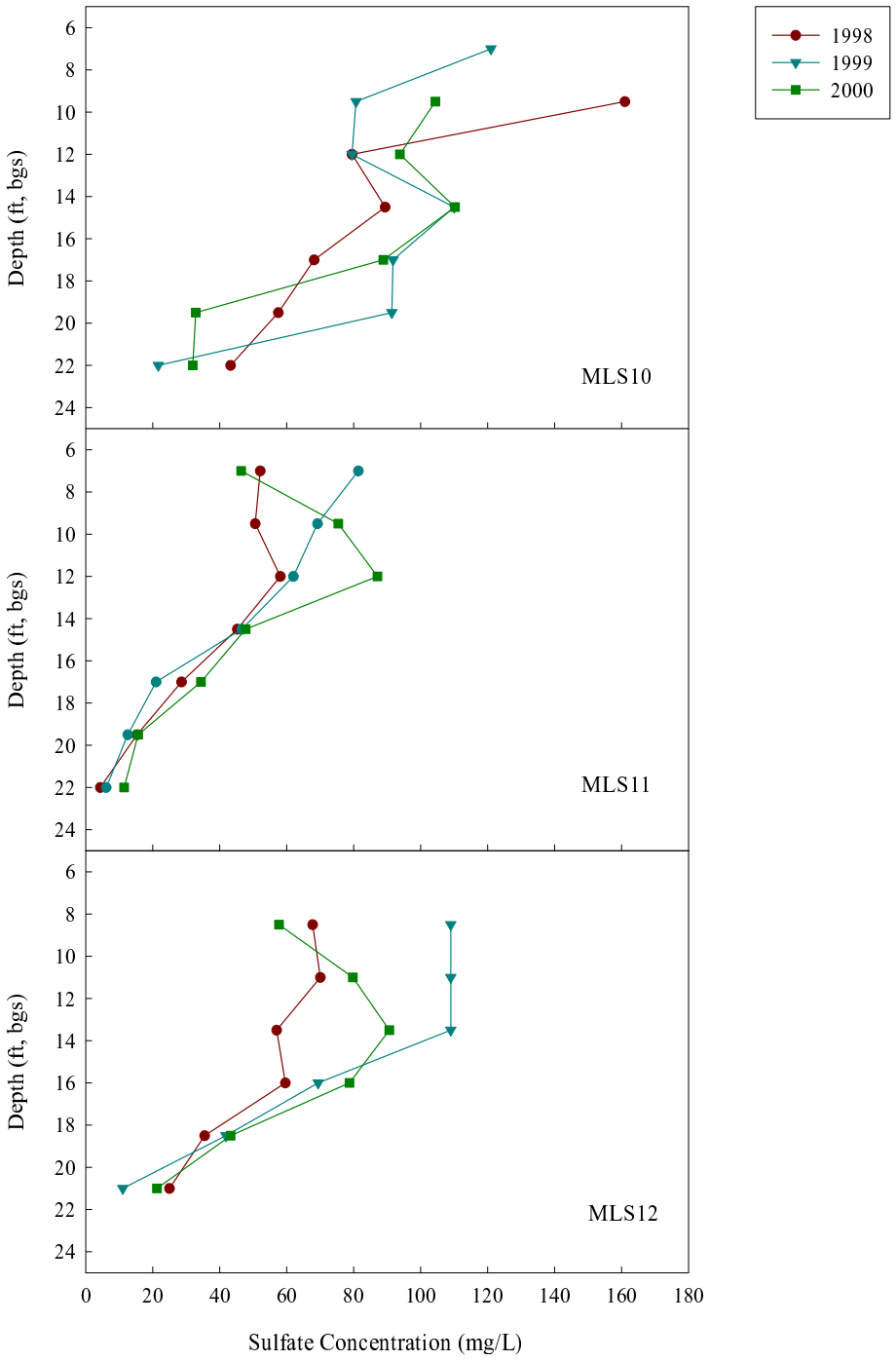

Figure 3.14: The groundwater concentrations of sulfate for the 1998, 1999, and 2000 sampling rounds at MLS10, MLS11 and MLS12.

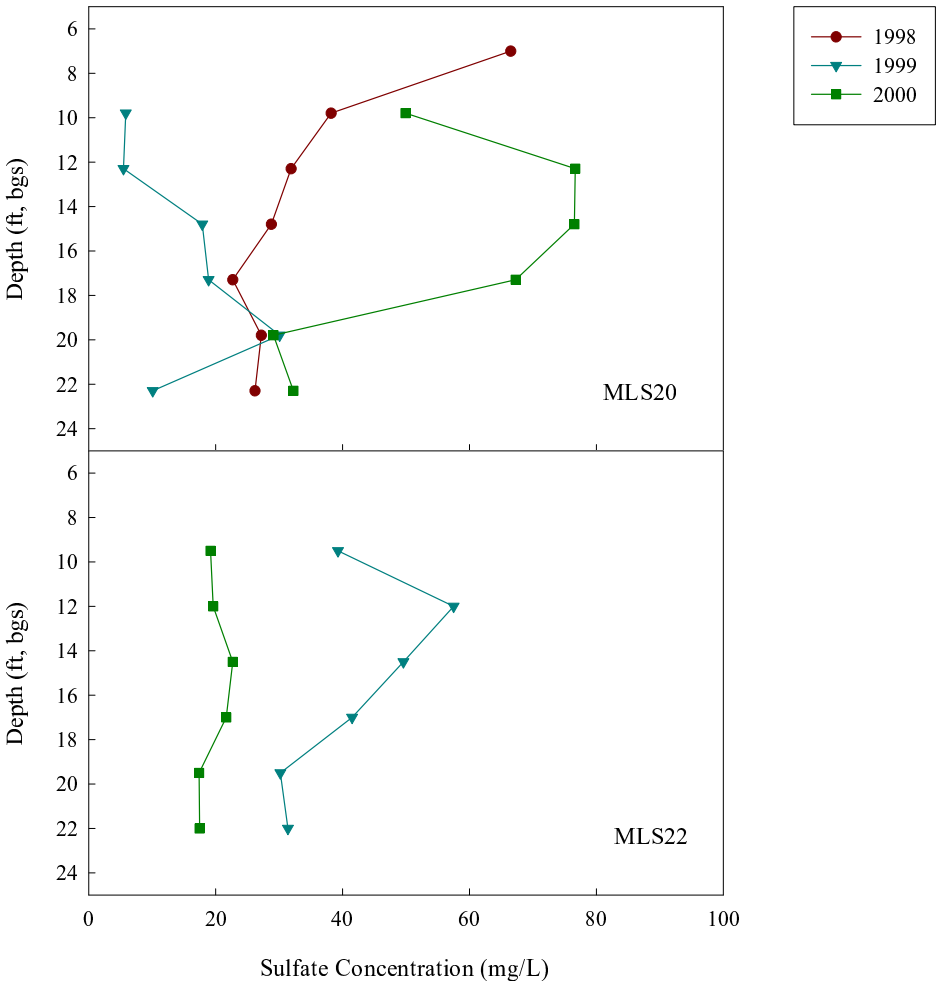

Figure 3.15: The groundwater concentrations of sulfate for the 1998, 1999, and 2000 sampling rounds at MLS20 and MLS22.

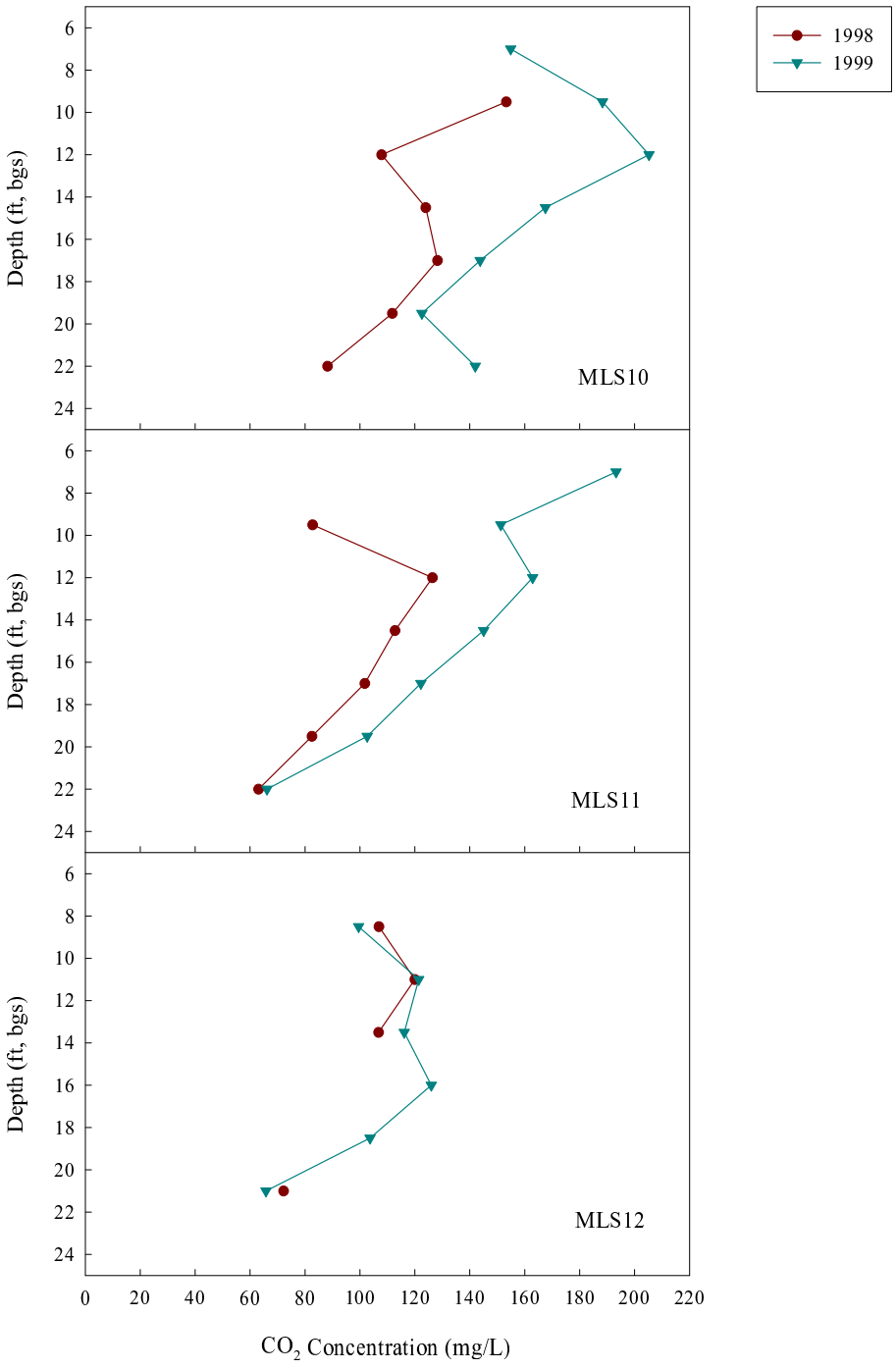

Figure 3.16: The groundwater concentrations of CO_2 for the 1998 and 1999 sampling rounds at MLS10, MLS11, and MLS12.

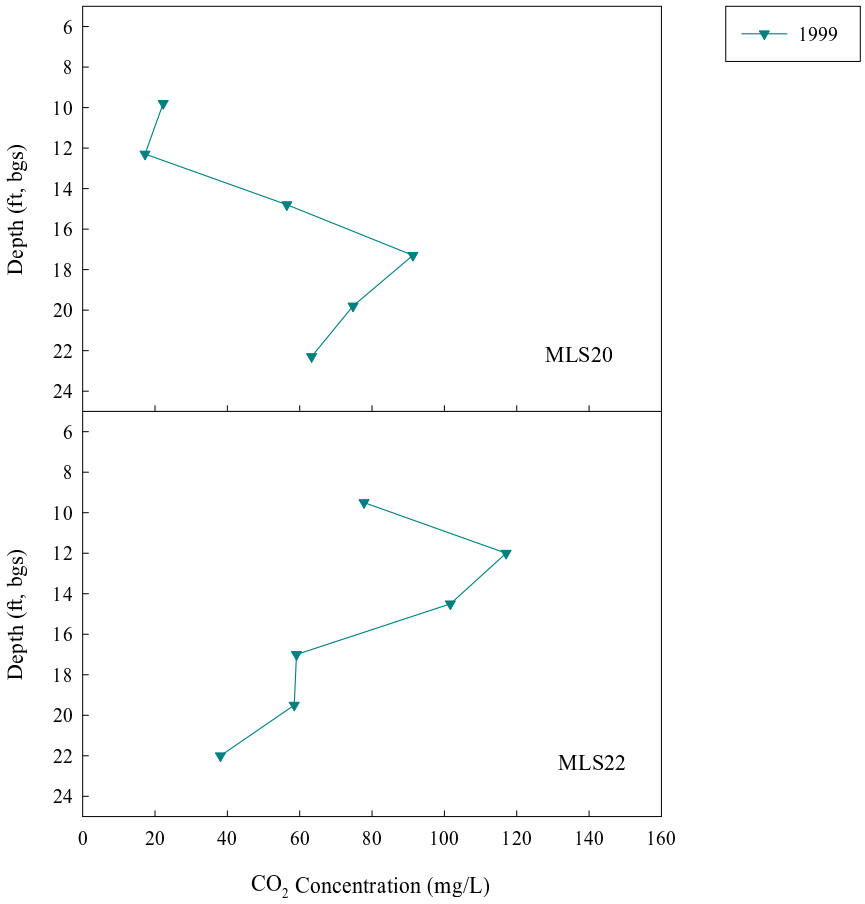

Figure 3.17: The groundwater concentrations of CO_2 for the 1999 sampling rounds at MLS20 and MLS22.

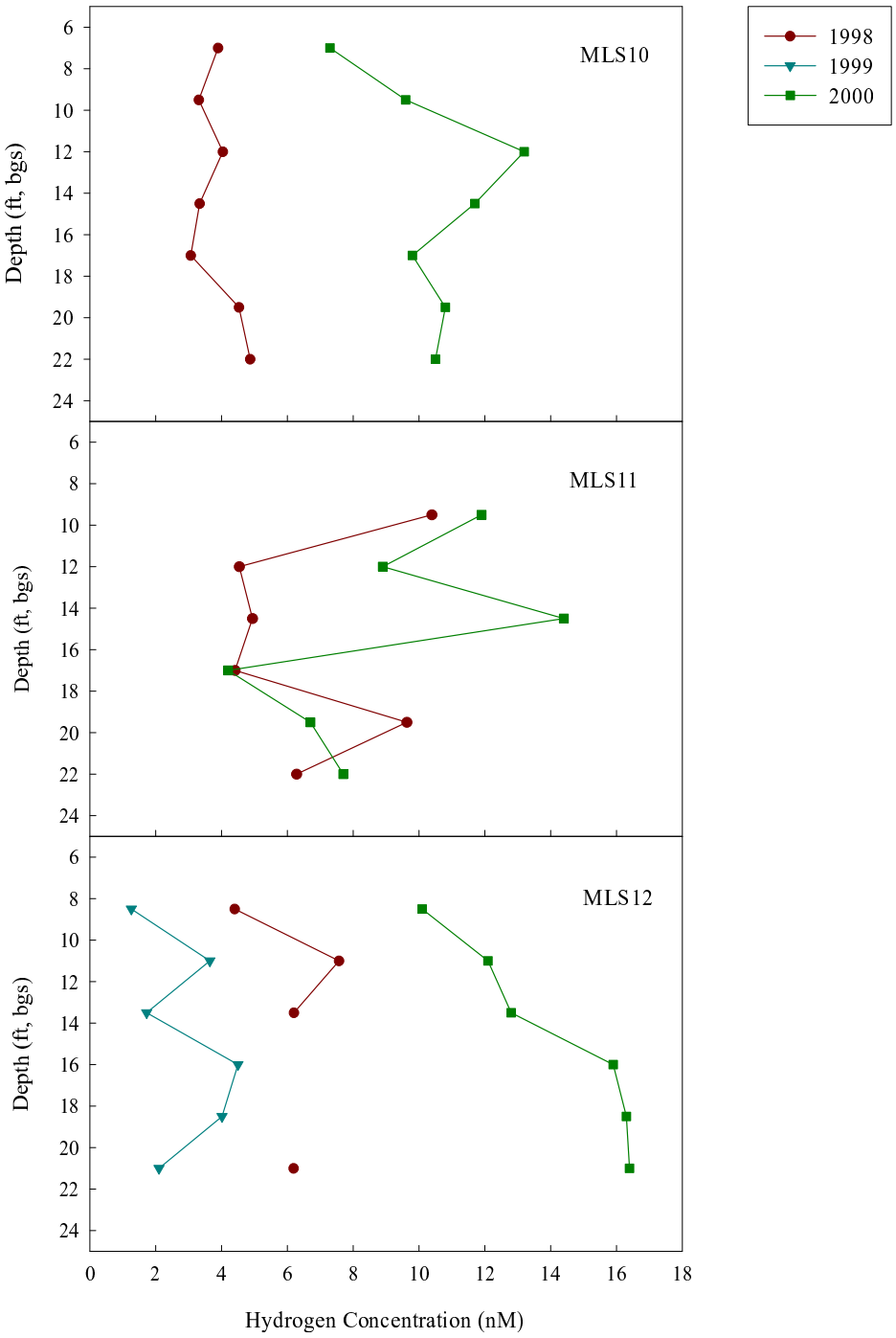

Figure 3.18: The groundwater concentrations of H_2 for the 1998, 1999, and 2000 sampling rounds at MLS10, MLS11, and MLS12.

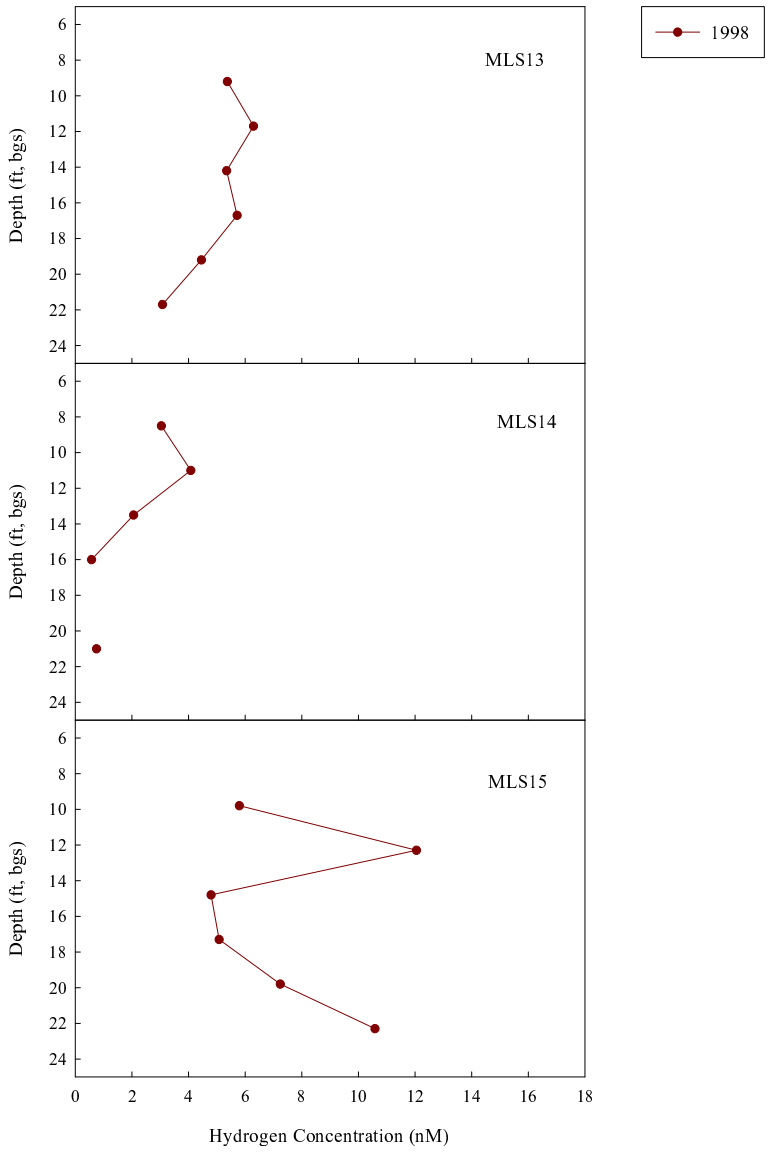

Figure 3.19: The groundwater concentrations of H_2 for the 1998 sampling round at MLS13, MLS14, and MLS15.

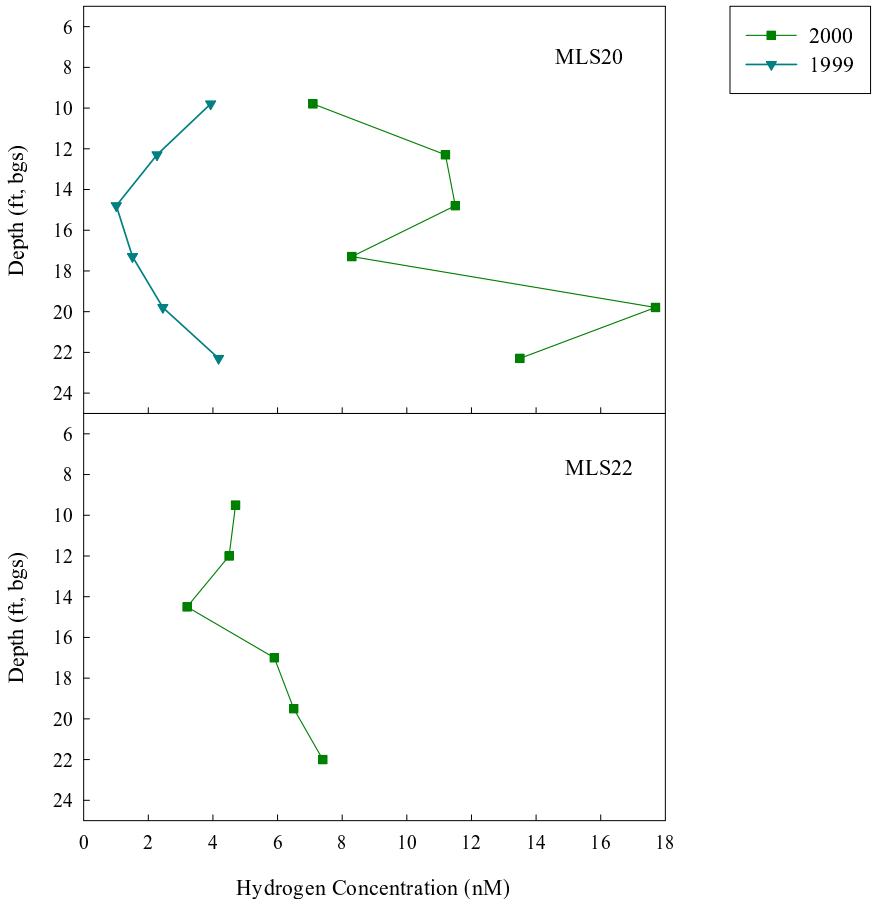

Figure 3.20: The groundwater concentrations of H_2 for the 1999 and 2000 sampling rounds at MLS20 and MLS22.

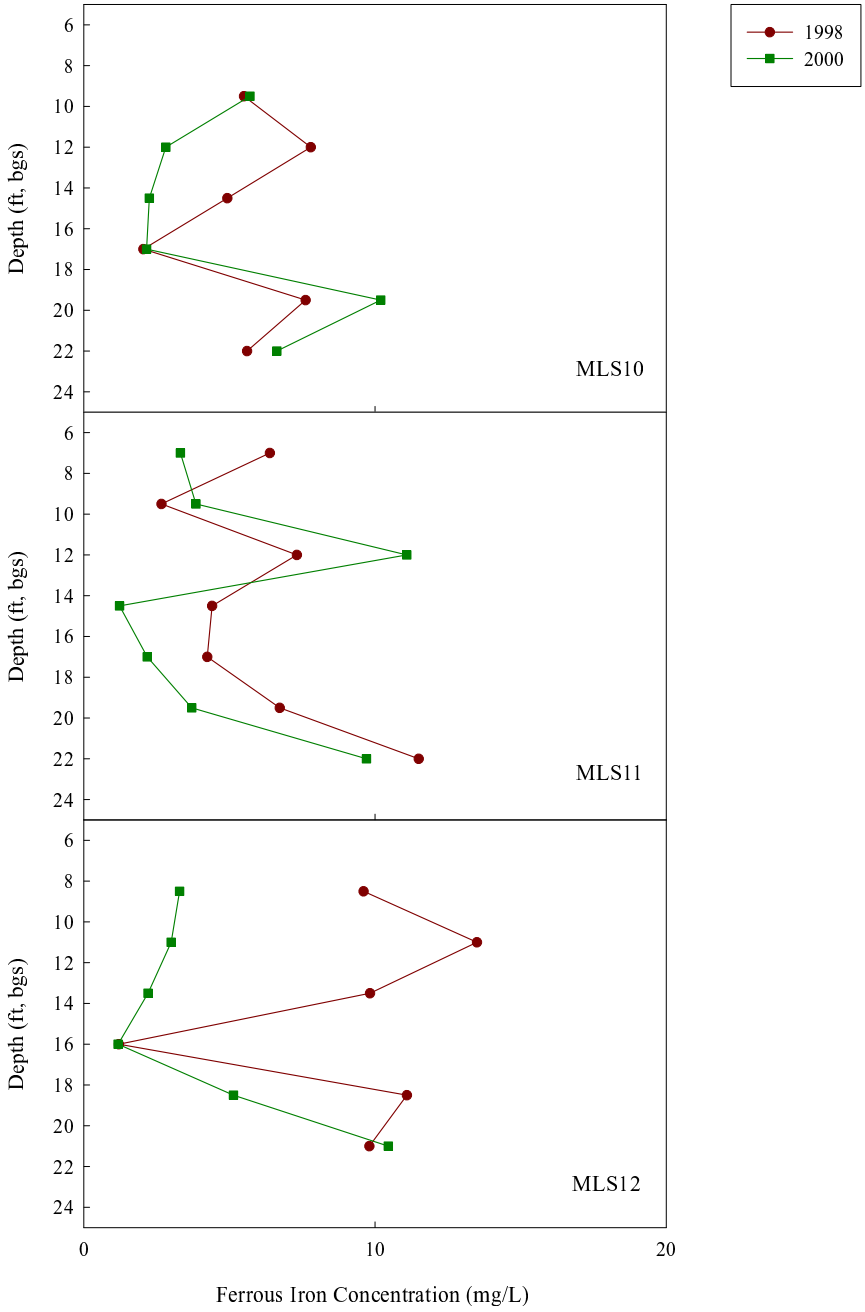

Figure 3.21: The groundwater concentrations of ferrous iron for the 1998, and 2000 sampling rounds at MLS10, MLS11, and MLS12.

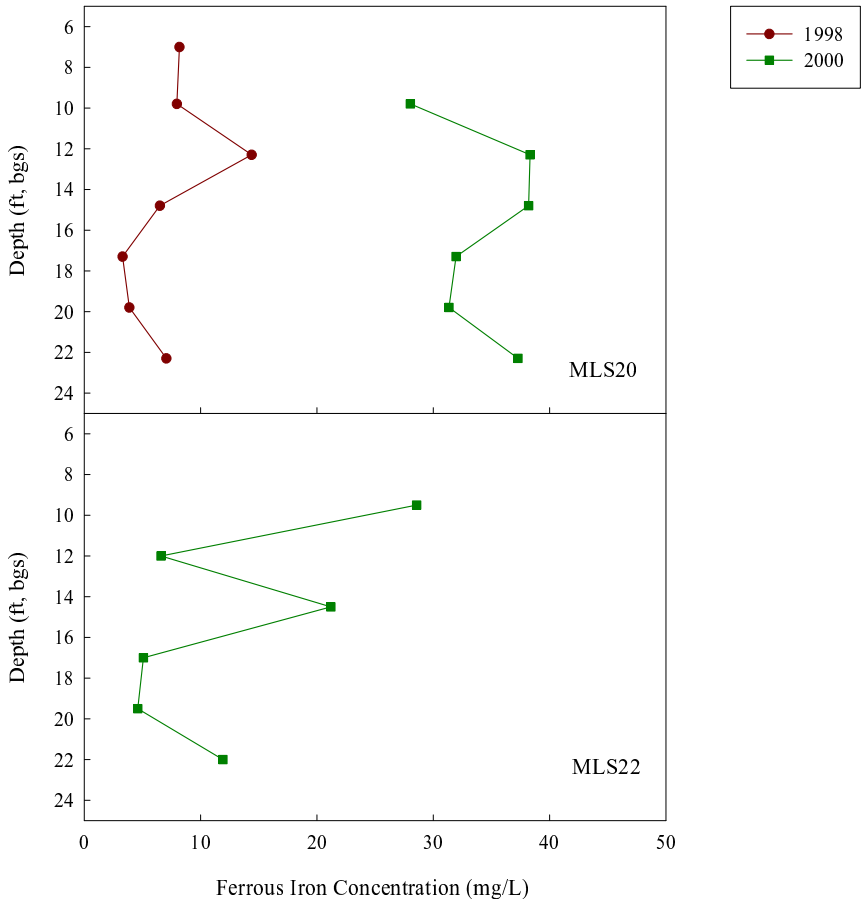

Figure 3.22: The groundwater concentrations of ferrous iron for the 1998 and 2000 sampling rounds at MLS20 and MLS22.

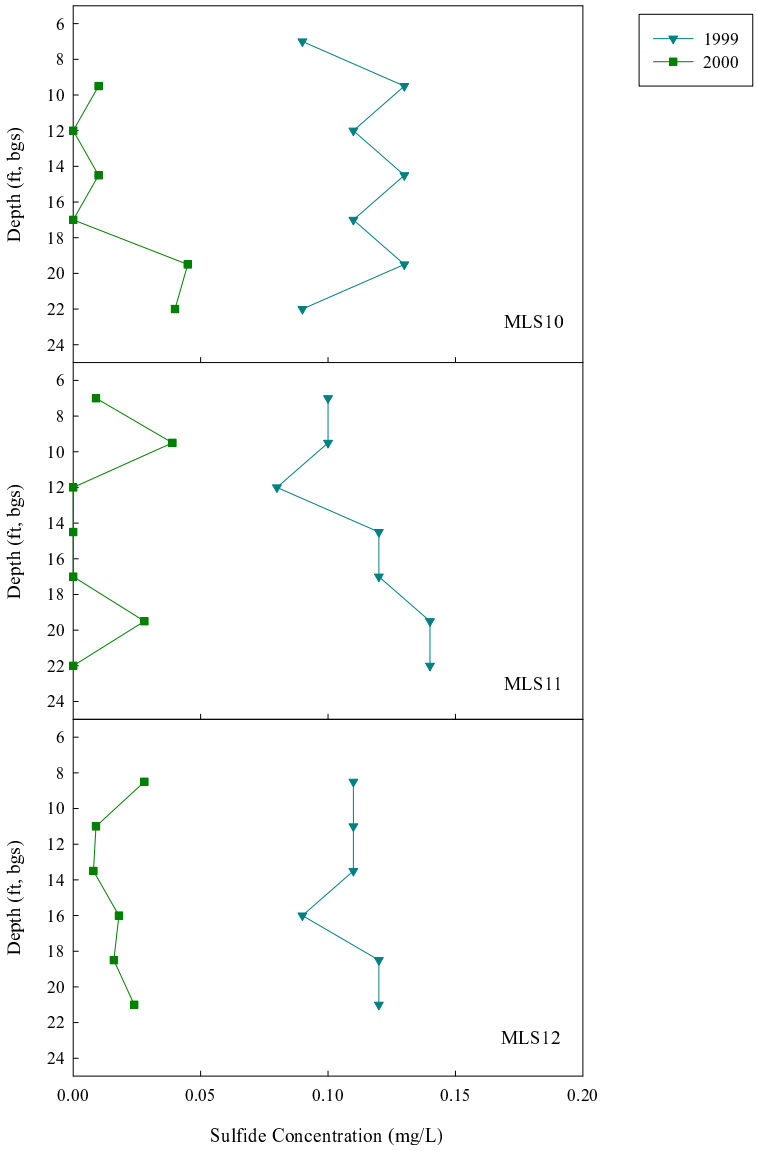

Figure 3.23: The groundwater concentrations of sulfide for the 1999 and 2000 sampling rounds at MLS10, MLS11, and MLS12.

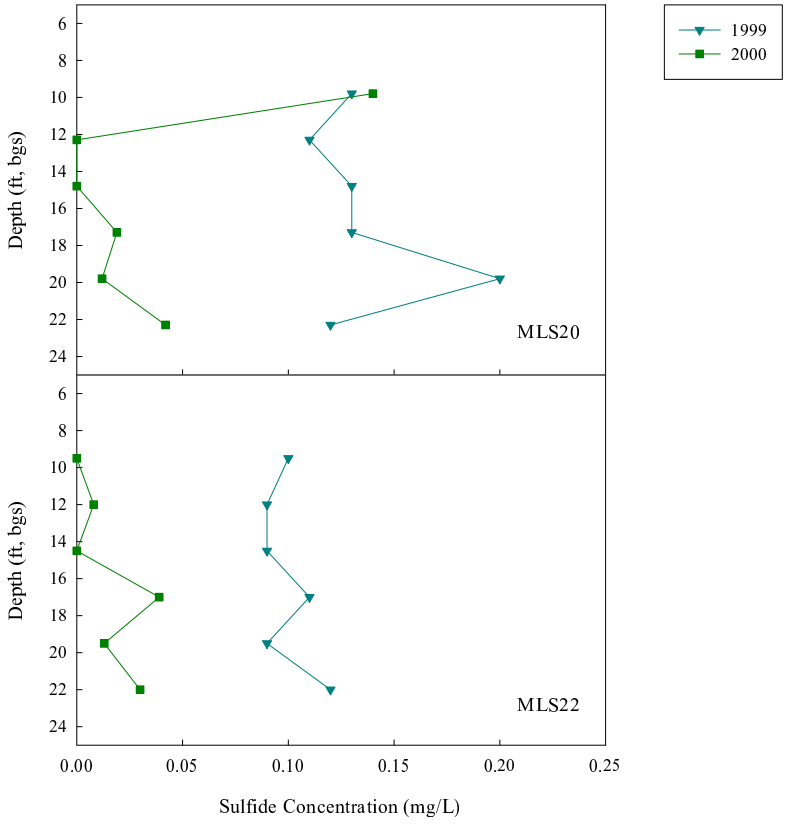

Figure 3.24: The groundwater concentrations of sulfide for the 1999 and 2000 sampling rounds at MLS20 and MLS22.

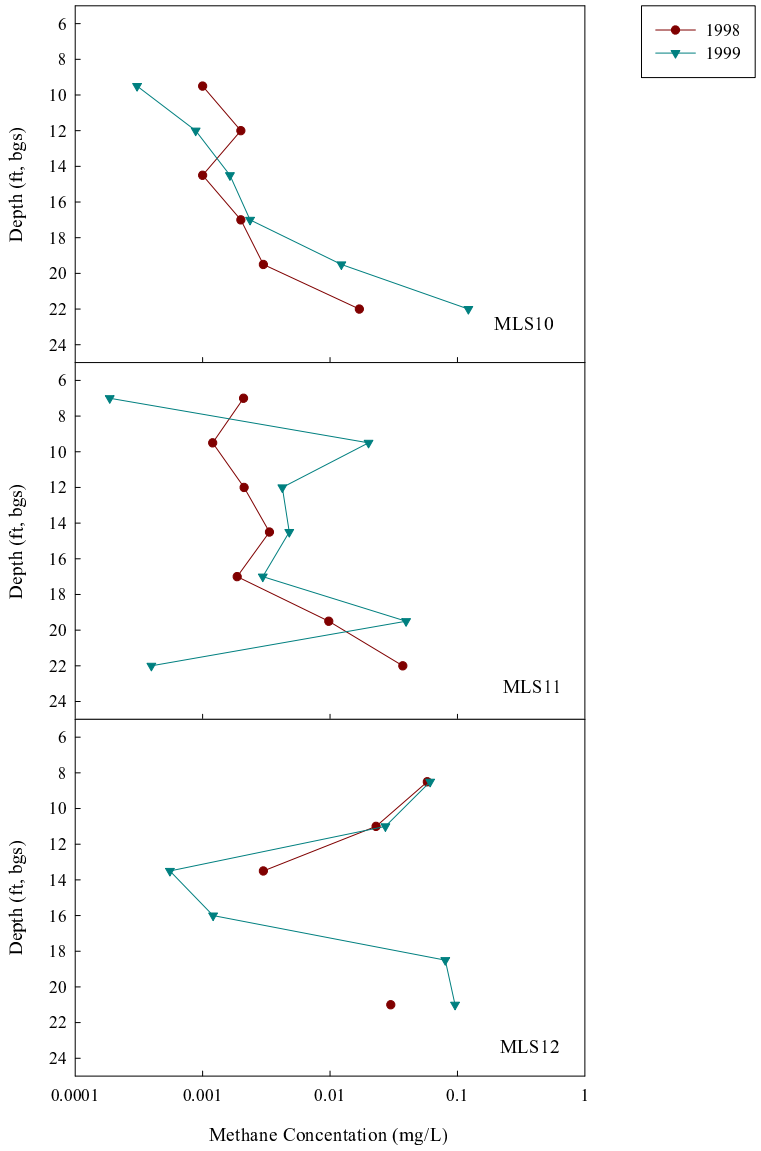

Figure 3.25: The groundwater concentrations of methane for the 1998 and 1999 sampling rounds at MLS10, MLS11, and MLS12.

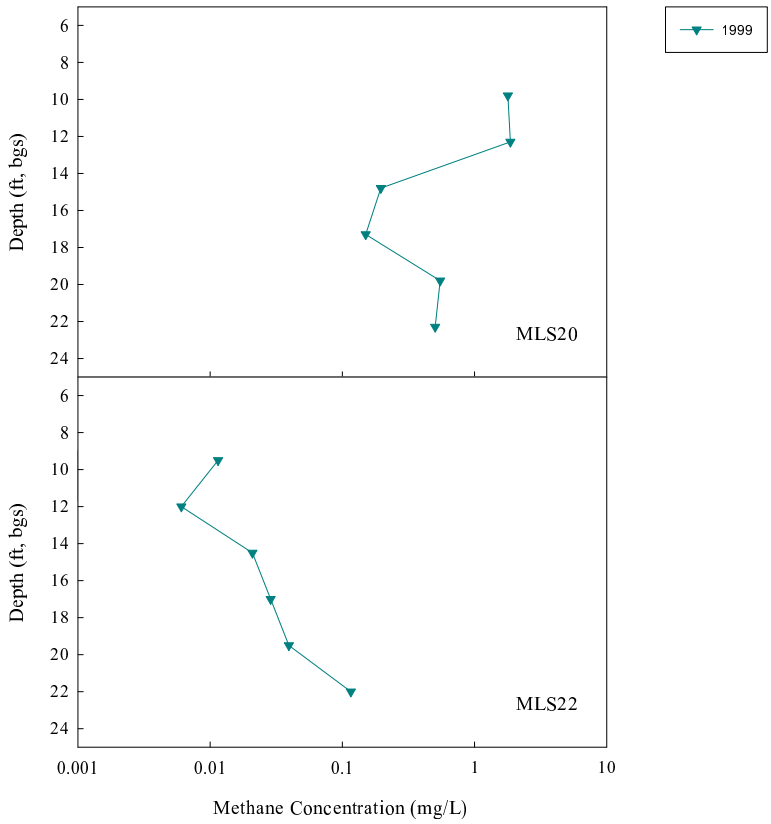

Figure 3.26: The groundwater concentrations of methane for the 1999 sampling rounds at MLS20 and MLS22.

Chapter 4

Experimental Microcosm Design

4.1 Introduction

Microcosm experiments are listed as the third line of evidence for assessing the capabilities of a site to use MNA as part of a viable remediation strategy (EPA., 1998). Groundwater analysis detected the presence of the daughter products of PCE. Therefore, a microcosm study was undertaken in 1998 to demonstrate the ability of aquifer sediment to degrade PCE and its daughter products. Initially, microcosms were constructed using 7 g of aquifer sediment and 10 mL of groundwater containing 25 μM of a specified chlorinated ethene (For a complete description of microcosms, see Widdowson et al., 2000). Microcosms were sacrificed in triplicate for analysis every six weeks. Results from this initial study suggested that the sacrificial interval, 6 weeks, was too long to obtain rate data for TCE. Nevertheless, the results established the presence of microbes capable of partial PCE degradation at MLS12-Shallow. Furthermore, one set of the microcosms was only exposed to *cis*-1,2-DCE and VC and did not exhibit degradation of the chlorinated ethenes. The ability of these microcosms to degrade PCE could not be assessed since PCE was not added. Therefore, a second microcosm study was designed to evaluate the extent of microbial degradation of the chlorinated ethenes at NAB Little Creek Site 12 and to provide concentration versus time data to estimate the associated biodegradation rates of the chlorinated ethenes.

The new microcosm design called for an increase in the sampling interval of the microcosms. The new sampling interval should accurately follow the sequential degradation of PCE through TCE to *cis*-1,2-DCE. A weekly sampling interval was chosen based on availability of the analytical

equipment and the rough degradation estimate provided by the 1998 microcosm data. Furthermore, the prospect of no TCE detection, as in the 1998 microcosm study, dictated the construction of a second set of microcosms to be amended with TCE. This second set of microcosms insured the measurement of a TCE degradation rate. The additional microcosm set and the increased sampling interval dramatically expanded the required number of sacrificial microcosms to be constructed for the 1999 microcosm experiment. Therefore, a non-sacrificial type or continuous microcosm design was selected to accommodate weekly sampling from the same microcosm.

4.2 Chlorinated Ethene Properties

The chlorinated ethenes belong to the alkene class of organic compounds which is designated by a carbon-carbon double bond. The structures of the chlorinated ethenes are shown in Figure 4.1. The pertinent chemical and physical properties of the chlorinated ethenes are listed in Table 4.2.1.

Table 4.1: Chemical and Physical Properties of the Chlorinated Ethenes

Compound	MW	Specific Gravity	Water Solubility	Vapor Pressure	log Koc
PCE	165.83 (g/mol)	1.62	150 (mg/L)	14 (mm Hg)	2.82 (mg/L)
TCE	131.39 (g/mol)	1.46	1100 (mg/L)	57.8 (mm Hg)	2.1 (mg/L)
cis-1,2-DCE	96.92 (g/mol)	1.28	3500 (mg/L)	200 (mm Hg)	1.86 (mg/L)
VC	62.5 (g/mol)	0.91	1100 (mg/L)	2580 (mm Hg)	0.91 (mg/L)

Table adapted from CH2MHill, 2000.

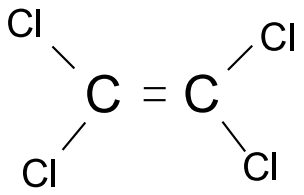

Tetrachloroethene

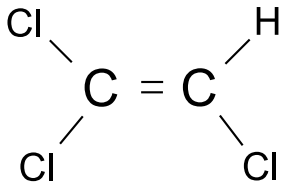

Trichloroethene

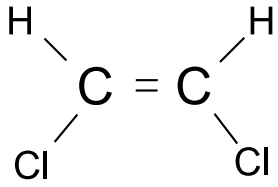

Dichloroethene

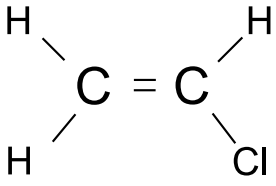

Monochloroethene

Figure 4.1: The molecular structures of PCE, TCE, *cis*-1,2-DCE and VC.

4.3 Aquifer Sediment Sample Collection

The three sample locations for June 1999 were selected based on the results of 1998 microcosm experiments and groundwater analysis. First, aquifer sediment for new microcosm construction was collected from an established active microbial location (MLS12-Shallow) and an uncontaminated area (SB 204) as shown in Figure 3.3. Secondly, a potential source area (SB 201) located between MLS10 and MLS11 was sampled for the presence of contamination. Finally, the installation of a new multi-level sample (MLS22) provided the opportunity to evaluate the degradation properties of the aquifer sediment adjacent to the leaky sewer line.

Aquifer sediment was collected from NAB Little Creek Site 12 using a traditional split-spoon drill assembly. The sample collection procedure began with a two step decontamination process of the split spoon sampler. First, the sampler was scrubbed using methanol. This step removed attached aquifer sediment and free product from the sampler. After the sampler was throughly scrubbed, the sampler was rinsed with distilled water. The acetate liners were sterilized by soaking them in a 10 ppm chlorine solution for 10 minutes and rinsing with autoclaved distilled water. The sterilized acetate liners reduced the potential to introduce exogenous microorganisms to the collected aquifer sediment samples. The sterile acetate liner was inserted into the decontaminated spit spoon sampler, and the system was driven then into the aquifer to the appropriate depth. After the liner was retrieved, the ends were immediately capped. If a portion of the liner was empty, the liner was cut to minimize exposure to the aerobic ambient environment before capping the liner. The liner containing aquifer sediment was weighed, labeled and placed in a glove bag under a nitrogen environment. The glove bag was stored in a cooler with frozen ice-packs. All soils were transported to the Environmental Engineering Laboratory at Virginia Tech, in Blacksburg, VA and stored at 5 ^{o}C . The microcosms were constructed within 2 weeks of sample collection.

4.4 Continuous Microcosm Construction

Aquifer sediment samples were collected from MLS12-Shallow, MLS22-Shallow and MLS22-Deep for construction continuous microcosms. Duplicate sets of microcosms were constructed for each well location. Each continuous microcosm contained 150 g wt/w of aquifer sediment, approximately

200 mL of MLS12-Shallow groundwater, and 30 μM of a specified chlorinated ethene (Table 4.2). These larger, continuous microcosms were constructed in 300 mL Erlenmeyer flasks that were retrofitted by a glass blower to house a Mininert^{TM} valve. Figure 4.2 provides a schematic that represents the retrofitted Erlenmeyer flasks.

The microcosms were prepared under anaerobic conditions using a disposable glove bag. The step by step procedure for microcosm construction was as follows:

- Autoclave groundwater (15 minutes 121 ^{o}C) and place under nitrogen gas while cooling
- Add 5000 mg/L stock solution of $Na_2S\bullet$ $9H_20$ x for 10 ppm of S^{-2} to groundwater
- Place all required items in glove bag
- Evacuate air from glove bag using vacuum pump and replenish with nitrogen that was scrubbed by a Hungate apparatus
- Remove caps from acetate liners and waste first inch of aquifer sediment on either end
- Homogenize aquifer sediment
- Purge flask for one minute with nitrogen
- Add 150 g wt/w of aquifer sediment into flask
- Purge flask for 2 minutes with nitrogen
- Fill flask with groundwater
- Inject appropriate amount of chlorinated ethene into flask
- Immediately cap with Mininert valve tops
- Place inverted and covered at 20 ^{o}C under nitrogen until sampled

The controls were prepared in a similar manner to the live microcosms. However, autoclaved aquifer sediment (5 cycles for 30 minutes at 121 ^{o}C) and groundwater (15 minutes at 121 ^{o}C) were used.

Table 4.2: Microcosm Experimental Setup Matrix

MLS Sampling Location	Chlorinated Ethene	Sample Depth (ft, bgs)
MLS12-Shallow	PCE	8-12
MLS12-Shallow	TCE	8-12
MLS22-Shallow	PCE	8-12
MLS22-Shallow	TCE	8-12
MLS22-Deep	PCE	18-22
MLS22-Deep	TCE	18-22

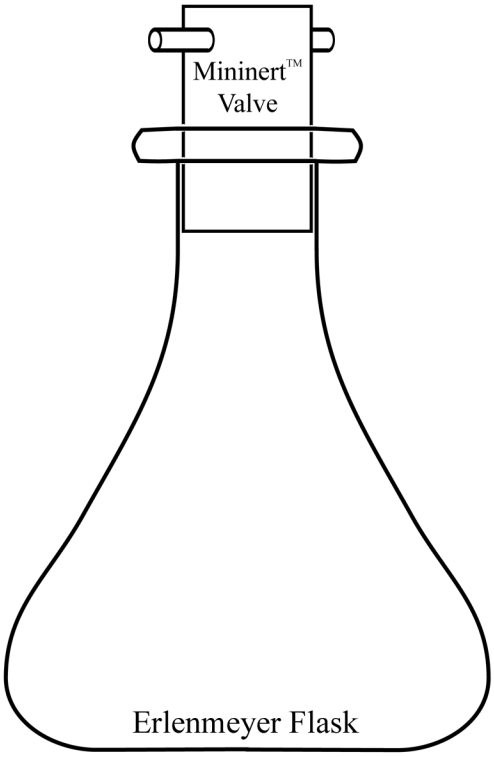

Figure 4.2: Retrofitted microcosm flask

4.5 Continuous Microcosm Sampling Method

At each sampling round, the microcosms were sampled for hydrocarbon gases and aqueous chlorinated ethenes. To sample the hydrocarbon gases, 100 μL of the headspace was removed from the microcosms. The headspace gases were analyzed with the method described in 4.6.1. After the headspace gases were sampled, the aqueous phase of the chlorinated ethenes was analyzed. First, the microcosms had 0.5 mL and 1 mL of the groundwater removed via a syringe under a nitrogen environment (glove bag). While the samples were first attempted to be removed with the microcosm inverted, aquifer sediment clogged the valve over time; so samples were removed with the microcosm in an upright position. Then, the 0.5 mL and 1 mL aqueous samples were injected into the purge and trap unit per analytical method in 4.6.2. Finally, 4.5 mL and 4 mL of distilled water was injected into the purge unit for a total volume of 5 mL. Therefore, the resultant chlorinated ethene concentration for each microcosm was an average of two different dilutions. Between samples, the syringes were rinsed with methanol once and distilled water three times. The multiple rinses eliminated cross contamination between samples by removing trace quantities of the chlorinated ethenes from the syringe.

4.6 Analytical Methods

4.6.1 Gases

Hydrocarbon Gases The hydrocarbon gases measurable by this method included methane, ethene, and ethane. The gases were measured using a HP 5890A flame ionization detector (Hewlett Packard, Wilmington, DE) equipped with a Carbosieve S-III Carbon Molecular Sieve (Supelco, Bellefonte, PA) packed column. The detection method started at an initial temperature of 125 ^{o}C with no initial holding time. The first temperature program increased at a rate of 25 ^{o}C/minute with a final temperature of 175 ^{o}C and no holding time. Then, the second level rose at a rate of 10 ^{o}C/minute with a final temperature of 200 ^{o}C which was held for 10 minutes. The detector and injection temperatures were 225 ^{o}C and 175 ^{o}C, respectively. The carrier gas (nitrogen) flowed at 30 mL/minute with hydrogen and air gas for the FID at 30 mL/minute and 300 mL/minute, respectively. The gases were compared to a Scotty II gas mix standard with the hydrocarbon

gases at a concentration of 1% by mole. The retention times for the compounds were 2.07 minutes for methane, 7.89 minutes for ethene, and 10.54 minutes for ethane. The detection limits for hydrocarbon gases were 10 μL/L.

Hydrogen Hydrogen was measured using the bubble-sampling method developed by Chapelle, et al. (1995). In the field, the gas sampling tube was first filled with approximately 225 mL of groundwater to create a gas bubble with roughly a 25 mL volume. With a groundwater flow rate of 150 mL/minute, the dissolved gases in the groundwater reached equilibrium with the 25 mL bubble in 20 minutes. Then, a 10 mL gas sample was taken from the bubble with a gas tight glass syringe. The gas sample was analyzed using a reduced gas detector (RGD, Trace Analytical, Menlo Park, CA) with a detection limit of 0.05 μL/L. Samples were analyzed within 15 minutes of collection.

4.6.2 Chlorinated Ethenes

The chlorinated ethene concentrations were measured using a purge and trap assembly that fed into a GC using a Hall detector. The purge and trap system used a 16 port Tekmar autosampler Model 2016 which was attached to a Tekmar 3000 Purge and Trap Concentrator (Tekmar Co., Cincinnati, OH). After a 5 mL aqueous sample was injected into the purge unit, the sample was purged with Helium for 11 minutes. The volatile compounds were condensed onto a Tenex/silica gel/charcoal trap (Tekmar trap No 3). After the completion of the purge cycle, the trap was heated to 225 ^{o}C. When the 10 minute trap bake cycle started at 225 ^{o}C, the Helium carrier gas (flow rate 25 mL/minute) brought the chlorinated ethenes to a Tremetrics 9001 GC (Tremetrics Inc., Austin, TX) equipped with a RTX-Volatiles megabore capillary column (Restek, Bellefonte, CA) and a Tracor 1000 Hall detector (Tracor Instruments, Austin, TX). A ramped temperature program was used to aid in separating the chlorinated ethenes. The temperature program started at an initial temperature of 35 ^{o}C which was held for 5 minutes. The first level rose at a rate of 6 ^{o}C/minute to a temperature of 95 ^{o}C with no holding time. The second level rose at a rate of 25 ^{o}C/minute to a final temperature of 225 ^{o}C with no holding time. The Hall detector operated at 842 ^{o}C with a hydrogen gas flow of 25 mL/minute. The retention times for the chlorinated ethenes were 2.2 minutes for VC, 3.2 minutes for *trans*-1,2-DCE, 4.9 minutes for *cis*-1,2-DCE, 8 minutes for TCE, and 12 minutes for PCE. The detection limit for the chlorinated ethenes was 1 μg/L.

Chapter 5

Microcosm Model

The continuous microcosms were modeled using the groundwater flow model MODFLOW and contaminant fate model SEAM3D (Sequential Electron Acceptor Model, 3 Dimensional) to estimate the biodegradation rates of PCE and its daughter products. MODFLOW simulates a variety of aquifer conditions through a cell centered, finite difference approach. SEAM3D also utilizes the cell centered, finite difference approach to simulate contaminant fate and transport. In the microcosm model, MODFLOW was used to produce the hydraulic head distribution file to describe the microcosm's head distribution. SEAM3D used the head file generated by MODFLOW as an input file, since SEAM3D does not calculate the hydraulic head distribution for a specified aquifer condition.

A single layer finite difference grid consisting of four rows and four columns was constructed to simulate the microcosm configuration. Each cell was 1 m by 1 m with a cell thickness of 10 m. The saturated, static groundwater conditions of the microcosms were simulated using MODFLOW by applying no flow boundary conditions to the edges of the model grid. These boundary conditions produced a uniform piezometric surface across the model. The unformatted head and flow file generated by the MODFLOW simulation provided the hydraulic head distribution required as input for the contaminant fate model. The fate of the chlorinated ethenes were modeled by SEAM3D. The concentration versus times results of the microcosms were used in calibrating the biodegradation rates of the chlorinated ethenes generated by SEAM3D.

5.1 Conceptual Model

The microcosm model was simulated with a uniform distribution of the chlorinated ethene concentrations throughout all model cells. Static groundwater flow conditions removed the effect of advection on the contaminant fate. Initial concentrations were assigned for the chlorinated ethene throughout the model grid which eliminated concentration gradients between adjacent cells. This removed the effect of dispersion on contaminant fate. Based on desorption experiments (Widdowson et al., 2000) and the continuous microcosm experiments, the effects of desorption were negligible compared to the amended concentrations of the chlorinated ethenes. Consequently, sorption was not included in the microcosm model. Therefore, biodegradation via reductive dechlorination became was the only mechanism responsible for the reduction of the chlorinated ethene concentrations over time.

The reductive dechlorination package (beta v 2.0) of SEAM3D was used to model the degradation of the chlorinated ethenes occurring the microcosm experiments. The reductive dechlorination package uses Monod kinetics as it considers aspects of the reductive dechlorination process including the stoichiometric conversion of PCE to ethene and the anaerobic oxidation of DCE and VC to CO_2. Given the design of the microcosms, CO_2 production by the dechlorinating microorganisms was not quantifiable. Therefore, the anaerobic oxidation option was omitted in the microcosm model. Another aspect of SEAM3D not incorporated in the microcosm model was growth kinetics of the PCE and TCE degrading microorganism population since the initial lag period in the microcosms was not explicitly modeled. Therefore, the biomass of the PCE and TCE degrading microorganism population was considered to be in steady state. The microcosm model was run over a period of 200 days at a 0.5 day time step with the explicit finite difference solution technique.

5.2 Mathematical Model

5.2.1 Reductive Dechlorination Equations

SEAM3D models the reductive dechlorination process as a series of inter-related microbial sink reactions where the rate of reactions can be generally expressed as

$$\frac{dC}{dt} = -R^{bio} \tag{5.1}$$

where C is the concentration [M_s L^{-3}], t is the time [T], and -R^{bio} is represented by Monod kinetics such that

$$\frac{dC}{dt} = -R^{bio} = -\frac{M}{\Theta}\nu^{max}\left[\frac{C}{K+C}\right] \tag{5.2}$$

where ν_{max} is the maximum specific utilization rate [M_s $M_b{}^{-1}$ T^{-1}], M is the biomass [M_b], Θ is the effective porosity, and K is the half saturation coefficient [M_s L^{-3}].

The first rate of reaction in the reductive dechlorination process begins with PCE degradation such that

$$\frac{dC_{PCE}}{dt} = -R^{bio}_{PCE} = -\frac{M_1}{\Theta}\nu_{PCE} = -\frac{M_1}{\Theta}\nu^{max}_{PCE}\left[\frac{C_{PCE}}{C_{PCE}+K_{PCE}}\right] \tag{5.3}$$

where C_{PCE} is the concentration of PCE, $M_1$is the microbial population of PCE and TCE degraders, ν_{PCE} is the rate of reaction for PCE, ν^{max}_{PCE} is the maximum specific utilization rate for PCE, and K_{PCE} is the half saturation coefficient for PCE.

TCE degradation is modeled in a similar manner to PCE degradation. However, the basic microbial sink expression not only incorporates TCE degradation but also includes TCE production via PCE degradation such that

$$\frac{dC_{TCE}}{dt} = -R^{bio}_{TCE} + \xi_{PCE}R^{bio}_{PCE} \tag{5.4}$$

where R^{bio}_{TCE} is the rate of TCE degradation, ξ_{PCE} is the production coefficient of TCE generated by PCE degradation based on the stoichiometry of the reductive of PCE to TCE [M_{TCE}/M_{PCE}],

and R^{bio}_{PCE} is the rate of PCE degradation. The TCE biodegradation rate also includes an inhibition function where high levels of PCE can effectively shut down TCE degradation.

$$\frac{dC_{TCE}}{dt} = -\frac{M_1}{\Theta}\nu_{TCE} = -\frac{M_1}{\Theta}\nu^{max}_{TCE}\left[\frac{C_{TCE}}{K_{TCE}+C_{TCE}}\right]\left[\frac{K_{PCE/TCE}}{K_{PCE/TCE}+C_{PCE}}\right] + \xi_{PCE}R^{bio}_{PCE} \tag{5.5}$$

where C_{TCE} is the concentration of TCE, ν_{TCE} is the rate of reaction for TCE, ν^{max}_{TCE} is the maximum specific utilization rate for TCE, K_{TCE} is the half saturation coefficient for TCE, and $K_{PCE/TCE}$ is the coefficient of TCE inhibition by PCE.

In the reductive dechlorination package of SEAM3D, two sets of microbial populations are modeled. The first set incorporates the PCE and TCE degrading microorganisms, while the second set incorporates the *cis*-1,2-DCE and VC degrading microorganisms. The microbial population for the PCE and TCE degraders can be further developed as

$$\frac{1}{M_1}\frac{dM_1}{dt} = Y_{PCE}\nu_{PCE} + Y_{TCE}\nu_{TCE} - k_{d_1} \tag{5.6}$$

where Y_{PCE} is the yield coefficient for PCE [$M_b\ {M_{PCE}}^{-1}$], ν_{PCE} is the rate of reaction for PCE [$M_{PCE}\ {M_b}^{-1}\ T^{-1}$], Y_{TCE} is the yield coefficient for TCE [$M_b\ {M_{TCE}}^{-1}$], ν_{TCE} is the rate of reaction for TCE [$M_{TCE}\ {M_b}^{-1}\ Y^{-1}$], and k_{d_1} is the decay coefficient for the microbial population of PCE and TCE degraders [T^{-1}]. The microbial population for the *cis*-1,2-DCE (referred to as DCE within the formulae) and VC degraders can also be expressed as

$$\frac{1}{M_2}\frac{dM_2}{dt} = Y_{DCE}\nu_{DCE} + Y_{VC}\nu_{VC} - k_{d_2} \tag{5.7}$$

where Y_{DCE} is the yield coefficient for DCE [$M_b\ {M_{DCE}}^{-1}$], ν_{DCE} is the rate of reaction for DCE reductive dechlorination [$M_{DCE}\ {M_b}^{-1}\ T^{-1}$], Y_{VC} is the yield coefficient for VC [$M_b\ {M_{VC}}^{-1}$], ν_{VC} is the rate of reaction for VC reductive dechlorination [$M_{VC}\ {M_b}^{-1}\ T^{-1}$], and k_{d_2} is the decay coefficient for the microbial population of DCE and VC dechlorinators [T^{-1}].

The general expression for DCE degradation adds another microbial sink term to account for anaerobic oxidation of DCE to CO_2 as follows

$$\frac{dC_{DCE}}{dt} = -R^{bio}_{DCE,RD} - R^{bio}_{DCE,DO} + \xi_{TCE}R^{bio}_{TCE} \tag{5.8}$$

where C_{DCE} is the concentration of DCE, $R^{bio}_{DCE,RD}$ is the rate of DCE degradation due to reductive dechlorination, $R^{bio}_{DCE,DO}$ is the rate of DCE degradation due to anaerobic oxidation, ξ_{TCE} is the production coefficient of DCE generated by TCE degradation, and R^{bio}_{TCE} is the rate of TCE degradation (due to reductive dechlorination). Since the system under consideration is intrinsically anaerobic, aerobic contributions to the degradation of DCE are not included. Each of the microbial sink terms can be expanded for further evaluation. The degradation of DCE due to reductive dechlorination includes inhibition by PCE and TCE and can be expressed as

$$R^{bio}_{DCE,RD} = \frac{M_2}{\Theta}\nu_{DCE,RD} = \frac{M_2}{\Theta}\nu^{max}_{DCE,RD}\left[\frac{C_{DCE}}{C_{DCE}+K_{DCE,RD}}\right]\left[\frac{K_{PCE/DCE}}{K_{PCE/DCE}+C_{PCE}}\right]\left[\frac{K_{TCE/DCE}}{K_{TCE/DCE}+C_{TCE}}\right] \quad (5.9)$$

where M_2 is the microbial population of DCE and VC degraders, $\nu_{DCE,RD}$ is the rate of reaction for the reductive dechlorination of DCE, $\nu^{max}_{DCE,RD}$ is the maximum specific utilization rate for DCE during reductive dechlorination, C_{DCE} is the concentration of DCE, $K_{DCE,RD}$ is the half saturation coefficient for DCE during reductive dechlorination, $K_{PCE/DCE}$ is the coefficient of DCE inhibition by PCE, and $K_{TCE/DCE}$ is the coefficient of DCE inhibition by TCE.

The degradation of DCE by anaerobic (or direct) oxidation is also modeled using Monod kinetics such that the microbial sink term is summed over all terminal electron accepting processes (TEAP) where anaerobic oxidation could occur. The general expression is

$$R^{bio}_{DCE,DO} = \sum^{TEAP} \frac{M}{\Theta}\nu^{max}_{DCE,DO}\left[\frac{C_{DCE}}{C_{DCE}+K_{DCE,DO}}\right]\left[\frac{E}{E+K_e}\right] \quad (5.10)$$

where M is the microbial population of the anaerobic oxidizers for a specific TEAP, $\nu^{max}_{DCE,DO}$ is the maximum specific utilization rate for DCE during anaerobic oxidation for a specific TEAP, $K_{DCE,DO}$ is the half saturation coefficient for DCE during anaerobic oxidation for a specific TEAP, E is the concentration of the electron acceptor associated with the TEAP, and K_e is effective half saturation constant for the electron acceptor associated with the TEAP. As stated previously, the anaerobic oxidation option is omitted in the microcosm model. The contribution of anaerobic oxidation to the reduction in mass of the contaminants is calculated in the biological package, however, the DCE specific parameters are entered into SEAM3D in the reductive dechlorination package.

The degradation of VC is similar to DCE degradation in that VC degradation includes the reductive

dechlorination of VC and the anaerobic oxidation of VC to CO_2. The general expression for VC degradation is as follows

$$\frac{dC_{VC}}{dt} = -R^{bio}_{VC,RD} - R^{bio}_{VC,DO} + \xi_{DCE} R^{bio}_{DCE,RD} \tag{5.11}$$

where C_{VC} is the concentration of VC, $R^{bio}_{VC,RD}$ is the rate of VC degradation due to reductive dechlorination, $R^{bio}_{VC,DO}$ is the rate of VC degradation due to anaerobic oxidation, ξ_{DCE} is the production coefficient of VC generated by DCE dechlorination, and $R^{bio}_{DCE,RD}$ is the rate of DCE degradation due to reductive dechlorination. Since the system under consideration is anaerobic by nature, aerobic contributions to the degradation of VC are not included.The microbial sink term due to reductive dechlorination can be further expressed as

$$R^{bio}_{VC,RD} = -\frac{M_2}{\Theta}\nu_{VC,RD} = -\frac{M_2}{\Theta}\nu^{max}_{VC,RD}\left[\frac{C_{VC}}{C_{VC}+K_{VC,RD}}\right]\left[\frac{K_{PCE/VC}}{K_{PCE/VC}+C_{PCE}}\right]\left[\frac{K_{TCE/VC}}{K_{TCE/VC}+K_{TCE}}\right]\left[\frac{K_{DCE/VC}}{K_{DCE/VC}+C_{DCE}}\right] \tag{5.12}$$

where $\nu_{VC,RD}$ is the rate of reaction for the reductive dechlorination of VC, $\nu^{max}_{VC,RD}$ is the maximum specific utilization rate for VC during reductive dechlorination, $K_{VC,RD}$ is the half saturation coefficient for VC during reductive dechlorination, $K_{PCE/VC}$ is the coefficient of VC inhibition by PCE, $K_{TCE/VC}$ is the coefficient of VC inhibition by TCE, and $K_{DCE/VC}$ is the coefficient of VC inhibition by DCE.

The microbial sink term for anaerobic oxidation of VC to CO_2 is the same as equation 5.10 with the exception that VC subscripts are used instead of DCE as shown below

$$R^{bio}_{VC,DO} = \sum^{TEAP} \frac{M}{\Theta}\nu^{max}_{VC,DO}\left[\frac{C_{VC}}{C_{VC}+K_{VC,DO}}\right]\left[\frac{E}{E+K_e}\right] \tag{5.13}$$

where $\nu^{max}_{VC,DO}$ is the maximum specific utilization rate for VC during anaerobic oxidation for a specific TEAP, C_{VC} is the concentration of VC, $K_{VC,DO}$ is the half saturation coefficient for VC during anaerobic oxidation for a specific TEAP, E is the concentration of the electron acceptor associated with the TEAP, and K_e is effective half saturation constant for the electron acceptor associated with the TEAP. As stated previously, the contribution of anaerobic oxidation to the reduction of VC is calculated in the biological package with the VC specific parameters being housed in the reductive dechlorination package.

The production of ethene is also calculated by the reductive dechlorination package and can be expressed as

$$\frac{dC_{ETH}}{dt} = \xi_{VC} R^{bio}_{VC,RD} \tag{5.14}$$

where C_{ETH} is the concentration of ethene, ξ_{VC} is the production coefficient of ethene generated by VC dechlorination, and $R^{bio}_{VC,RD}$ is the rate of VC degradation due to reductive dechlorination.

5.2.2 Reductive Dechlorination Parameters

A microcosm model was developed for each microcosm: MLS12-Shallow, MLS22-Shallow, and MLS22-Deep. The reductive dechlorination input parameters for the MLS12-Shallow microcosm model were based on calculated estimates performed on the concentration versus time microcosm data using Excel to simulate the Monod kinetics. The MLS22-Shallow microcosm model used the resultant rate parameters from the calibrated MLS12-Shallow model as input parameters. Similarly, the MLS22-Deep microcosm model used the results from the calibrated MLS22-Shallow model for its input parameters. The degradation parameters (substrate utilization factor and half saturation coefficient) were calibrated individually for each chlorinated compound such that the chlorinated ethene under investigation was simulated as the sole amended compound. Then, the inhibitory functions were calibrated as the model sequentially degraded the chlorinated ethenes beginning with PCE. The calibrated reductive dechlorination parameters are shown in Tables 5.1-5.3. Furthermore, the conceptual model developed for the reductive dechlorination package of SEAM3D could not accurately simulate the observed TCE data in the MLS22-Shallow and MLS22-Deep microcosms. Therefore, the reported degradation parameters for TCE are artificially high and do not represent aqueous phase degradation. The production coefficient for mass units were calculated based on the 1:1 stoichiometry of the reductive dechlorination process in molar units (Table 5.4). The production coefficient for VC was set to zero for the MLS22 microcosms because no VC was observed.

To model steady state microbial kinetics, the two microbial populations were set initially equal to the porosity. The subsequent parameters of growth, the yield coefficient and decay coefficient, were set equal to zero. The microcosms' measured concentration versus time profiles were shifted to remove the lag phase that occurred at the beginning of the microcosm experiments. The initial

concentration of PCE for the model was set equal to initial PCE concentration on the adjusted concentration versus time profile for each microcosm (Table 5.5). These adjusted concentration versus time profiles were used in fitting the reductive dechlorination parameters for biodegradation rate determination. The microbial population of the *cis*-1,2-DCE degrading microorganisms was included later in the MLS22 microcosm models after the microcosm concentration versus time profile could not be predicted under the steady state microbial population assumption (Table 5.6). It should be noted that biomass was not measured in the microcosms for an initial biomass concentration for use in the model. While the second microbial population initially included both the *cis*-1,2-DCE and VC degrading microorganisms, the MLS22 microcosms did not produce VC. Therefore, the second microbial population was limited to the effects by the *cis*-1,2-DCE concentrations.

Table 5.1: Maximum specific utilization rate of the chlorinated ethenes (CE) (ν_{CE}^{max}, day^{-1}) for the three microcosm models.

Microcosm	PCE	TCE	DCE	VC
MLS12-Shallow	0.4	0.42	0.05	0.25
MLS22-Shallow	0.4	1.00*	0.06	na
MLS22-Deep	0.4	1.50*	0.07	na

* - Artificially high rate to simulate limited production of TCE
na - Not applicable

Table 5.2: Half saturation coefficients (K_{CE}, mg/L) of the chlorinated ethenes for the three microcosm models.

Microcosm	PCE	TCE	DCE	VC
MLS12-Shallow	0.41	0.01	0.07	0.02
MLS22-Shallow	0.57	0.20*	1.30	na
MLS22-Deep	1.00	0.30*	2.10	na

* - Artificially high rate to simulate limited production of TCE
na - Not applicable

Table 5.3: Inhibition Coefficients (mg/L) of one chlorinated ethene on the degradation of another chlorinated ethene for the three microcosm models.

Microcosm	$K_{PCE/TCE}$	$K_{PCE/DCE}$	$K_{TCE/DCE}$	$K_{PCE/VC}$	$K_{TCE/VC}$	$K_{DCE/VC}$
MLS12-Shallow	0.01	0.01	0.01	0.01	0.01	0.15
MLS22-Shallow	1.90*	0.10	0.60	na	na	na
MLS22-Deep	1.90*	0.40	0.50	na	na	na

* - Artificially high rate to simulate limited production of TCE
na - Not applicable

Table 5.4: The production coefficient (ξ) of one chlorinated ethene generated by the degradation of another chlorinated ethene.

Microcosm	ξ_{PCE}	ξ_{TCE}	ξ_{DCE}	ξ_{VC}
MLS12-Shallow	0.79	0.74	0.64	0.45
MLS22-Shallow	0.79	0.74	0	0
MLS22-Deep	0.79	0.74	0	0

Table 5.5: The initial concentrations ($\mu g/L$)o f the PCE spike used by the model.

Microcosm	C_{PCE}
MLS12-Shallow	5.80
MLS22-Shallow	3.40
MLS22-Deep	4.10

Table 5.6: The initial microbial population M_2 (g), yield coefficient Y_{DCE} (g g^{-1}), and microbial death rate k_d (day^{-1}) for the *cis*-1,2-DCE degrading microbial population (M_2) in the MLS22 microcosms.

Microcosm	M_2	Y_{DCE}	k_d
MLS22-Shallow	0.030	0.65	0.004
MLS22-Deep	0.020	0.75	0.004

Chapter 6

Results and Discussion

6.1 Groundwater Parameter Assessment

6.1.1 Contaminant Distribution

The chlorinated ethene distribution through the years of 1998, 1999, and 2000 elucidated two aspects which aid in understanding the nature of the contamination at the site. The first aspect suggests that there are at least two locations of high contamination within the source zone as indicated by relatively high concentrations of PCE at 22 ft bgs in MLS12 (Figure 3.8) and 6 ft bgs in MLS11 (Figure 3.6). Both MLS12 and MLS11 are located adjacent to the former exchange laundry/dry cleaning facility. The second aspect suggests the depth of the contamination is directly related to the phase of the released waste. The shallow depth of the high PCE concentrations at MLS11 implies that the PCE waste was released in an aqueous phase that remained in the upper portion of the aquifer. Conversely, the deep depth of the PCE detected at MLS12 suggests that the PCE waste was released in a non-aqueous or pure form. Since PCE as a pure solvent has a higher density than water, the PCE migrated through the Columbia Aquifer until the contaminant reached the Yorktown confining unit.

The detection of PCE's daughter products, TCE, *cis*-1,2-DCE, VC and ethene, in the aquifer suggest that reductive dechlorination is occurring at Site 12 (Figures 3.6-3.13). However, detection of daughter products does not implicitly support that reductive dechlorination is activity degrading the contamination in a manner suited for MNA. Furthermore, the decreasing concentrations of the

daughter products suggests that the extent of the dechlorination process and efficiency of the degradation process should be evaluated. Therefore, successive chlorinated ethene concentrations (on a molar basis) were compared to elucidate the progression of the reductive dechlorination process between the 1998, 1999, and 2000 sampling rounds (Tables 6.1-6.4). The comparison used a ratio format to facilitate numerical comparisons of the reductive dechlorination process between sampling rounds and MLS locations. Moreover, the numerical ratios represent a non-unique method of evaluation. Consequently, the ratio may misrepresent the changes in contaminant concentration when one contaminant increases and the other decreases in a relative quantity. Therefore, the evaluation the ratios also incorporated the concentrations of the chlorinated ethenes.

A numerical ratio >1 states that the majority of the contamination is detected as the first compound in the ratio. It follows that as the ratio approaches unity, the chlorinate ethenes are being stoichiometrically degraded. When the ratio <1, this signifies that the majority of the contamination has been converted to the second compound in the ratio. A ratio >200 means that the second compound in the ratio was not detected and a ratio of 0.00 means that the second compound was detected but the first compound was not detected.

Evaluation of PCE, TCE, and *cis*-1,2-DCE

A comparison of each MLS between the sampling rounds indicates that in general PCE is being degraded to TCE while TCE degradation to *cis*-1,2-DCE was limited to discrete locations. The MLS11 PCE:TCE ratio decreased in the blue port between 1998, 1999, and 2000 while the contaminant ratio remained constant at the other ports (Table 6.1). Upon investigation of the PCE and TCE concentrations, the constant PCE:TCE ratio understated the decrease in PCE concentration and increase in TCE concentration observed in 2000 for the black port. However, *cis*-1,2-DCE was not observed at MLS11 in 1999 and 2000. Therefore, MLS11 exhibited partial dechlorination to TCE over the course of three years. At MLS12, the PCE:TCE ratio for the yellow port dropped from 14.02 to 7.31 to 3.83 between years while the PCE:TCE ratio in the red port increases between 1998 from 4.86 to 12.45 (Table 6.2). This increase illustrated the decrease in TCE production for 1999 and a possible decrease in reductive dechlorination activity. Concentration of *cis*-1,2-DCE also decreased in the yellow port between 1998 and 1999 and no *cis*-1,2-DCE was detected in

the red, purple, and orange ports. The high levels of PCE contamination (> 6000 μg/L) may be contributing to the low levels or lack of *cis*-1,2-DCE generation. The green and blue ports at MLS12 show a decrease in PCE:TCE and TCE:DCE ratios over 1998, 1999 and 2000. The green port in 2000 had a PCE:TCE ratio of 0.80 and a TCE:DCE of 0.51 accompanied with decreased concentrations of PCE, TCE and *cis*-1,2-DCE. This indicates substantial reductive dechlorination activity at the blue port. Since the concentrations of PCE in the upper ports are <4000 μg/L, this further indicates that high PCE concentrations may be inhibiting TCE degradation. Furthermore, the contaminant concentrations at MLS20 were below 2000 μg/L and substantial dechlorination activity was observed (Table 6.3). While the PCE:TCE ratios decreased only slightly, the PCE and TCE concentrations decreased between each sampling round. The TCE:DCE ratios decreased between 1998, 1999 and 2000. By 2000, the majority of the contamination at MLS20 was detected as TCE and *cis*-1,2-DCE as illustrated in PCE:TCE and TCE:DCE ratios less than one. MLS22 exhibited a decrease in PCE:TCE ratio between 1999 and 2000 and a connection between PCE concentrations and *cis*-1,2-DCE production (Table 6.4). While the 1999 PCE concentration in the red port was 8800 μg/L, *cis*-1,2-DCE production was similar to MLS12 yellow, where PCE concentration was >12000 μg/L. In 1999, the PCE concentrations over purple and the blue ports were between 2200 and 4500 μg/L. *Cis*-1,2-DCE was detected all the ports except the blue port. By 2000, the PCE and TCE concentrations were under 10 μg/L in the purple through the blue ports and little to no *cis*-1,2-DCE was detected. Overall, the groundwater concentrations of the PCE, TCE and *cis*-1,2-DCE demonstrated reductive dechlorination activity at Site 12 and indicated a possible inhibitory relationship between elevated PCE levels and *cis*-1,2-DCE production.

Evaluation of VC and Ethene

The detection of VC and ethene were limited to the above mentioned areas of substantial reductive dechlorination activity. MLS12 exhibited decreases in VC and ethene between 1998 and 1999. However, the concentrations of VC or ethene were not necessarily related to one another. MLS20 produced VC in 1998 but no ethene was present. In 1999, ethene was observed along with VC. Furthermore, the low levels or non-detects of VC and ethene imply that the microorganisms with the ability to degrade *cis*-1,2-DCE were absent or inactive. As the reductive dechlorination process proceeds the chlorinated ethenes become more reduced. More energy is required to dehalogenate

cis-1,2-DCE in contrast to PCE. Therefore, the low concentrations of VC and ethene may stem from partial dechlorination due to energy limitations in the aquifer. Conversely, *cis*-1,2-DCE has been shown to directly oxidize to CO_2 under Fe(III)-reducing, sulfate-reducing and methanogenic conditions while low levels of VC, ethene and ethane were observed (Bradley et al., 1998; Bradley and Chapelle, 1998b). This degradation pathway my be contributing to the observed low levels of VC, ethene and ethane (Figures 3.9 and 3.11, ethane data not shown). However, the detection of VC and ethene was limited to discrete locations at MLS12 and MLS20. Research by Flynn et al. (2000) has shown that two microbial populations were responsible for PCE degradation to ethene. One population dechlorinated PCE to *cis*-1,2-DCE and another population degraded *cis*-1,2-DCE or VC to ethene. The localized areas of activity at MLS12 and MLS20 could result from isolated pockets of *cis*-1,2-DCE and VC degraders. Therefore, the partial dechlorination may be due to a lack of *cis*-1,2-DCE and VC degrading microbes present throughout Site 12. Overall, the contaminant groundwater data suggests that reductive dechlorination to *cis*-1,2-DCE is occurring at the site with limitations on the further steps in the reductive dechlorination process.

Summary of Chlorinated Ethene Distribution

The groundwater concentrations of the PCE, TCE and *cis*-1,2-DCE demonstrated reductive dechlorination activity at Site 12 and indicated a possible inhibitory relationship between elevated PCE levels and *cis*-1,2-DCE production. Furthermore, the detection of VC and ethene was limited to discrete locations at MLS12 and MLS20. In the areas of VC production, the concentrations of PCE were at or below 18 μM for all three sampling rounds. This suggests that PCE must be below a threshold concentration for VC production to occur. A PCE concentration at or below 18 μM in conjunction with the detection of *cis*-1,2-DCE occurred 20 times in the 1998, 1999, and 2000 groundwater data. However, VC was detected 11 out of those 20 times (55%). To confirm the hypothesis of a PCE threshold concentration affecting the degradation of VC at Site 12 would require further investigation. Alternatively, the localized areas of activity at MLS12 and MLS20 could result from isolated pockets of *cis*-1,2-DCE and VC degraders. Therefore, the partial dechlorination may be due to either a lack of *cis*-1,2-DCE and VC degrading microbes present throughout Site 12 or elevated levels of PCE that inhibit *cis*-1,2-DCE production and degradation. Overall, the biological component of the fate of the aqueous chlorinated ethenes indicates that partial reductive

dechlorination is occurring at Site 12.

While the abiological component of the fate of the chlorinated ethenes were not explicitly evaluated in this study, the abiological effects can be discussed in terms of the groundwater flow at Site 12. As stated in the Chapter 3 Section 3.2.3 the groundwater flow is dominated by the leaky sanitary sewer line that traverses Site 12 (See Figure 3.2 for Potentiometric Surface). This groundwater flow pattern provides hydraulic control on the extent of the plume and the advective forces effectively flush the contaminated area with fresh groundwater. As a result of a combination of advection, diffusion, and sorption, the concentrations of PCE and TCE decline along the flow path. Monitoring of the sewer line showed concentrations of PCE below 15 μg/L, TCE below 2 μg/L, and non-detectable concentrations of *cis*-1,2-DCE and VC (CH2MHill, 2000). Therefore, through a combination of biological and abiological components the chlorinated ethene concentrations at Site 12 decreased from 1998 to 2000.

Table 6.1: Sequential chlorinated ethene ratios for MLS11

1998 Sampling Round

Port Color	PCE:TCE	TCE:DCE	DCE:VC	VC:ETH
Black (7.0 ft bgs)	48	2	UL	0
Blue (9.5 ft bgs)	167	2	UL	0
Green (12 ft bgs)	22	2	UL	0
Orange (14.5 ft bgs)	38	0.9	UL	0
Purple (17 ft bgs)	24	UL	UL	0
Red (19.5 ft bgs)	15	UL	UL	0
Yellow (22 ft bgs)	UL	UL	UL	0

1999 Sampling Round

Port Color	PCE:TCE	TCE:DCE	DCE:VC	VC:ETH
Black (7.0 ft bgs)	UL	UL	UL	UL
Blue (9.5 ft bgs)	58	UL	UL	0
Green (12 ft bgs)	23	UL	UL	0
Orange (14.5 ft bgs)	UL	UL	UL	0
Purple (17 ft bgs)	19	UL	UL	UL
Red (19.5 ft bgs)	UL	UL	UL	UL
Yellow (22 ft bgs)	UL	UL	UL	UL

2000 Sampling Round

Port Color	PCE:TCE	TCE:DCE	DCE:VC	VC:ETH*
Black (7.0 ft bgs)	48	UL	UL	
Blue (9.5 ft bgs)	10	UL	UL	
Green (12 ft bgs)	6	UL	UL	
Orange (14.5 ft bgs)	11	UL	UL	
Purple (17 ft bgs)	39	UL	UL	
Red (19.5 ft bgs)	23	UL	UL	
Yellow (22 ft bgs)	UL	UL	UL	

*Ethene was not analyzed

Table 6.2: Sequential chlorinated ethene ratios at MLS12

1998 Sampling Round

Port Color	PCE:TCE	TCE:DCE	DCE:VC	VC:ETH
Blue (8.5 ft bgs)	2	2	3	1
Green (11.0 ft bgs)	2	1	4	8
Orange (13.5 ft bgs)	1	UL	UL	0
Purple (16 ft bgs)	6	UL	UL	UL
Red (18.5 ft bgs)	5	UL	UL	UL
Yellow (21.7 ft bgs)	14	5	UL	0

1999 Sampling Round

Port Color	PCE:TCE	TCE:DCE	DCE:VC	VC:ETH
Blue (8.5 ft bgs)	1	0.6	4	1
Green (11.0 ft bgs)	1	0.9	21	2
Orange (13.5 ft bgs)	2	UL	UL	0
Purple (16 ft bgs)	3	UL	UL	0
Red (18.5 ft bgs)	12	UL	UL	0
Yellow (21.7 ft bgs)	7	9	UL	0

2000 Sampling Round

Port Color	PCE:TCE	TCE:DCE	DCE:VC	VC:ETH*
Blue (8.5 ft bgs)	1	0.5	UL	
Green (11.0 ft bgs)	0.8	0.5	UL	
Orange (13.5 ft bgs)	0.4	UL	UL	
Purple (16 ft bgs)	2	UL	UL	
Red (18.5 ft bgs)	10	7	UL	
Yellow (21.7 ft bgs)	4	8	UL	

*Ethene was not analyzed

Table 6.3: Sequential chlorinated ethene ratios at MLS20

1998 Sampling Round

Port Color	PCE:TCE	TCE:DCE	DCE:VC	VC:ETH
Black (8 ft bgs)	5	5	UL	UL
Blue (10.5 ft bgs)	5	4	11	UL
Green (13 ft bgs)	0.06	5	6	UL
Orange (15.5 ft bgs)	6	4	7	UL
Purple (18 ft bgs)	7	5	6	UL
Red (20.5 ft bgs)	6	4	9	UL
Yellow (23 ft bgs)	3	4	8	UL

1999 Sampling Round

Port Color	PCE:TCE	TCE:DCE	DCE:VC	VC:ETH
Black (8 ft bgs)	4	UL	UL	UL
Blue (10.5 ft bgs)	1	2	UL	UL
Green (13 ft bgs)	4	UL	UL	UL
Orange (15.5 ft bgs)	9	UL	UL	UL
Purple (18 ft bgs)	8	2	UL	0
Red (20.5 ft bgs)	4	4	UL	0
Yellow (23 ft bgs)	3	2	UL	0

2000 Sampling Round

Port Color	PCE:TCE	TCE:DCE	DCE:VC	VC:ETH*
Black (8 ft bgs)*				
Blue (10.5 ft bgs)	0.1	0.2	UL	
Green (13 ft bgs)	0.3	0.4	UL	
Orange (15.5 ft bgs)	2	0.4	UL	
Purple (18 ft bgs)	4	1	UL	
Red (20.5 ft bgs)	2	0.7	2	
Yellow (23 ft bgs)	UL	0	UL	

* Not analyzed

Table 6.4: Sequential chlorinated ethene ratios for MLS22

1999 Sampling Round

Port Color	PCE:TCE	TCE:DCE	DCE:VC	VC:ETH
Blue (9.5 ft bgs)	6	UL	UL	0
Green (12 ft bgs)	6	9	UL	0
Orange (14.5 ft bgs)	5	10	UL	0
Purple (17 ft bgs)	3	15	UL	0
Red (19.5 ft bgs)	4	11	UL	0
Yellow (22 ft bgs)	2	UL	UL	0

2000 Sampling Round

Port Color	PCE:TCE	TCE:DCE	DCE:VC	VC:ETH*
Blue (9.5 ft bgs)	5	0.4	UL	
Green (12 ft bgs)	UL	UL	UL	
Orange (14.5 ft bgs)	0.2	UL	UL	
Purple (17 ft bgs)	3	UL	UL	
Red (19.5 ft bgs)	2	8	UL	
Yellow (22 ft bgs)	0.7	3	UL	

*Ethene not analyzed

6.1.2 Redox Indicators

An evaluation of the redox indicators was used to determine the prevalent terminal electron accepting precess/es (TEAP) occurring in the aquifer. The importance of understanding the TEAP within the extent of the contaminant plume has been demonstrated through the investigations of petroleum hydrocarbon contamination (Yager et al., 1997; Chapelle et al., 1995). This research has shown that the TEAP is a primary factor in determining the efficacy of biodegradation. Similarly, the extent of reductive dechlorination has been shown to be affected by the predominant TEAP (Bradley, 2000; Lendvay et al., 1998). As the chlorinated ethene becomes more reduced, it requires a more reduced environment is required for dechlorination. For example, the highly oxidized nature of PCE enables degradation to TCE under all anaerobic conditions whereas TCE degradation requires at least Fe(III)-reducing conditions. Consequently, the determination of the TEAP at Site 12 will aid in predicting the extent or fate of reductive dechlorination.

An evaluation of the redox indicators began with examining the concentrations of electron acceptors and the final redox products. The nitrate/nitrate concentrations were below detection for all three sampling rounds within the extent of the plume. Upgradient from the plume in the lower ports of MLS10 background nitrate concentrations were 0.9 mg/L. These low levels of nitrate/nitrite suggest that strong reducing conditions exist within the plume. The concentrations of sulfate were highest (40-100 mg/L) in the upper portions of the aquifer and lowest (20-40 mg/L) in the lower portions of the aquifer (Figures 3.14 and 3.15). Similarly, the concentrations of CO_2 were also highest (100-200 mg/L) in the upper portions of the aquifer and lowest (20-100 mg/L) in the lower portions of the aquifer (Figures 3.16 and 3.17). The lower levels of sulfate and CO_2 in the low portions of the aquifer may indicate that microbial processes have consumed the election donors. In general, the levels of ferrous iron, a final redox product, were below 15 mg/L throughout the aquifer in 1998 and 2000. However, in 2000 MLS20 and MLS22 showed higher concentrations of ferrous iron. MLS20 exhibited an increase in ferrous iron concentrations of 25 mg/L and MLS22 exhibited spikes of ferrous iron above 20 mg/L in the sixth and fourth ports. The levels of sulfide were generally at or below the detection limits in 1998 and 2000. The concentrations of methane in 1998 and 1999 were between 0.001 to 0.01 mg/L throughout the aquifer with the higher levels of methane in the lower portion of the aquifer. In 2000, MLS20 exhibited higher levels of methane

in the range of 0.1 to 2 mg/L. Overall, the final redox products exhibited little variation between MLS. The increased methane concentrations in the first and second ports of the MLS support the observed methanogenic levels of hydrogen.

Since hydrogen is a short lived intermediate product of fermentation, measurements of hydrogen concentrations can indicate the predominate TEAP at location sampled without possible bias from upstream flow of groundwater constituents. Based on work by Chapelle et al. (1995), the relationship between the hydrogen concentrations and the TEAP is listed in Table 2.1. The relationship between the hydrogen concentration and the predominate TEAP was used in assessing the redox conditions in the aquifer at Site 12. In 1998, the upper portion of the aquifer showed border line sulfate-reducing to methanogenic conditions while the lower portion of the aquifer showed predominately methanogenic conditions. In 1999, fewer wells were sampled for hydrogen (Figures 3.18 and 3.20). MLS12 and MLS20 produced hydrogen concentrations in the range sulfate-reducing conditions (1 to 4 nM). In 2000, the dissolved hydrogen levels throughout the aquifer were indicative of methanogenic conditions. The levels of hydrogen (5 to 10 nM) were slightly lower in the upper portion of the aquifer. The lower portion of the aquifer exhibited highly methanogenic conditions with hydrogen levels between 10-18 nM.

The laboratory employed by CH2MHill for 1999 sampling round used the Microseeps hydrogen bubbler technique rather than the glass gas sampler technique recommended by Chapelle et al. (1995). This change in sampling produce may have resulted in an underestimation of the hydrogen concentrations in the aquifer. In 2000, the Chapelle method was used by Virginia Tech. The hydrogen levels showed methanogenic conditions throughout the aquifer. Therefore, both sampling rounds that used the Chapelle gas bubbler technique (1998 and 2000) exhibited mainly methanogenic conditions while the Microseeps method (1999) exhibited sulfate-reducing conditions. However, upon further investigation, data from the 1999 sampling round did show other differences. For example, the sulfide concentrations throughout the aquifer were higher in the 1999 sampling round as opposed to the 1998 and 2000 sampling rounds. The higher sulfides could result from a shift to sulfate reduction. Unfortunately, ferrous iron concentrations were not measured in 1999 to corroborate the sulfide trend. Nevertheless, the sulfate-reducing conditions exhibited through the hydrogen sampling may have correctly indicated the prevalent TEAP.

Given that the hydrogen concentrations predicted sulfate-reducing conditions in the upper portion of the aquifer for 1999, the depletion of sulfate would be expected. However, the concentrations of sulfate were high and there was little measured sulfide accumulation. The high levels of sulfate could be due to a release of sulfate from the aquifer's confining beds (Chapelle et al., 1995). As the sulfate-reducing microbes utilize the sulfate, the confining bed could release sulfate from its pore water. This replenishment of the sulfate in the groundwater from the aquifer and subsequent sulfate reduction should generate a considerable amount of sulfide. However, the levels of sulfide were below 0.15 mg/L throughout the aquifer in 1998, 1999, and 2000. These observed low levels of sulfide could be a result of interactions between the newly generated sulfide and the dissolved ferrous iron in the groundwater (Chapelle et al., 1995). This stripping action would remove the sulfide from solution as the sulfide is produced by sulfate reduction. Based on pH and dissolved CO_2 of the groundwater, the critical pH for FeS formation is 5.69 and the critical pH for $FeCO_3$ formation is 6.8. The groundwater at Site 12 fluctuates between a pH of 5.2 to 6.5. Therefore, FeS formation is possible in discrete locations depending on the pH while $FeCO_3$ formation would not be expected. Further evaluation of the groundwater parameters would be warranted to confirm this phenomena in which pE-pH considerations of the system could predict the formations of the minerals pyrite and sederite.

Under sulfate-reducing and methanogenic conditions *cis*-1,2-DCE can anaerobically oxidize to CO_2 with low levels of VC, ethene and ethane production (Bradley and Chapelle, 1998a,b, 1997; Bradley et al., 1998). This pathway may account for the general increase of CO_2 levels in the upper portion of the aquifer. Furthermore, the detection of low levels of VC (100 μM) and ethene at MLS12 were in the upper ports of MLS12. Furthermore, MLS20 is an exception to the CO_2 concentration trend with higher concentrations of CO_2 in the lower portion of the aquifer. And, MLS20 had VC production detected in the lower portion of the aquifer in 1998 and 2000. These observations of high CO_2 production corresponding to VC and ethene detection suggest that anaerobic oxidation may be a contributing pathway to the biodegradation processes occurring at Site 12.

The combination of sulfate, CO_2, and hydrogen concentrations suggest that the aquifer differs in TEAP with increased depth. The high levels of sulfate in the upper portion of the aquifer suggest that although some upper well ports exhibited hydrogen concentrations at methanogenic levels, the

terminal electron accepting process is dominated by sulfate reduction. As the sulfate levels decrease with depth in the aquifer, the hydrogen levels conversely increase with depth in the aquifer. A transitional zone between sulfate reduction and methanogenesis is located in the middle of aquifer as the sulfate and hydrogen levels invert. At the lower depths in the Columbia Aquifer, where the sulfate levels are the lowest and the hydrogen levels are the highest, methanogenic conditions dominate.

6.2 Microcosm Study

In the microcosm study, the production of TCE and *cis*-1,2-DCE was observed in all of the microcosms while VC production was only detection in the MLS12-Shallow experiments. Ethene and ethane production was not observed in any of the experiments. The observation of black precipitates, presumed to be iron sulfides, indicated sulfate reduction in the microcosms. Methane was detected around 3 months which indicated methanogenic conditions. These redox indicators confirmed that highly reduced conditions which foster reductive dechlorination were present in the microcosms. The time zero measurements for the microcosms could not be taken due to problems experienced with the analytical equipment. Consequently, the first measurement was taken 9 days after construction of the microcosms. The reported measurements were averages of duplicate samples (5x and 10x dilutions). The microcosm experiments produced concentration versus time results that were used in estimating the degradation rate parameters associated with the MLS12-Shallow, MLS22-Shallow and MLS-Deep locations.

In both the control and live TCE amended microcosms, PCE desorption was observed. The desorption concentrations averaged 0.26 μM $\pm$0.23 μM and 0.18 μM $\pm$0.17 μM in the shallow and deep sediment, respectively. Since desorption of PCE was observed in the TCE amended microcosms, it was assumed PCE desorption also occurred in the PCE amended microcosms at roughly the same concentrations. Based on the desorbed concentrations in the TCE amended microcosms, the levels of PCE desorption in the PCE amended microcosms would be 0.8% and 0.6% of the total amended PCE for the shallow and deep sediment, respectively. Therefore, the desorption of the PCE was considered negligible.

The control microcosms maintained a loss under 20% of the amended chlorinated ethene during the first 145 days of the experiment (Figure 6.1). However, at day 245 losses of 50% were observed. As stated previously, low levels of PCE were observed in the TCE amended controls and were attributed to desorption. Low levels of the TCE in the range of 0.05 to 0.08 μM were also observed in the shallow and deep PCE amended controls. Since TCE concentrations were less than 0.25% of the amended PCE, the observed TCE was assumed to be a result of desorption. Therefore, the lack of stoichiometric chlorinated ethene daughter production observed in the controls substantiated that biological activity was responsible for the reduction of chlorinated ethenes in the live microcosms.

Loss mechanisms in the microcosms consisted of mass removal due to aqueous samples (0.5 mL and 1 mL), decreases in aqueous phases concentrations due to partitioning into the headspace, and mass loss due to gas pressure releases with methane samples. Over the course of 14 sampling rounds, a total of 20.0 mL of groundwater was removed and 1.9 % of amended chlorinated ethene was removed. As the groundwater volume decreased, the headspace volume increased. The larger headspace volume resulted in higher quantities of mass partitioning into the headspace. Therefore as gas production increased the pressure inside the microcosm, more mass could be lost when methane sampling allowed the microcosm to depressurize to gauge pressure. In the worst case scenario of complete mass loss in the headspace per methane sample, a total of 1.4 % of *cis*-1,2-DCE would be lost and 11.2 % of VC would be lost for MLS12-Shallow. The same scenario could be applied to the loss mechanisms when the caps on the microcosms were replaced at day 161. However, the one time act of replacing the caps contributed to the loss of 3.0 % of VC while the repeated methane sampling contributed to 13.1 % of the mass loss in the microcosms. Therefore, the replacement of the microcosm caps was negligible in comparison to the loss of mass from the aqueous and methane sampling.

MLS12-Shallow

The microcosms amended with PCE produced TCE, *cis*-1,2-DCE and VC. After the detection of TCE production and degradation and subsequent production of *cis*-1,2-DCE, the microcosm sampling interval was decreased from weekly to every three weeks. The frequent sampling interval enabled the detection of TCE production beginning on day 13 and TCE degradation beginning on

day 50 (Figure 6.2). As with the 1998 microcosms, *cis*-1,2-DCE production was observed beginning on day 28. The transformation of *cis*-1,2-DCE to VC was first detected on day 60 at a concentration of 0.15 μM. The TCE amended microcosms (See Figure 6.3) also produced *cis*-1,2-DCE after a lag period of 28 days. The subsequent production of VC began on day 85. As mention previously, low levels of PCE due to desorption were observed throughout the study. The maximum PCE concentration was 0.53 μM on day 20 and decreased to 0.04 μM. Methane was measured in the head space of both sets of microcosms from day 85 in the range of 0.06 to 0.21 mole/L.

In contrast to the 1998 microcosm experiments, the continuous MLS12-Shallow microcosms produced VC. A possible reason for the production of VC could be due to an incorporation of *cis*-1,2-DCE degrading organisms in the continuous microcosms. As stated previously, research has shown that certain microorganisms can only degrade PCE and TCE to the end product of *cis*-1,2-DCE (Miller, et al., 1997). Thus, the chance of obtaining a pocket of *cis*-1,2-DCE degrading microorganisms was higher in the 1999 microcosms because the 1999 microcosms used 150 g of aquifer sediment rather than of 7 g of aquifer sediment as in the 1998 microcosms. Another possible reason for the production of VC could be due to inhibition of VC production by PCE. In the continuous microcosms prior to the onset of VC production, the concentration of PCE in the PCE and TCE amended microcosms dropped from over 0.13 μM to less than 0.02 μM. This decrease in PCE concentration may be related to the production of VC. The presence of PCE at high concentrations may inhibit the degradation of *cis*-1,2-DCE to VC. Therefore, when the PCE concentration is lowered, the reduction of *cis*-1,2-DCE to VC can proceed. The groundwater at MLS12 and MLS20 also exhibited a PCE threshold concentration, however, the threshold concentration was 18 μM. The difference in threshold concentrations implies that the *cis*-1,2-DCE and VC degrading microorganisms in the aquifer may require a micro-environment in order to reductively dechlorinate *cis*-1,2-DCE and VC.

MLS22-Shallow

The MLS22-Shallow microcosms produced partial dechlorination to *cis*-1,2-DCE. After a lag period, the PCE amended microcosms from MLS22-Shallow began degrading PCE on day 38 (Figure 6.4). TCE production was first detected on day 44 with TCE degradation beginning shortly after day 61.

The production of *cis*-1,2-DCE was detected on day 61. As of day 186, no VC had been detected. Methane was measured from day 85 in the range of 0.001 to 0.144 mole/L. The TCE amended microcosms from MLS22-Shallow began degrading TCE on day 38 and producing *cis*-1,2-DCE on day 44 (Figure 6.5). The microbial population may have required an acclimation period. However, after adjusting the MLS22-Shallow microbial community degraded TCE at a rapid rate in a similar manner to the MLS22- Shallow PCE amended microcosms. Methane was measured from day 85 in the range of 0.001 to 0.32 mole/L.

The degradation capability of the aquifer soil amended with PCE from location MLS22-Shallow differed from the MLS12-Shallow soil in three aspects. First, the onset of degradation for MLS22-Shallow was delayed by 2 to 3 weeks (Figure 6.4). This delay could suggest that the microorganisms from MLS22-Shallow required an adjustment or acclimation time period before the organisms could begin the reductive dechlorination process. On the other hand, the delay could suggest fewer chlorinated ethene-degraders were present in the aquifer soil during microcosm construction. Hence, more time was needed to see a microbial response. The second difference between MLS22- Shallow and MLS12-Shallow was the quantity of TCE detected in the microcosms. Over 35.5 μM of TCE was detected in MLS12-Shallow while only 1.9 μM of TCE was detected in MLS22-Shallow. This difference could result from differences in the activity of the TCE degraders or differences in their numbers. Similar amounts of TCE could have been produced, but the microbial community in the MLS22-Shallow microcosms may have quickly degraded the TCE. Another explanation for the smaller quantity of TCE detected in the MLS22-Shallow microcosms could be that the microorganism reduce PCE to *cis*-1,2-DCE before releasing the reduced chlorinated ethene to the aqueous environment. Holliger and Schumacher (1994) proposed that PCE degrading organisms produce *cis*-1,2-DCE. through intracellular TCE production where TCE is degraded to *cis*-1,2-DCE and then released to the aqueous environment. If this is the case, another organism, which can directly produce *cis*-1,2-DCE from PCE, may be responsible for the dechlorination activity at MLS22-Shallow. The final aspect that differentiates the MLS12 and MLS22 microcosms is that VC was produced in the MLS12 microcosms and not in the MLS22 microcosms. The groundwater analysis at MLS22 substantiates the results of the MLS22-Shallow microcosms. This lack of VC production supports the theory that the degradation of PCE at Site 12 is controlled by a microbial consortium with at least two sets of microbes. Moreover, the lack of the *cis*-1,2-DCE degrading organisms in

the MLS22-Shallow microcosms and groundwater samples indicate the sparse distribution of the *cis*-1,2-degrading microbial population.

MLS22-Deep

Because the deep sample from MLS22 is less sandy and contains more silt and clay than the shallow sediment, it would be expected that the degradation capabilities of the microbes at MLS22-Deep might differ from the capabilities of the MLS22-Shallow microbes. In the 1998 microcosm studies, no degradation was observed in any deep aquifer sediment. Therefore, the lag period seen in the MLS22-Deep microcosm was expected. The PCE-amended microcosms began *cis*-1,2-DCE production beginning at day 85 (Figure 6.6). The TCE amended microcosms slowly degraded TCE through day 186 (Figure 6.7). However, since production of *cis*-1,2-DCE in the TCE amended microcosms did not begin until day 137, a portion of the decrease in TCE was due to mass loss from aqueous and methane sampling. Methane was measured beginning from day 85 in the range of 0.0011 to 0.304 mole/L.

Zero Order Rate Calculations

The concentration versus time profiles from the microcosm experiments were used to estimate zero order decay rates. The rate constants were calculated via a linear regression through the concentration versus time profile. However, only the points that exhibited zero order decay were used when calculating the rate constants. Therefore, the initial lag phase and *cis*-1,2-DCE lag phase were omitted in the calculations. The PCE amended microcosms demonstrate repeatability in the PCE loss rate whereas the MLS22 microcosms show a difference in the TCE degradation rate versus the MLS12-Shallow microcosm. Furthermore, the MLS12-Shallow microcosms exhibit similar TCE degradation rates between the PCE and TCE amended microcosms. Conversely, the MLS22 TCE amended microcosms exhibit differences in the TCE degradation rates between the PCE and TCE amended microcosms. Since MLS12-Shallow microcosm demonstrated the conventional sequential reductive dechlorination pathway, the degradation rates of *cis*-1,2-DCE and VC were slower than those of PCE and TCE (Haston and McCarty, 1999). However, the *cis*-1,2-DCE degradation in the MLS22 microcosms is subject to question because of no VC production. The *cis*-1,2-DCE

degradation rate for the MLS22 microcosms are only a factor of two higher than the rate of mass loss due to aqueous and methane sampling. Nevertheless, the *cis*-1,2-DCE loss rates for all four MLS22 microcosms were similar and fit the linear regression with a R^2>0.99.

Table 6.5: Zero order decay rates (ppm day^{-1}) for the continuous microcosm experiments

MLS Location	Amendment	PCE Loss	TCE Loss	*cis*-1,2-DCE Loss	VC Production
MLS12-Shallow	PCE	0.07	0.19	0.02	0.005
MLS12-Shallow	TCE	na	0.23	0.01	0.005
MLS22-Shallow	PCE	0.07	0.007	0.0001	na
MLS22-Shallow	TCE	na	0.14	0.0001	na
MLS22-Deep	PCE	0.11	0.007	0.0001	na
MLS22-Deep	TCE	na	0.02	0.0001	na

na -not applicable

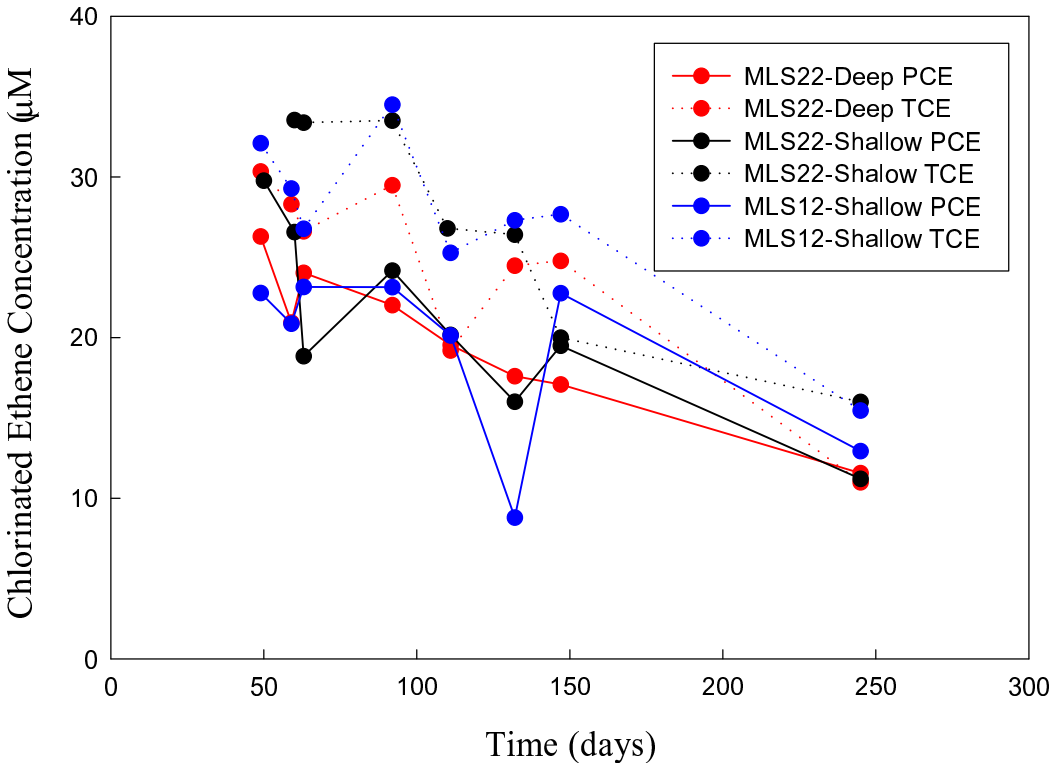

Figure 6.1: The measured concentrations of the chlorinated ethenes in the control microcosm MLS12-Shallow, MLS22-Shallow and MLS22-Deep experiments.

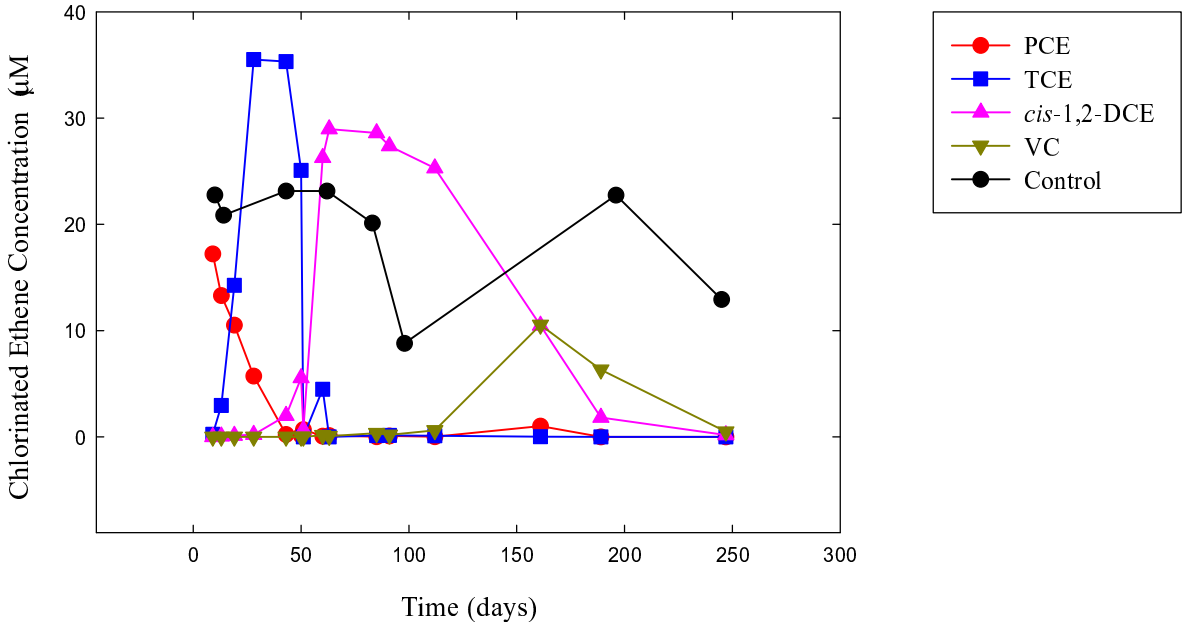

Figure 6.2: The measured concentrations of the chlorinated ethenes in MLS12-Shallow microcosm experiment amended with PCE.

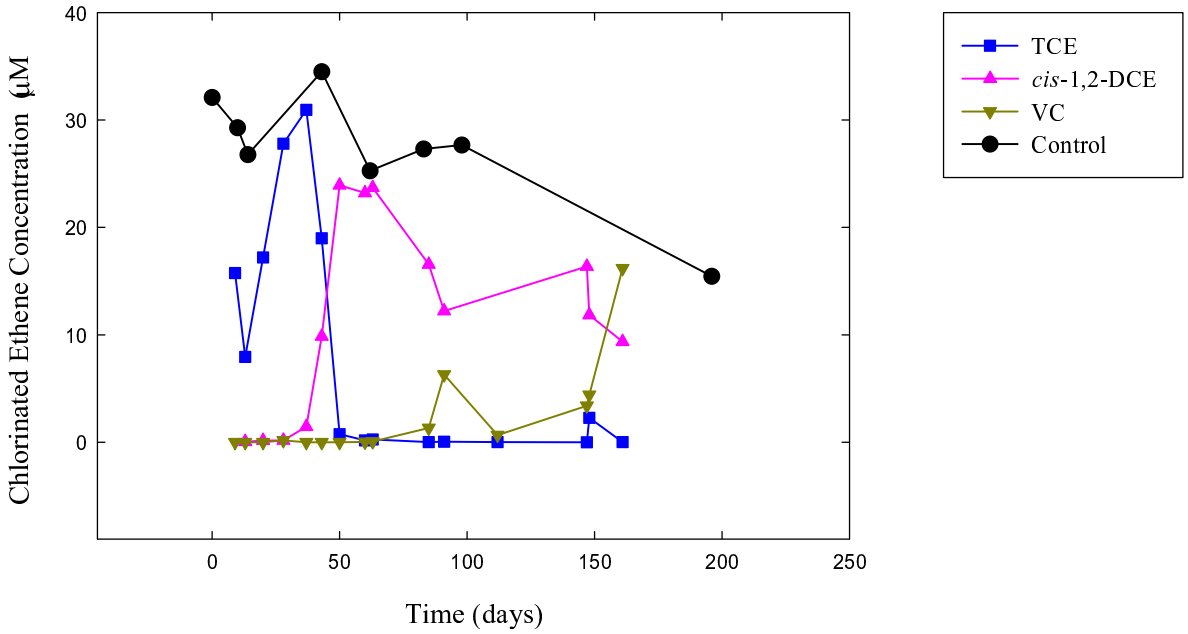

Figure 6.3: The measured concentrations of the chlorinated ethenes in MLS12-Shallow microcosm experiment amended with TCE.

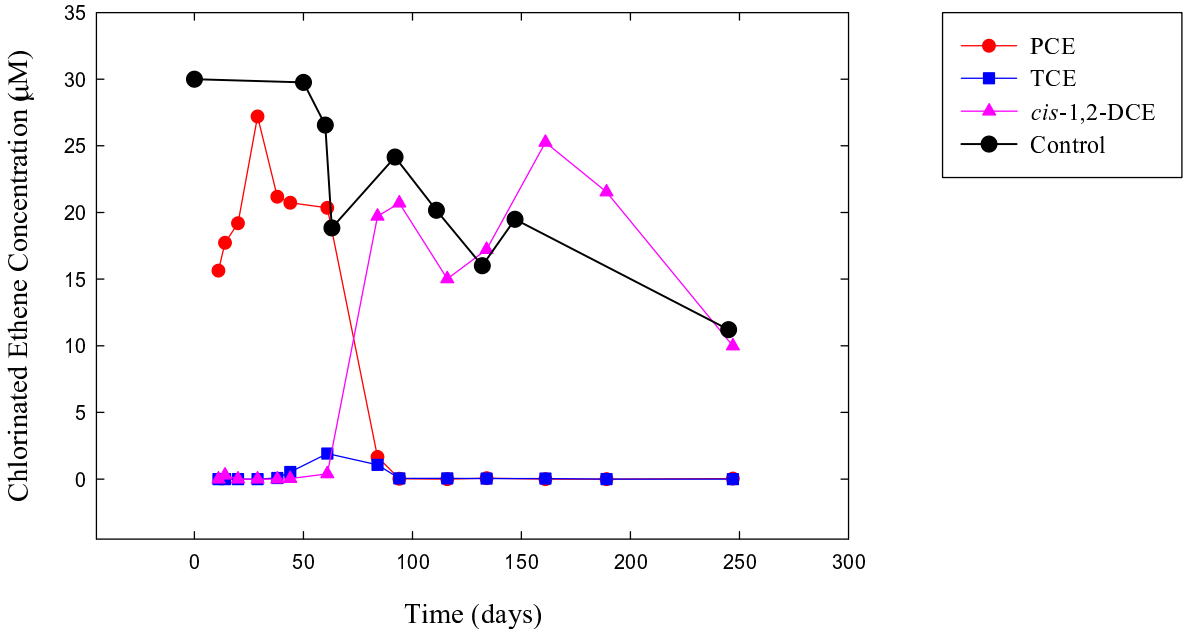

Figure 6.4: The measured concentrations of the chlorinated ethenes in MLS22-Shallow microcosm experiment amended with PCE.

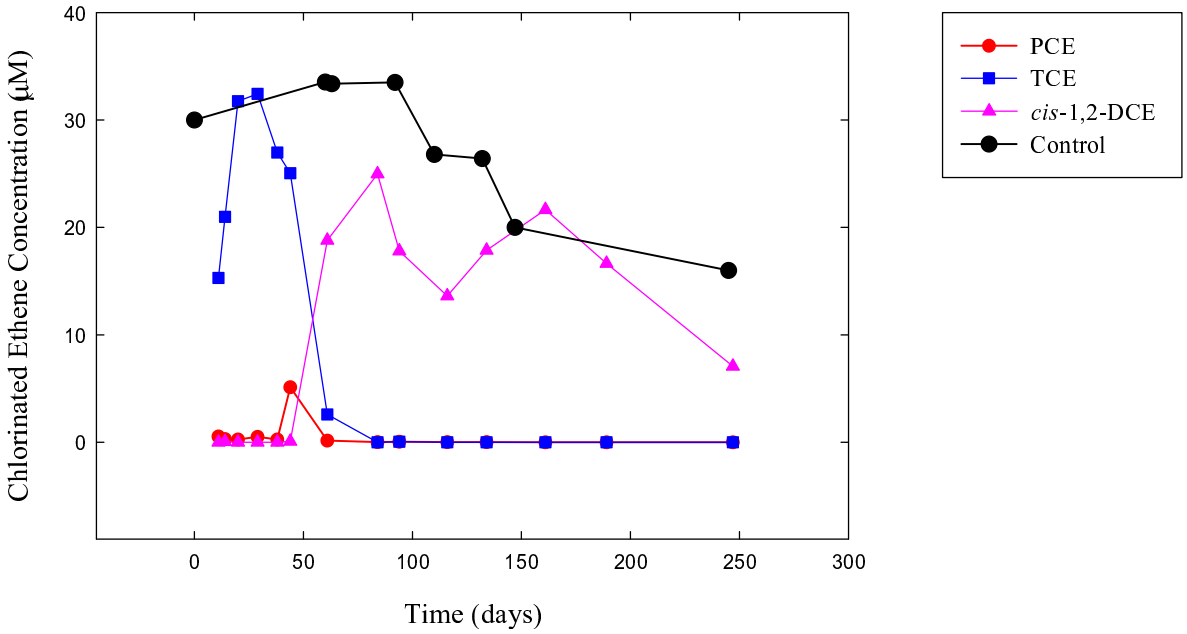

Figure 6.5: The measured concentrations of the chlorinated ethenes in MLS22-Shallow microcosm experiment amended with TCE.

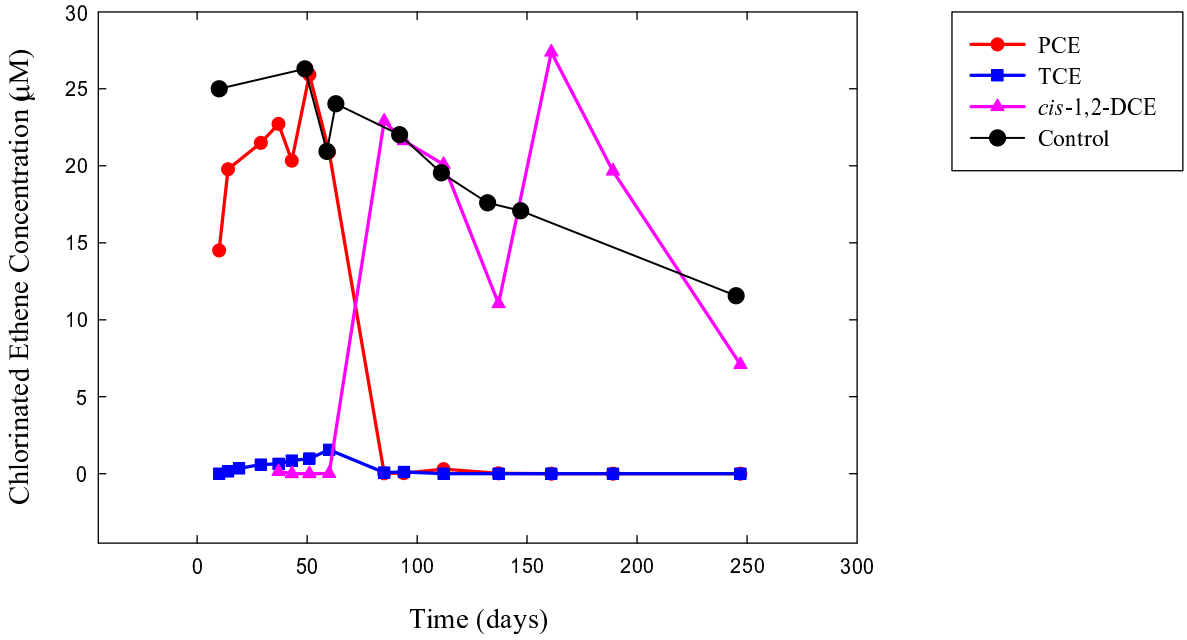

Figure 6.6: The measured concentrations of the chlorinated ethenes in MLS22-Deep microcosm experiment amended with PCE.

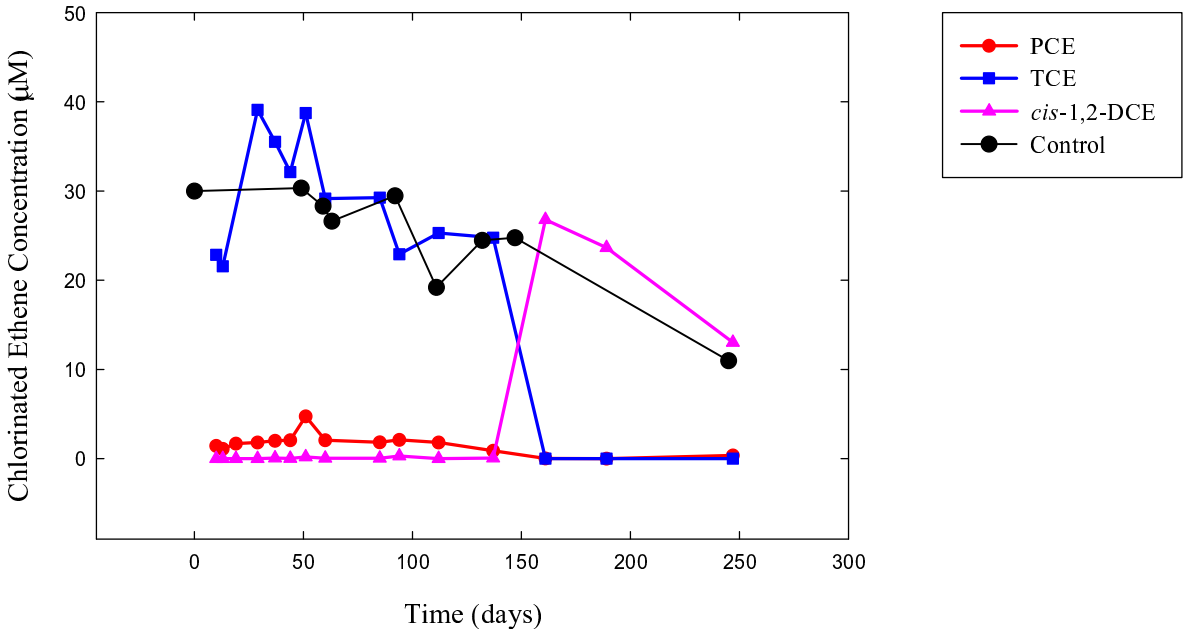

Figure 6.7: The measured concentrations of the chlorinated ethenes in MLS22-Deep microcosm experiment amended with TCE.

6.3 Microcosm Model

The microcosm models estimated the chlorinated ethene degradation parameters for the MLS12-Shallow, MLS22-Shallow, and MLS22-Deep microcosms. Predicted concentrations of the chlorinated ethenes were fit to the measured concentrations of the chlorinated ethenes from the continuous microcosms. The results from the three microcosm models are shown in Figures 6.8-6.10. The final estimated biodegradation rate parameters are shown in Tables 5.1-5.3. The generation of three values for each degradation parameter enabled the comparison of the degradation rates between three locations in the aquifer.

The maximum substrate utilization rate for PCE was the same for the three locations. While the PCE half saturation coefficients for the shallow microcosms were similar, the PCE half saturation coefficient for MLS22-Deep increased by a factor of two in comparison to the shallow microcosms. The higher half saturation coefficient suggests that deep aquifer sediment would degrade the PCE slower than the shallow aquifer sediment.

The TCE degradation parameters differed between the three microcosms because the detected quantities of TCE production were dissimilar between microcosms. The MLS12-Shallow microcosm followed the conventional reductive dechlorination process, which was the basis of the conceptual model for reductive dechlorination in SEAM3D. The maximum substrate utilization rate for TCE was similar to the maximum substrate utilization rate for PCE. The half saturation coefficient for TCE was smaller than PCE's by an order of magnitude which would indicate that low levels of TCE would be degraded faster than low levels of PCE. The MLS22 microcosms from the shallow and deep locations had small quantities of TCE detected. Therefore, the TCE amended microcosms were used to estimate the TCE degradation rates for the MLS22-Shallow and MLS22-Deep microcosms. These degradation rates were then applied to the PCE amended MLS22-Shallow and MLS22-Deep microcosms. However, manipulation of the inhibitory function of PCE on TCE degradation ($K_{PCE/TCE}$) could not simulate the observed TCE concentrations in the PCE amended microcosms as seen in Figures 6.11-6.12.

This inability to simulate the degradation of TCE by SEAM3D indicated that the TCE degradation in the microcosms did not follow the conceptual reductive dechlorination pathway of sequential

degradation. But rather, PCE was degraded to *cis*-1,2-DCE before the reduced chlorinated ethene was released to the aqueous environment. Holliger and Schumacher (1994) proposed that PCE degrading organisms produce *cis*-1,2-DCE through intracellular TCE production. Upon in vivo *cis*-1,2-DCE production, the cell releases the *cis*-1,2-DCE to the aqueous environment. In order to simulate the observed TCE concentrations in the MLS22 microcosms, the maximum specific utilization rate of TCE was artificially increased. Therefore, the reported values for TCE degradation do not reflect aqueous phase degradation rates. The rates could indicate intracellular rates of TCE degradation.

The maximum substrate utilization rate for *cis*-1,2-DCE were similar between the three microcosms. However, the half saturation coefficients differed between microcosms. These rates were determined by simulating the degradation of *cis*-1,2-DCE as the sole amended chlorinated ethene. Then, the maximum substrate utilization rate and half saturation coefficient were placed in a simulation beginning with PCE so that the inhibitory functions could be calibrated. However, the MLS22 microcosm model could not accurately predict the lag phase observed in *cis*-1,2-DCE degradation. Thus, the microbial population was included in the models for the MLS22 microcosms. Because no VC was detected in the MLS22 microcosms, no degradation parameters for VC for the MLS22 microcosms were calculated. Conversely, the production of VC in the MLS12-Shallow microcosm enabled the fitting of degradation parameters to VC.

The results of the microcosm models show that PCE and TCE degradation rates are higher than *cis*-1,2-DCE and VC degradation rates. This result was expected due to the indication of partial reductive dechlorination by the groundwater analysis. Haston and McCarty (1999) also reported higher degradation rates for PCE and TCE in comparison to *cis*-1,2-DCE and VC. Furthermore, the MLS22 microcosm data suggest that PCE may be directly converted to *cis*-1,2-DCE. Moreover, the microcosm models illustrate the variability in degradation rates and microorganism populations within Site 12.

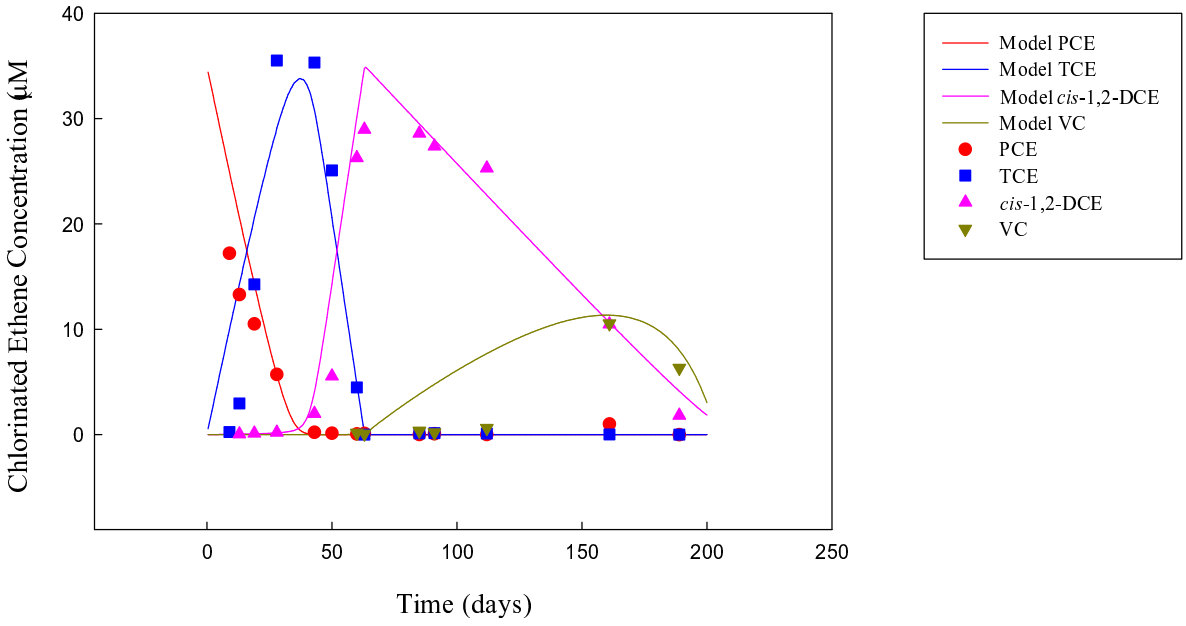

Figure 6.8: A comparison between measured (symbols) and predicted (lines) concentrations of the chlorinated ethenes in the MLS12-Shallow microcosm.

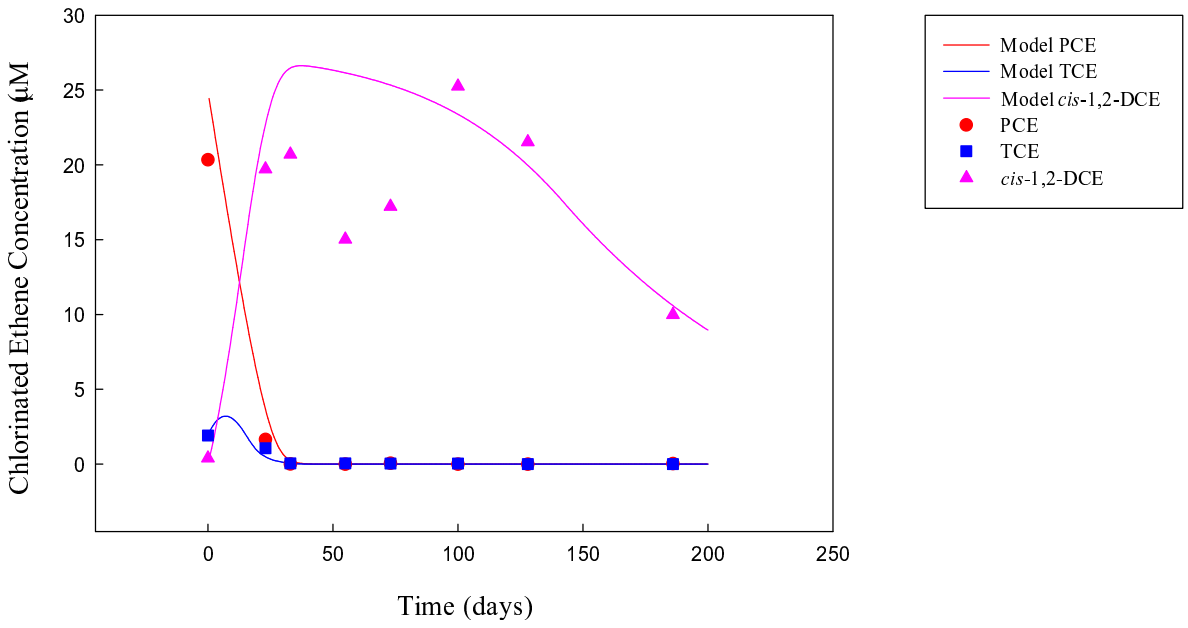

Figure 6.9: A comparison between measured (symbols) and predicted (lines) concentrations of the chlorinated ethenes in the MLS22-Shallow microcosm

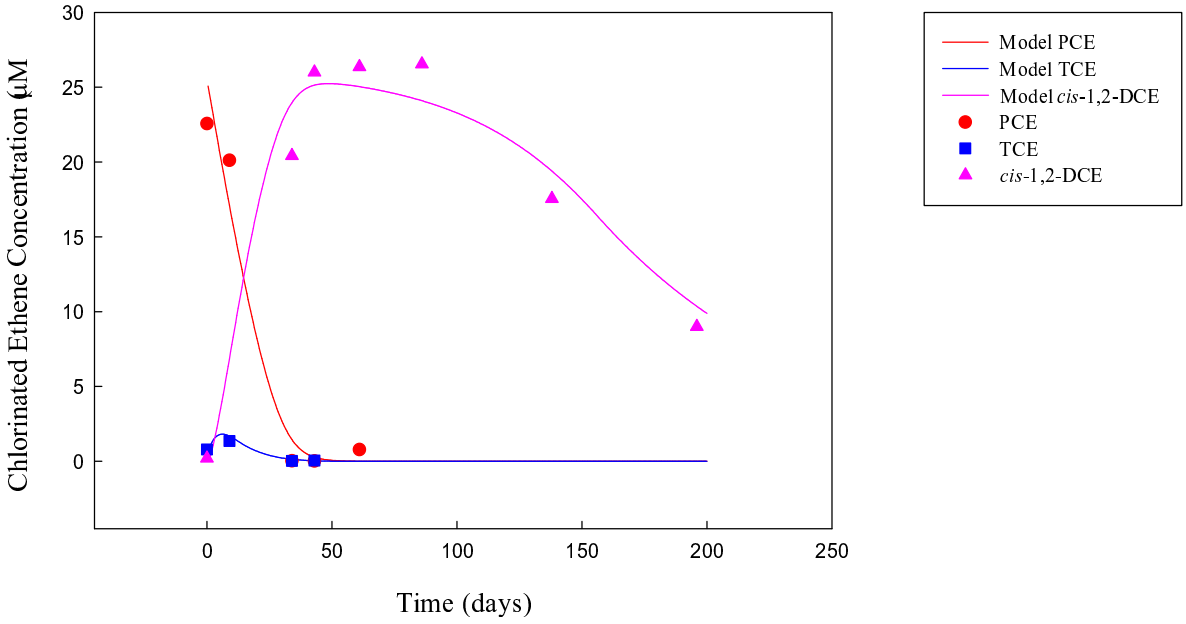

Figure 6.10: A comparison between measured (symbols) and predicted (lines) concentrations of the chlorinated ethenes in the MLS22-Deep microcosm

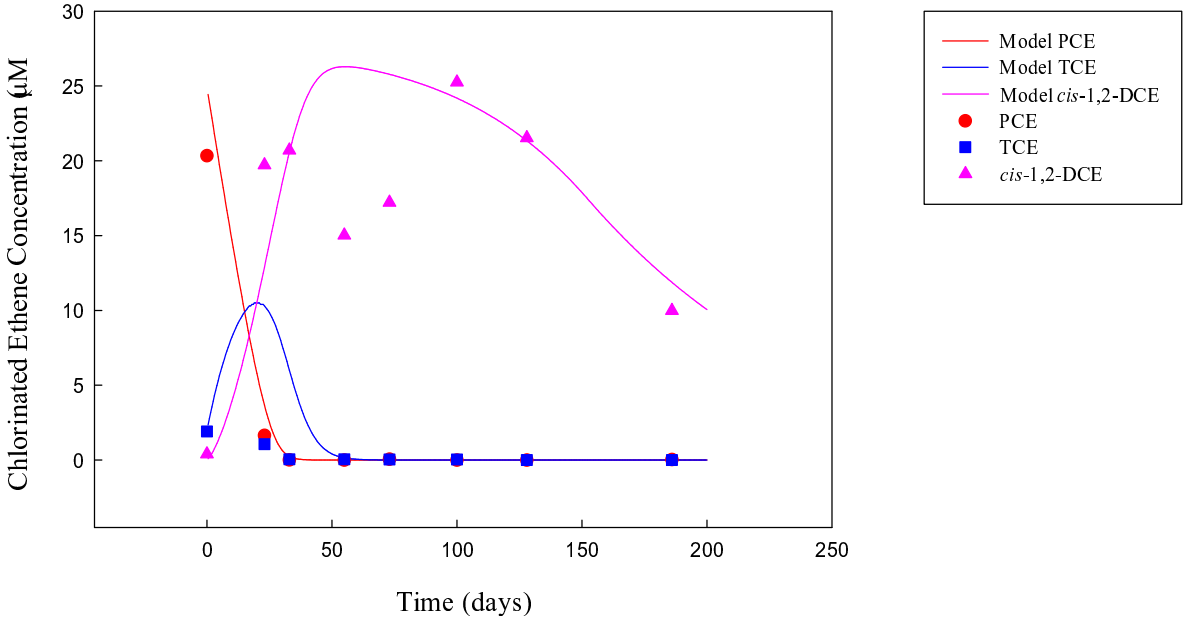

Figure 6.11: A comparison between measured (symbols) and predicted (lines) concentrations of the chlorinated ethenes in the MLS22-Shallow microcosm where TCE degradation rates were calculated based on the TCE amended microcosm.

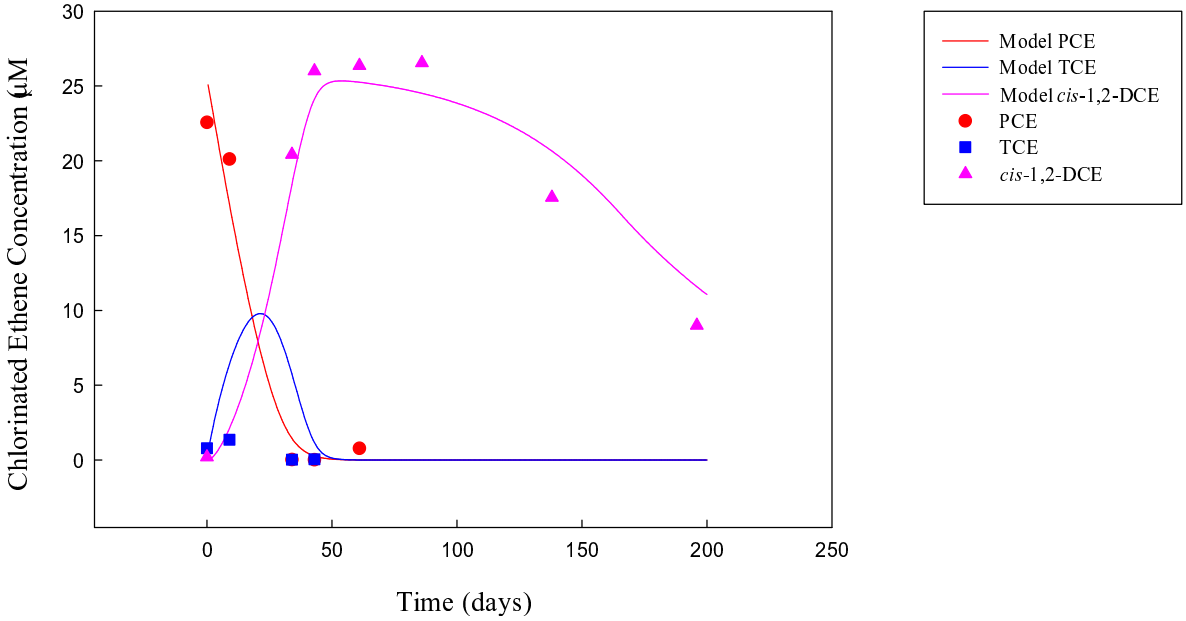

Figure 6.12: A comparison between measured (symbols) and predicted (lines) concentrations of the chlorinated ethenes in the MLS22-Deep microcosm where TCE degradation rates were calculated based on the TCE amended microcosm.

Chapter 7

Conclusions

To assess the potential of Monitored Natural Attenuation as a remediation strategy at Site 12, groundwater parameter analysis, microcosm experiments and three microcosm models were undertaken. In the groundwater analysis, contaminant characteristics and redox indicators were evaluated to assess the reductive dechlorination potential of Site 12. The microcosm experiments were designed to evaluate the extent of microbial degradation of the chlorinated ethenes at Site 12 and to provide concentration versus time data for the estimation of the chlorinated ethenes' biodegradation rates. The microcosm model used SEAM3D to simulate the results of the microcosm experiments (concentration versus time data) to estimate the biodegradation rates of PCE and its daughter products.

The groundwater analysis of the chlorinated ethenes indicated that there are at least two locations of high contamination within the source zone and the depth at which the high concentrations are detected was a result of the phase in which the PCE waste was released. Groundwater concentrations of the PCE, TCE and *cis*-1,2-DCE demonstrated reductive dechlorination activity at Site 12. Moreover, the contaminant distribution between the 1998, 1999, and 2000 sampling rounds exhibited a decrease in the extent of the plume over time. The decrease in total chlorinated ethene concentration at MLS locations between the 1998, 1999, and 2000 sampling rounds can be attributed to a combination of reductive dechlorination and radial groundwater flow pattern induced by the leaky sanitary sewer line. The ratios of chlorinated ethene parent compound to daughter product indicated a possible inhibitory relationship between elevated PCE levels (above 4000 μg/L) and *cis*-1,2-DCE and VC production. The low levels or non-detects of VC and ethene

suggested partial dechlorination may be occurring due to energy limitations in the aquifer, insignificant numbers of *cis*-1,2-DCE degrading microbes present throughout the aquifer, or inhibitory levels of PCE for *cis*-1,2-DCE and VC degradation. The redox indicators suggest that the aquifer TEAP differs with depth. Sulfate reduction appears to be prevalent in the upper five feet of the aquifer. A transitional zone between sulfate reduction and methanogenesis follows in the middle of aquifer. The lower five feet of the aquifer is dominated by methanogenic conditions. Observations of high CO_2 levels corresponding to VC and ethene detection suggest that anaerobic oxidation may be a contributing pathway to the biological transformation of *cis*-1,2-DCE and VC. Overall, the groundwater analysis indicated that Site 12 exhibits partial reductive dechlorination to *cis*-1,2-DCE and possible anaerobic oxidation of *cis*-1,2-DCE and VC to CO_2 under sulfate-reducing and methanogenic conditions.

The continuous microcosms established that biological transformation of the chlorinated solvent occurs in aquifer sediment sample from Site 12 at both MLS12 and MLS22. Degradation of PCE, TCE and *cis*-1,2-DCE were observed in the MLS12 experiments, as well as, production of TCE, *cis*-1,2-DCE, and VC. In the MLS22-Shallow and MLS22-Deep microcosms, partial degradation of the chlorinated ethenes (PCE and TCE) to *cis*-1,2-DCE was observed. The results of the microcosm experiments can be compared to the groundwater analysis to evaluate the consistency of the reductive dechlorination process between field and laboratory observations. As stated previously, the groundwater analysis detected PCE, TCE, DCE, and ethene at MLS11, MLS12, MLS20, and MLS22 and detected VC at MLS12 and MLS20. The MLS12-Shallow (8-12 ft bgs) microcosm produced TCE, DCE and VC from an original spike of PCE. However, the microcosms did not produce ethene. The groundwater analysis between 8 to 12 ft bgs detected PCE, TCE, DCE, VC and ethene. MLS22-Shallow (8-12 ft bgs) microcosms and groundwater both showed TCE and DCE production. The TCE production in the microcosms was minimal while the concentrations of TCE in the groundwater were substantial in comparison to the PCE concentrations. The TCE concentration in the groundwater in 2000 at a depth of 9 ft bgs was 50% of the PCE concentration (in mass units). Similarly, MLS22-Deep (18-22 ft bgs) microcosms and groundwater analysis produced TCE and DCE with small quantities of TCE in the microcosms and considerable quantities of TCE in the groundwater. VC was not observed in either MLS22 microcosm or in the groundwater. The MLS22 microcosms also did not produce ethene while ethene was observed in

the groundwater. Overall, the microcosms produced the same PCE daughter products that were observed in the groundwater analysis with the exceptions that the microcosms did not produce ethene and low TCE concentrations were observed in the MLS22 microcosms.

The microcosm results demonstrated the effects of PCE levels on subsequent chlorinated ethene degradation. In the MLS12-Shallow microcosm, the PCE levels were below 0.15 μM before *cis*-1,2-DCE production started and below 0.02 μM before VC production started. Conversely, the PCE amended MLS22-Shallow microcosm had *cis*-1,2-DCE production (19.72 μM) with a PCE level of 1.66 μM. The TCE amended MLS22-Shallow microcosm required a similar PCE level (0.16 μM) as the MLS12-Shallow microcosms. The MLS22-Deep microcosms exhibited PCE levels of 0.03 μM with *cis*-1,2-DCE production. Similarly, the groundwater analysis indicated a relationship between PCE levels (>4.14 μM) and inhibition of *cis*-1,2-DCE production. Furthermore, the groundwater data suggested a PCE threshold of 18 μM of aqueous PCE before VC production was observed. The MLS12-Shallow microcosm data also exhibited a PCE threshold before VC production, however the PCE threshold was 0.01 μM. These differences in PCE threshold concentrations between the groundwater and microcosms imply that the *cis*-1,2-DCE producing and degrading microorganisms may require a micro-environment similar to the microcosms aqueous concentration for reductive dechlorination and therefore are located in pockets within the aquifer matrix.

The microcosm models used the measured concentrations of the chlorinated ethenes over time from the continuous microcosms to fit the predicted concentrations of the chlorinated ethenes and generate biodegradation parameters for the chlorinated ethenes at MLS12-Shallow, MLS22-Shallow, and MLS22-Deep. The degradation parameters were based on Monod kinetics and illustrated the differences in the microbial population and degradation pathways between the MLS12 and MLS22, shallow and deep, locations. The MLS12-Shallow microcosm followed the conventional reductive dechlorination process, which was the basis of the conceptual model for reductive dechlorination in SEAM3D. Conversely, the TCE degradation in the MLS22 microcosms did not follow the conceptual reductive dechlorination pathway of sequential degradation. But rather, it is hypothesized that PCE was degraded to *cis*-1,2-DCE intracellularly then released to the aqueous environment. The results will serve as degradation rate input parameters for the Site 12 model.

In terms of the reductive dechlorination potential of Site 12, the combination of the groundwater

analysis and the microcosm experiments established that reductive dechlorination to *cis*-1,2-DCE is occurring under sulfate-reducing and methanogenic conditions, but degradation beyond *cis*-1,2-DCE is isolated to localized pockets within the aquifer. The groundwater analysis and microcosm experiments revealed these localized pockets of VC and ethene production which may be a result of isolated *cis*-1,2-DCE and VC degrading microorganisms. In both the MLS12-Shallow microcosms and the MLS12 groundwater data VC was observed, while no VC activity was observed in either the MLS22 microcosms or the MLS22 groundwater data. Furthermore, the groundwater and microcosm data also demonstrated that *cis*-1,2-DCE production is dependent on PCE levels. The groundwater data suggested PCE levels be below 4.14 μM for *cis*-1,2-DCE production while the microcosm data suggested that PCE levels should be below 1.66 μM. These differences in PCE threshold concentrations between the groundwater and microcosms further imply that the *cis*-1,2-DCE producing and degrading microorganisms may require a micro-environment in order to reductively dechlorinate *cis*-1,2-DCE and are subsequently located in pockets within the aquifer matrix. Therefore, despite the observed hydrogen levels throughout the aquifer, Site 12 is not an efficient system for complete reductive dechlorination. This lack of efficiency, as indicated by the groundwater and microcosm data, may stem from sparse microbial populations capable of reducing *cis*-1,2-DCE or the aquifer may contain levels of PCE which inhibit the further reduction of *cis*-1,2-DCE. Based on the observed inhibitory relationship between PCE and *cis*-1,2-DCE and VC production, source removal would reduce the PCE levels and encourage further reductive dechlorination at Site 12. Therefore, the recommended first step for a monitored natural attenuation-based remediation strategy at Site 12 should be source removal. The reduction in PCE mass and concentration will accelerate the remediation time frame and increase efficiency.

Chapter 8

Recommendations

Through the site assessment process, three areas called for further analysis. Based on the groundwater parameters analysis, the source area was shown to be complex and span over a considerable portion of the site. For a complete understanding of the source area, additional MLS samplers should be installed. One possible area for further investigation with a new MLS is in between MLS11 and the sewer along the groundwater flow path. Monitoring well data has indicated that this area also contains high concentrations of PCE, but without a MLS the vertical distribution of the contamination can not be understood. Secondly, anaerobic oxidation was suggested through the groundwater analysis but the design of the microcosms experiments did not enable the measurement of CO_2 that was generated specifically from anaerobic oxidation. Since the potential for anaerobic oxidation to contribute to the complete biodegradation of the chlorinated ethene to an innocuous end product is high, this avenue should be further studied. Radiolabed microcosm studies would determine the relative impact that this degradation mechanism has on the site. Finally, the extent of modeling in the thesis was limited to simulating the microcosm experiments. The modeling effort should be expanded to address the contaminant fate and transport for the entire site. This site model could evaluate the scenarios of fixing the leaky sewer and/or removing the source. Such scenarios would aid in assessing the long term remediation goals for the site.

Bibliography

Bradley, P. (2000). Microbial degradation of chloroethenes in groundwater systems. *Hydrogeology Journal 8*, 104–111.

Bradley, P. M. and F. H. Chapelle (1996). Anaerobic mineralization of vinyl chloride in Fe(III)-reducing, aquifer sediments. *Environmental Science and Technology 30*, 2084–2086.

Bradley, P. M. and F. H. Chapelle (1997). Kinetics of DCE and VC mineralization under methanogenic and Fe(III)-reducing conditions. *Environmental Science and Technology 31*, 2692–2696.

Bradley, P. M. and F. H. Chapelle (1998a). Effect of contaminant concentration on aerobic microbial mineralization of DCE and VC in stream-bed sediments. *Environmental Science and Technology 31*, 2692–2696.

Bradley, P. M. and F. H. Chapelle (1998b). Microbial mineralization of VC and DCE under different terminal electron accepting conditions. *Anaerobe 4*, 81–87.

Bradley, P. M. and F. H. Chapelle (2000). Aerobic microbial mineralization of dichloroethene as sole carbon substrate. *Environmental Science and Technology 34*, 221–223.

Bradley, P. M., F. H. Chapelle, and D. R. Lovely (1998). Humic acids as electron acceptors for anaerobic microbial oxidation of vinyl chloride and dichloroethene. *Applied and Environmental Microbiology 64*, 3102–3105.

Butler, E. and K. Hayes (1999). Kinetics of the transformation of trichloroethylene and tetrachloroethylene by iron sulfide. *Environmental Science and Technology 33*, 2021–2027.

Cabirol, N., F. Jocab, J. Perrier, B. Fouillet, and P. Chambon (1998). Interaction between methanogenic and sulfate-reducing microorganisms during dechlorination of a high concentration of tetrachloroethylene. *Journal of Applied Microbiology 44*, 297–301.

Cabirol, N., J. Perrier, F. Jacob, B. Fouillet, and P. Chambon (1996). Role of methanogenic and sulfate-reducing bacteria in the reductive dechlorination of tetrachloroethylene in mixed culture. *Bullet of Environmental Contaminant Toxicology 56*, 817–824.

CH2MHill (2000, January). Draft supplemental remedial investigation for site 12. Technical report, CH2MHill.

Chapelle, F. H. and P. M. Bradley (1998). Selecting remediation goals by assessing the natural attenuation capacity of groundwater systems. *Bioremediation Journal 2*, 227–238.

Chapelle, F. H., P. B. McMahon, N. M. Dubrovsky, R. F. Fujii, E. T.Oaksford, and D. A. Vroblesky (1995). Deducing the distribution of terminal electron-accepting processes in hydrologically diverse groundwater systems. *Water Resources Research 31*, 359–371.

deBruin, W. P., M. J. Kotterman, M. A. Posthumus, G. Schraa, and A. Zehnder (1992). Complete biological reductive transformation of tetrachloroethene to ethane. *Applied and Environmental Microbiology 58*, 1996–2000.

EPA., U. (1998). Technical protocol for evaluating natural attenuation of chlorinated solvents in groundwater. *EPA/600/R-98/128*.

Fennell, D. and J. Gossett (1997). Comparison of butyric acid, ethanol, lactic acid, and propionic acid as hydrogen donors for the reductive dechlorination of tetrachloroethene. *Environmental Science and Technology 31*, 918–926.

Fetzner, S. (1998). Bacterial dehalogenation. *Applied Microbiology and Biotechnology 50*, 633–657.

Gao, J., R. Skeen, B. Hooker, and R. Quesenberry (1997). Effects of several electron donors on tetrachloroethylene dechlorination in anaerobic soil microcosms. *Water Resources 31*, 2479–2486.

Harkness, M., A. Bracco, M. Brennan, K. Deweerd, and J. Spivack (1999). Use of bioaugmentation to stimulate complete reductive dechlorination of trichloroethene in Dover soil columns. *Environmental Science and Technology 33*, 1100–1109.

Haston, Z. and P. L. McCarty (1999). Chlorinated ethene half-velocity coefficients for reductive dechlorination. *Environmental Science and Technology 33*, 223–226.

Hollinger, C. and W. Schumacher (1994). Reductive dehalogenation as a repiratory process. *Antonie van Leeuwenhoek 66*, 239–246.

Lendvay, J., S. Dean, and P. Adriaens (1998). Temporal and spatial trend in biogeochemical conditions at a groundwater-surface water interface: implications for natural bioattenuation. *Environmental Science and Technology 32*, 3472–3478.

Magnuson, J., R. Stern, J. Gossett, S. Zinder, and D. Burris (1998). Reductive dechlorination of tetrachloroethene to ethene by a two-component enzyme pathway. *Applied and Environmental Microbiology 64*, 1270–1275.

Smatlak, C. R., J. M. Gossett, and S. H. Zinder (1996). Comparative kinetics of hydrogen utilization for reductive dechlorination of tetrachloroethene and methanogenesis in an anaerobic enrichment culture. *Environmental Science and Technology 30*, 2850–2858.

Widdowson, M. A., J. T. Novak, D. F. Berry, H. V. Rectanus, and F. Wang (2000, July). Task 4 report. Technical report, Virginia Tech.

Wu, W., M. Kitagawa, S. Taniguchi, and M. K. Jain (1998). Anaerobic dechlorination of perchloroethylene (PCE) in soil by a dechlorinating microbial consortium. *Journal of Fermentation and Bioengineering 86*, 588–594.

Yager, R., S. E. Bilotta, C. Mann, and E. Madsen (1997). Metabolic adaption and in situ attenuation of chlorinated ethenes by naturally occurring microorganisms in a fractured dolomite aquifer near Niagara Falls, New York. *Environmental Science and Technology 31*, 3138–3147.

Yang, Y. and P. L. McCarty (1998). Competition for hydrogen within a chlorinated solvent dehalogenating anaerobic mixed culture. *Environmental Science and Technology 32*, 3591–3597.

Appendix A

Groundwater Data

Table A.1: Chlorinated ethene groundwater data for the 1998 sampling round

z (feet)	MLS	PCE (ppb)	TCE (ppb)	cDCE (ppb)	tDCE (ppb)	1,1-DCE (ppb)	VC (ppb)
-9.3	10	0	1.3	0	0	0	0
-6.8	10	0	13	0	0	0	0
-4.3	10	0	17	0	0	0	0
-1.8	10	0	14	0	0	0	0
0.7	10	0	8.5	0	0	0	0
3.2	10	0	0	0	0	0	0
-10.8	11	150	0	0	0	0	0
-8.3	11	89	4.7	0	0	0	0
-5.8	11	390	13	0	0	0	0
-3.3	11	580	12	10	0	0	0
-0.8	11	1700	62.6	22.2	0	0	0
1.7	11	9900	47.1	15.2	0	0	0
4.2	11	4000	66.4	20.6	0	0	0
-9.8	12	23000	1300	193	0	0	0
-7.3	12	3800	620	0	0	0	0
-4.8	12	352	43.9	0	0	0	0
-2.3	12	330	240	0	0	0	0
-0.2	12	2300	840	532	11.6	0	74.9
2.7	12	2700	1000	440	18.4	0	104.4
-10.8	20	2467	570	97.5	17.3	1.8	7.7
-8.3	20	2775	370	70	12.6	0.8	4.8
-5.8	20	1381	159	24	7	0.5	2.5
-3.3	20	433	56	10.4	2.1	0.2	0.9
-0.8	20	5.84	76	11.6	2.4	0	1.2
1.7	20	754	129.5	21.3	4.5	0	1.2
4.2	20	578	101	16.4	3.5	0	0

Table A.2: TEAP parameters for the 1998 sampling round-Part A

MLS	DO (mg/L)	T (degree C)	pH	CO2 (mg/l)	CH4 (mg/l)	Ethane (ng/l)	Ethene (ng/l)	H2 (nm/l)	Fe ll (mg/l)
10	0.93	22	5.97	88.23	0.017	37.8	27.9	6.28	5.61
10	0.66	22.2	5.86	111.78	0.003	29.3	28.3	9.63	7.62
10	0.5	22.4	5.3	128.27	0.002	22.5	29.7	4.41	2.05
10	0.45	22.2	5.36	123.99	0.001	45.1	35.2	4.94	4.93
10	0.53	22.8	5.51	107.87	0.002	160.3	101.9	4.54	7.8
10	0.72	24	5	153.29	0.001	102.6	31.8	10.39	5.5
11	0.45	23	6.22	63.1	0.03727	32.1	52.1	4.87	11.5
11	0.47	23.5	5.73	82.5	0.00979	17.2	30.6	4.53	6.73
11	0.42	24	5.4	101.8	0.00187	40.8	51.1	3.07	4.24
11	0.45	24.7	5.38	112.8	0.00335	30.4	80.4	3.34	4.41
11	0.38	25.7	5.5	126.4	0.00212	117.6	105.9	4.04	7.32
11	0.49	27.9	5.48	82.8	0.00124	78.9	53.4	3.31	2.67
11					0.0021	84.5	92.8	3.9	6.39
12	0.37	22.9	5.93	72.2	0.03	219.6	457.2	6.19	9.81
12	0.56	25.1	5.75						11.1
12									1.21
12	0.37	23.8	5.56	106.8	0.003	89.9	219.6	6.2	9.83
12	0.37	24.6	5.69	120	0.023	512.4	3965.3	7.57	13.5
12	0.43	26.2	6.04	106.9	0.058	553.5	42692.3	4.4	9.61
20	0.2	21	5.9						7.06
20	0.2	21	5.8						3.88
20	0.2	21	5.5						3.3
20	0.2	21	5.5						6.5
20	0.2	21	5.7						14.4
20	0.2	23	5.6						7.97
20	0.2	24	6						8.19

Table A.3: TEAP parameters for the 1998 sampling round-Part B

MLS	Chloride (mg/l)	Nitrite (mg/l)	Nitrate (mg/l)	Sulfate (mg/l)	Sulfide (ppm)	Alkalinity (ppm)
10	24.8	<0.5	<0.5	43.3	<0.06	20
10	26.6	<0.5	<0.5	57.5	<0.06	25
10	28.8	<0.5	<0.5	68.2	<0.06	<10
10	28.1	<0.5	0.5	89.4	<0.06	<10
10	27.1	<0.5	0.5	79.5	<0.06	11
10	48.3	<0.5	0.9	161	<0.06	<10
11	24.3	0.5	<0.5	4.38	<0.06	22
11	25.8	0.5	0.5	15.3	<0.06	12
11	25.7	0.5	0.5	28.6	<0.06	10
11	25.7	0.5	0.5	45.3	<0.06	11
11	26.6	0.5	0.5	58.1	<0.06	13
11	32.6	0.5	1.55	50.6	<0.06	<10
11	28.2	0.5	0.58	52.1	<0.06	<10
12	62.4	0.5	<0.5	25	<0.06	20
12	44.5	0.5	0.28	35.5	<0.06	27
12	30		1.11	59.6		12
12	30.3	0.5	<0.5	57	<0.06	19
12	32.2	0.5	0.5	70.1	<0.06	25
12	24.6	0.5	0.5	67.8	<0.06	27
20	41.2		<0.05	26.2	<0.2	46
20	37		<0.05	27.2	<0.2	40
20	26.9		<0.05	22.7	<0.2	36
20	19		<0.05	28.8	<0.2	44
20	20.4		<0.05	31.9	<0.2	34
20	23.7		<0.05	38.2	<0.2	66
20	23.5		0.35	66.5	<0.2	48

Table A.4: Chlorinated ethene groundwater data for the 1999 sampling round

z (feet)	MLS	PCE (ppb)	TCE (ppb)	cDCE (ppb)	tDCE (ppb)	1,1-DCE (ppb)	VC (ppb)
-9.3	10	0	0	0	0	0	0
-6.8	10	0	12	1.1	0	0	0
-4.3	10	0	12	1.7	0	0	0
-1.8	10	0	8.7	1.5	0	0	0
0.7	10	0	3.5	0	0	0	0
3.2	10	0	0	0	0	0	0
7.8	10	0	0	0	0	0	0
-10.8	11	400	0	0	0	0	0
-8.3	11	380	0	0	0	0	0
-5.8	11	310	13	0	0	0	0
-3.3	11	940	0	0	0	0	0
-0.8	11	600	21	0	0	0	0
1.7	11	1400	19	0	0	0	0
4.2	11	12000	0	0	0	0	0
-9.8	12	12000	1300	110	0	0	0
-7.3	12	4400	280	0	0	0	0
-4.8	12	130	31	0	0	0	0
-2.3	12	81	33	0	0	0	0
-0.2	12	340	260	220	0	0	6.8
2.7	12	490	270	310	0	0	57
-9.9	22	2000	790	0	0	0	0
-7.4	22	8800	1700	110	0	0	0
-2.4	22	2800	730	35	0	0	0
0.1	22	4800	790	57	0	0	0
2.6	22	2500	350	29	0	0	0
5.1	22	4400	620	0	0	0	0
-10.8	20	1200	350	110	0	0	0
-8.3	20	3400	630	130	26	0	0
-5.8	20	860	86	30	0	0	0
-3.3	20	13	1.2	0	0	0	0
-0.8	20	6.8	1.4	0	0	0	0
1.7	20	6.8	4.2	1.6	0	0	0

Table A.5: TEAP parameters for the 1999 sampling round

MLS	CO2 (mg/L)	Methane (μg/L)	Ethane (ng/L)	Ethene (ng/L)	Hydrogen (nM)	Chloride (mg/L)	Nitrite (mg/L)	Nitrate (mg/L)	Sulfate (mg/L)	Sulfide (mg/L)
10	141.98	122.352	26	0		26.6	0	0	21.7	0.09
10	122.58	12.263	0	78		28	0	0	91.4	0.13
10	143.79	2.36	0	0		28	0	0	91.8	0.11
10	167.51	1.639	0	39		33.5	0	0.54	110	0.13
10	205.24	0.884	0	0		49.6	0	0	79.5	0.11
10	188.32	0.306	50	0		56.5	0	0.972	80.7	0.13
10	154.9	0.041	0	0		55.8	0	4.51	121	0.09
11	66.17	0.397	0	0		25	0	0	6.13	0.14
11	102.61	39.578	0	0		25.6	0	0	12.6	0.14
11	122.17	2.971	0	0		25.1	0	0	21	0.12
11	145.07	4.79	0	37		26.3	0	0	46.6	0.12
11	162.89	4.23	0	48		25.8	0	0	62	0.08
11	151.25	20.054	28	28		27	0	0	69.2	0.1
11	193.29	0.187	61	0		38.5	0	2.16	81.4	0.1
12	65.78	95.8	79	211	2.1	74.2	0	0	11.1	0.12
12	103.65	80.3	0	33	4.02	41.7	0	0	41.9	0.12
12	126.01	1.209	0	13	4.5	27.7	0	0	69.4	0.09
12	116.16	0.554	0	15	1.73	25.1	0	0	109	0.11
12	121.38	27.249	79	1606	3.65	25.1	0	0	109	0.11
12	99.51	61.13	171	18806	1.26	25.1	0	0	109	0.11
22	38.09	115.839	460	634		31.3			31.4	0.12
22	58.52	39.519	1444	2276		37.1			30.2	0.09
22	59.13	28.708	387	568		27.2			41.5	0.11
22	101.66	20.882	572	513		28.6			49.6	0.09
22	117.1	6.061	390	285		24.7		0.527	57.5	0.09
22	77.79	11.47	661	590		26.8			39.3	0.1
20	63.29	504.1	108	281	4.18	62.1			10.1	0.12
20	74.76	550.7	45	129	2.45	50.2			30.1	0.2
20	91.32	150.4	7	49	1.51	22.6			18.9	0.13
20	56.45	195.7	0	0	1.01	12.8			17.9	0.13
20	17.28	1870	0	0	2.27	13.4			5.48	0.11
20	22.31	1789.1	0	0	3.93	16.6			5.85	0.13

Table A.6: Chlorinated ethene groundwater data for the 2000 sampling round

z (feet)	MLS	VC (ppb)	1,1-DCE (ppb)	*trans*-1,2,DCE (ppb)	*cis*-1,2-DCE (ppb)	TCE (ppb)	PCE (ppb)
-9.30	10	0.00	0.00	0.00	0.00	0.00	36.86
-6.80	10	0.00	0.00	0.00	0.00	41.77	0.00
-4.30	10	0.00	0.00	0.00	0.00	44.79	0.00
-1.80	10	0.00	0.00	0.00	126.96	0.00	0.00
0.70	10	0.00	0.00	0.00	195.94	0.00	0.00
3.20	10	0.00	0.00	0.00	90.53	0.00	0.00
-10.80	11	0.00	0.00	0.00	0.00	0.00	683.45
-8.30	11	0.00	0.00	0.00	0.00	22.10	644.94
-5.80	11	0.00	0.00	0.00	0.00	34.53	1718.64
-3.30	11	0.00	0.00	0.00	0.00	66.10	923.27
-0.80	11	0.00	0.00	0.00	0.00	70.28	492.04
1.70	11	0.00	0.00	0.00	0.00	64.23	782.46
4.20	11	0.00	0.00	0.00	0.00	72.57	4416.05
-9.80	12	0.00	0.00	0.00	140.37	1247.11	6031.98
-7.30	12	0.00	0.00	0.00	41.38	460.12	5684.60
-4.80	12	0.00	0.00	0.00	0.00	44.03	85.19
-2.30	12	0.00	0.00	0.00	0.00	42.08	19.75
-0.20	12	0.00	0.00	0.00	156.93	108.44	109.15
2.70	12	0.00	0.00	0.00	325.69	225.55	308.55
-9.90	22	0.00	0.00	0.00	347.69	1221.06	1141.01
-7.40	22	0.00	0.00	12.41	403.71	4285.83	8627.19
-2.40	22	0.00	0.00	0.00	0.00	179.25	699.97
0.10	22	0.00	0.00	0.00	0.00	84.34	17.05
2.60	22	0.00	0.00	0.00	0.00	0.00	7.54
5.10	22	0.00	0.00	0.00	343.26	181.39	1044.03
-10.80	20	0.00	0.00	0.00	90.68	0.00	21.92
-8.30	20	238.70	0.00	4.23	699.08	664.71	1342.63
-5.80	20	0.00	0.00	0.00	86.03	163.13	769.12
-3.30	20	0.00	0.00	0.00	69.15	34.54	69.31
-0.80	20	0.00	0.00	0.00	65.59	35.05	14.88
1.70	20	0.00	0.00	2.56	78.98	22.25	3.12

Table A.7: TEAP parameters for the 2000 sampling round

MLS	T (C)	pH	D.O. (mg/L)	Hydrogen (nM)	Chloride (mg/L)	Nitrite (mg/L)	Nitrate (mg/L)	Sulfate (mg/L)	Sulfide (mg/L)	Ferrous Iron (mg/L)
10	18.00	5.78	0.00	7.70	30.88	0.00	0.10	31.99	0.04	6.63
10	18.00	5.68	0.00	6.70	26.45	0.00	0.10	32.85	0.05	10.20
10	18.00	5.59	0.00	4.20	32.36	0.00	0.00	88.87	0.00	2.16
10	19.00	5.37	0.10	14.40	36.73	0.10	0.38	110.29	0.01	2.25
10	19.00	5.37	0.20	8.90	37.13	0.00	0.16	93.85	0.00	2.82
10	17.50	5.34	0.00	11.90	44.76	0.00	0.40	104.42	0.01	5.71
11	17.00	6.22	0.00	10.50	28.92	0.00	0.00	11.47	0.00	9.71
11	17.00	5.80	0.00	10.80	27.78	0.00	0.00	15.67	0.03	3.71
11	17.00	5.35	0.00	9.80	30.26	0.00	0.10	34.42	0.00	2.18
11	20.00	5.13	0.20	11.70	30.23	0.32	0.19	47.78	0.00	1.23
11	19.00	5.23	0.00	13.20	40.42	0.00	0.00	87.13	0.00	11.09
11	20.00	5.24	0.20	9.60	33.47	0.29	0.41	75.44	0.04	3.85
11	20.00	5.42	0.00	7.30	36.21	0.28	1.50	46.43	0.01	3.32
12	21.00	6.11	0.00	16.40	48.99	0.10	0.10	21.28	0.02	10.46
12	21.00	5.95	0.10	16.30	41.18	0.00	0.13	43.28	0.02	5.14
12	21.00	5.08	0.40	15.90	30.55	0.00	0.42	78.75	0.02	1.18
12	22.00	5.62	0.00	12.80	28.35	0.00	0.10	90.68	0.01	2.21
12	22.00	5.18	0.00	12.10	27.65	0.00	0.00	79.79	0.01	3.00
12	22.00	5.73	0.00	10.10	28.61	0.00	0.10	57.74	0.03	3.29
22	17.00	5.86	0.40	7.40	29.16	0.00	0.00	17.48	0.03	11.93
22	19.00	5.77	0.20	6.50	35.82	0.00	0.00	17.39	0.01	4.61
22	18.00	5.41	0.40	5.90	23.74	0.00	0.00	21.69	0.04	5.09
22	17.00	5.65	0.30	3.20	19.62	0.00	0.00	22.70	0.00	21.20
22	17.00	5.81	0.30	4.50	21.34	0.00	0.00	19.63	0.01	6.61
22	16.00	5.73	0.30	4.70	22.71	0.00	0.00	19.21	0.00	28.57
20	18.00	6.54	0.00	13.50	45.42	0.00	0.73	32.27	0.04	37.29
20	17.00	6.77	0.00	17.70	56.20	0.00	0.10	29.12	0.01	31.36
20	17.00	6.24	0.00	8.30	33.96	0.00	0.00	67.30	0.02	31.96
20	15.00	6.12	0.10	11.50	32.86	0.00	0.00	76.54	0.00	38.20
20	15.00	6.35	0.00	11.20	30.81	0.00	0.00	76.67	0.00	38.32
20	15.00	6.38	0.00	7.10	34.31	0.10	0.10	49.94	0.14	28.04

Appendix B

Microcosm Data

Table B.1: Concentration (μM) versus time data for MLS12-Shallow PCE amended microcosm

MicroAbbr	ContamAbbr	Day	VC	1,1 DCE	tDCE	cDCE	TCE	PCE
MLS12-S	PCE-2	9	0.00	0.00	0.00	0.00	0.25	17.22
MLS12-S	PCE-2	13	0.00	0.00	0.00	0.06	2.96	13.31
MLS12-S	PCE-2	19	0.00	0.00	0.00	0.12	14.26	10.53
MLS12-S	PCE-2	28	0.00	0.00	0.00	0.22	35.52	5.73
MLS12-S	PCE-2	43	0.00	0.69	0.00	2.00	35.32	0.23
MLS12-S	PCE-2	50	0.00	0.00	0.00	5.56	25.08	0.15
MLS12-S	PCE-2	51	0.00	0.00	0.00	0.66	0.00	0.69
MLS12-S	PCE-2	60	0.15	0.02	0.00	26.27	4.48	0.08
MLS12-S	PCE-2	63	0.08	0.00	0.00	28.97	0.00	0.13
MLS12-S	PCE-2	85	0.35	0.00	0.00	28.61	0.12	0.02
MLS12-S	PCE-2	91	0.20	0.00	0.00	27.37	0.14	0.09
MLS12-S	PCE-2	112	0.61	0.00	0.00	25.29	0.11	0.02
MLS12-S	PCE-2	161	10.53	0.02	0.00	10.48	0.02	1.02
MLS12-S	PCE-2	189	6.32	0.00	0.00	1.83	0.00	0.00
MLS12-S	PCE-2	247	0.50	0.00	0.00	0.18	0.00	0.00

Table B.2: Concentration (μM) versus time data for Controls of MLS12-Shallow PCE amended microcosm

MicroAbbr	ContamAbbr	Day	VC	1,1 DCE	tDCE	cDCE	TCE	PCE
C MLS12-S	PCE	10	0.00	0.00	0.00	0.00	0.00	22.77
C MLS12-S	PCE	20	0.00	0.00	0.00	0.00	0.04	20.86
C MLS12-S	PCE	24	0.00	0.00	0.00	0.00	0.10	23.15
C MLS12-S	PCE	53	0.00	0.00	0.00	0.00	0.01	23.13
C MLS12-S	PCE	72	0.00	0.00	0.00	0.00	0.01	20.13
C MLS12-S	PCE	93	0.00	0.00	0.00	0.00	0.02	8.80
C MLS12-S	PCE	108	0.00	0.00	0.00	0.00	0.04	22.76
C MLS12-S	PCE	206	0.00	0.00	0.00	0.00	0.44	12.93

Table B.3: Concentration (μM) versus time data for MLS12-Shallow TCE amended microcosm

MicroAbbr	ContamAbbr	Day	VC	1,1 DCE	tDCE	cDCE	TCE	PCE
MLS12-S	TCE-1	9	0.00	0.00	0.00	0.00	15.75	0.25
MLS12-S	TCE-1	13	0.00	0.00	0.00	0.06	7.95	0.49
MLS12-S	TCE-1	20	0.00	0.00	0.00	0.16	17.20	0.53
MLS12-S	TCE-1	28	0.17	0.00	0.00	0.18	27.79	0.47
MLS12-S	TCE-1	37	0.00	0.00	0.00	1.45	30.94	0.35
MLS12-S	TCE-1	43	0.00	1.01	0.00	9.85	18.99	0.11
MLS12-S	TCE-1	50	0.00	0.08	0.00	23.93	0.76	0.07
MLS12-S	TCE-1	51	0.00	0.00	0.00	1.70	0.00	0.08
MLS12-S	TCE-1	60	0.04	0.07	0.00	23.21	0.18	0.33
MLS12-S	TCE-1	63	0.08	0.07	0.00	23.70	0.27	0.29
MLS12-S	TCE-1	85	1.34	0.11	0.00	16.56	0.02	0.30
MLS12-S	TCE-1	91	6.31	0.18	0.00	12.23	0.05	0.00
MLS12-S	TCE-1	112	0.67	0.00	0.00	0.00	0.02	0.04
MLS12-S	TCE-1	147	3.40	0.87	0.00	16.37	0.00	0.00
MLS12-S	TCE-1	148	4.41	0.63	0.00	11.85	2.28	0.04

Table B.4: Concentration (μM) versus time data for Controls of MLS12-Shallow TCE amended microcosm

MicroAbbr	ContamAbbr	Day	VC	1,1 DCE	tDCE	cDCE	TCE	PCE
CMLS12-S	TCE	10	0.00	0.00	0.00	0.00	30.00	0.00
CMLS12-S	TCE	49	0.00	0.00	0.00	0.00	32.10	0.13
CMLS12-S	TCE	59	0.00	0.00	0.00	0.00	29.28	0.43
CMLS12-S	TCE	63	0.00	0.00	0.00	0.00	26.77	0.39
CMLS12-S	TCE	92	0.00	0.00	0.00	0.00	34.50	0.15
CMLS12-S	TCE	111	0.00	0.00	0.00	0.00	25.28	0.00
CMLS12-S	TCE	132	0.00	0.00	0.00	0.00	27.30	0.64
CMLS12-S	TCE	147	0.00	0.00	0.00	0.00	27.67	0.00
CMLS12-S	TCE	245	0.00	0.00	0.00	0.00	15.46	0.05

Table B.5: Concentration (μM) versus time data for MLS22-Shallow PCE amended microcosm

MicroAbbr	ContamAbbr	Day	VC	1,1 DCE	tDCE	cDCE	TCE	PCE
MLS22-S	PCE-2	11	0.00	0.00	0.00	0.00	0.00	15.64
MLS22-S	PCE-2	14	0.00	0.00	0.00	0.29	0.00	17.72
MLS22-S	PCE-2	20	0.00	0.00	0.00	0.00	0.00	19.19
MLS22-S	PCE-2	29	0.00	0.00	0.00	0.00	0.00	27.21
MLS22-S	PCE-2	38	0.00	0.00	0.00	0.00	0.07	21.18
MLS22-S	PCE-2	44	0.13	0.00	0.00	0.03	0.53	20.73
MLS22-S	PCE-2	61	0.00	0.00	0.00	0.39	1.92	20.35
MLS22-S	PCE-2	84	0.00	0.00	0.00	19.72	1.07	1.66
MLS22-S	PCE-2	94	0.00	0.00	0.00	20.71	0.05	0.02
MLS22-S	PCE-2	116	0.00	0.00	0.00	15.02	0.05	0.00
MLS22-S	PCE-2	134	0.00	0.00	0.00	17.22	0.04	0.07
MLS22-S	PCE-2	161	0.00	0.00	0.00	25.26	0.04	0.00
MLS22-S	PCE-2	189	0.00	0.00	0.00	21.53	0.00	0.00
MLS22-S	PCE-2	247	0.00	0.05	0.00	9.98	0.00	0.04

Table B.6: Concentration (μM) versus time data for Controls of MLS22-Shallow PCE amended microcosm

MicroAbbr	ContamAbbr	Day	VC	1,1 DCE	tDCE	cDCE	TCE	PCE
CMLS22-S	PCE	10	0.00	0.00	0.00	0.00	0.02	29.77
CMLS22-S	PCE	20	0.00	0.00	0.00	0.00	0.00	26.56
CMLS22-S	PCE	23	0.00	0.00	0.00	0.00	0.04	18.84
CMLS22-S	PCE	52	0.00	0.00	0.00	0.00	0.05	24.16
CMLS22-S	PCE	71	0.00	0.00	0.00	0.00	0.08	20.16
CMLS22-S	PCE	92	0.00	0.00	0.00	0.00	0.04	16.01
CMLS22-S	PCE	107	0.00	0.00	0.00	0.00	0.04	19.49
CMLS22-S	PCE	205	0.00	0.00	0.00	0.00	0.11	11.21

Table B.7: Concentration (μM) versus time data for MLS22-Shallow TCE amended microcosm

MicroAbbr	ContamAbbr	Day	VC	1,1 DCE	tDCE	cDCE	TCE	PCE
MLS22-S	TCE-1	11	0.00	0.00	0.00	0.00	15.30	0.55
MLS22-S	TCE-1	14	0.00	0.00	0.00	0.06	20.98	0.31
MLS22-S	TCE-1	20	0.00	0.00	0.00	0.00	31.74	0.27
MLS22-S	TCE-1	29	0.00	0.00	0.00	0.00	32.43	0.52
MLS22-S	TCE-1	38	0.00	0.00	0.00	0.00	26.98	0.27
MLS22-S	TCE-1	44	0.00	0.00	0.00	0.10	25.04	5.12
MLS22-S	TCE-1	61	0.00	0.00	0.00	18.81	2.59	0.16
MLS22-S	TCE-1	84	0.00	0.00	0.00	24.97	0.00	0.02
MLS22-S	TCE-1	94	0.00	0.05	0.00	17.80	0.05	0.05
MLS22-S	TCE-1	116	0.00	0.00	0.00	13.63	0.01	0.02
MLS22-S	TCE-1	134	0.00	0.00	0.00	17.87	0.00	0.02
MLS22-S	TCE-1	161	0.00	0.00	0.00	21.64	0.00	0.00
MLS22-S	TCE-1	189	0.00	0.00	0.00	16.65	0.00	0.01
MLS22-S	TCE-1	247	0.00	0.04	0.00	7.08	0.00	0.00

Table B.8: Concentration (μM) versus time data for Controls of MLS22-Shallow TCE amended microcosm

MicroAbbr	ContamAbbr	Day	VC	1,1 DCE	tDCE	cDCE	TCE	PCE
CMLS22-S	TCE	10	0.00	0.00	0.00	0.00	30.00	0.25
CMLS22-S	TCE	59	0.00	0.00	0.00	0.00	33.54	0.53
CMLS22-S	TCE	63	0.00	0.00	0.00	0.00	33.38	0.09
CMLS22-S	TCE	92	0.00	0.00	0.00	0.00	33.50	0.00
CMLS22-S	TCE	111	0.00	0.00	0.00	0.00	26.79	0.02
CMLS22-S	TCE	132	0.00	0.00	0.00	0.00	26.40	0.00
CMLS22-S	TCE	147	0.00	0.00	0.00	0.00	20.00	0.00
CMLS22-S	TCE	245	0.00	0.00	0.00	0.00	16.00	0.00

Table B.9: Concentration (μM) versus time data for MLS22-Deep PCE amended microcosm

MicroAbbr	ContamAbbr	Day	VC	1,1 DCE	tDCE	cDCE	TCE	PCE
MLS22-D	PCE-2	10	0.00	0.00	0.00	0.00	0.00	15.63
MLS22-D	PCE-2	14	0.00	0.00	0.00	0.00	0.08	15.89
MLS22-D	PCE-2	19	0.00	0.00	0.00	0.00	0.38	0.00
MLS22-D	PCE-2	29	0.00	0.00	0.00	0.00	0.56	23.71
MLS22-D	PCE-2	37	0.00	0.00	0.00	0.07	0.60	25.58
MLS22-D	PCE-2	43	0.13	0.00	0.00	0.00	0.57	20.34
MLS22-D	PCE-2	51	0.17	0.10	0.00	0.20	0.79	22.57
MLS22-D	PCE-2	60	0.00	0.00	0.00	0.00	1.36	20.13
MLS22-D	PCE-2	85	0.00	0.00	0.00	20.42	0.03	0.04
MLS22-D	PCE-2	94	0.00	0.02	0.00	26.00	0.05	0.03
MLS22-D	PCE-2	112	0.00	0.00	0.00	26.36	0.00	0.79
MLS22-D	PCE-2	137	0.00	0.02	0.00	26.54	0.00	0.00
MLS22-D	PCE-2	189	0.00	0.00	0.00	17.55	0.00	0.00
MLS22-D	PCE-2	247	0.00	0.00	0.00	9.00	0.00	0.00

Table B.10: Concentration (μM) versus time data for Controls of MLS22-Deep PCE amended microcosm

MicroAbbr	ContamAbbr	Day	VC	1,1 DCE	tDCE	cDCE	TCE	PCE
CMLS22-D	PCE	10	0.00	0.00	0.00	0.00	0.09	26.29
CMLS22-D	PCE	20	0.00	0.00	0.00	0.00	0.11	20.94
CMLS22-D	PCE	24	0.00	0.00	0.00	0.00	0.07	24.03
CMLS22-D	PCE	53	0.00	0.00	0.00	0.00	0.09	22.02
CMLS22-D	PCE	72	0.00	0.00	0.00	0.00	0.06	19.54
CMLS22-D	PCE	93	0.00	0.00	0.00	0.00	0.07	17.60
CMLS22-D	PCE	108	0.00	0.00	0.00	0.00	0.09	17.08
CMLS22-D	PCE	206	0.00	0.00	0.00	0.00	0.04	11.56

Table B.11: Concentration (μM) versus time data for MLS22-Deep TCE amended microcosm

MicroAbbr	ContamAbbr	Day	VC	1,1 DCE	tDCE	cDCE	TCE	PCE
MLS22-D	TCE-2	10	0.00	0.00	0.00	0.00	22.85	1.45
MLS22-D	TCE-2	13	0.00	0.00	0.00	0.00	21.56	1.11
MLS22-D	TCE-2	19	0.00	0.00	0.00	0.00	0.00	1.70
MLS22-D	TCE-2	29	0.00	0.00	0.00	0.00	39.10	1.81
MLS22-D	TCE-2	37	0.00	0.00	0.00	0.07	35.51	2.02
MLS22-D	TCE-2	44	0.00	0.00	0.00	0.03	32.12	2.07
MLS22-D	TCE-2	51	0.30	0.00	0.00	0.20	38.75	4.75
MLS22-D	TCE-2	60	0.05	0.00	0.00	0.04	29.15	2.08
MLS22-D	TCE-2	85	0.00	0.06	0.00	0.05	29.25	1.84
MLS22-D	TCE-2	94	0.03	0.11	0.00	0.31	22.92	2.11
MLS22-D	TCE-2	112	0.08	0.00	0.00	0.02	25.30	1.83
MLS22-D	TCE-2	137	0.10	0.00	0.00	0.06	24.76	0.88
MLS22-D	TCE-2	161	0.00	0.08	0.00	26.80	0.01	0.03
MLS22-D	TCE-2	189	0.00	0.07	0.00	23.65	0.00	0.00
MLS22-D	TCE-2	247	0.10	0.00	0.00	13.04	0.00	0.36

Table B.12: Concentration (μM) versus time data for Controls of MLS22-Deep TCE amended microcosm

MicroAbbr	ContamAbbr	Day	VC	1,1 DCE	tDCE	cDCE	TCE	PCE
CMLS22-D	TCE	10	0.00	0.00	0.00	0.00	30.00	0.00
CMLS22-D	TCE	49	0.00	0.00	0.00	0.00	30.33	0.17
CMLS22-D	TCE	59	0.00	0.00	0.00	0.00	28.30	0.34
CMLS22-D	TCE	63	0.00	0.00	0.00	0.00	26.61	0.53
CMLS22-D	TCE	92	0.00	0.00	0.00	0.00	29.48	0.09
CMLS22-D	TCE	111	0.00	0.00	0.00	0.00	19.20	0.13
CMLS22-D	TCE	132	0.00	0.00	0.00	0.00	24.47	0.00
CMLS22-D	TCE	147	0.00	0.00	0.00	0.00	24.77	0.12
CMLS22-D	TCE	245	0.00	0.00	0.00	0.00	10.98	0.07

Appendix C

Model Data

MLS12-Shallow: Input file for reductive dechlorination package

```
 T        2                                  pceopt,ncdis
******** Chlor.  cpd.  minimum concs.  ********
       0.0                                   acmin(1)  PCE
       0.0                                   acmin(2)  TCE
       0.0                                   acmin(3)  DCE
       0.0                                   acmin(4)   VC
       0.0                                   acmin(5)  Eth
       0.0                                   acmin(6)  CL-
******** Microb.  pop.  init.  & min.  concs.  ********
         0     0.250                         ymold(1)
         0     0.250                         ymold(2)
     0.250                                   ymmin
Yield Coefficients
      0.0                                    yield(1) PCE
      0.0                                    yield(2) TCE
      0.0                                    yield(3) DCE
      0.0                                    yield(4)  VC
Inhibition Terms
PCE inhib.  by O2, Fe(III)
      0.10                                   akinhc(lj,lk) O2
     20.00                                   akinhc(lj,lk) FE3
TCE inhib.  by O2, Fe(III) PCE
      0.10                                   akinhc(lj,lk) O2
     20.00                                   akinhc(lj,lk) FE3
      0.01                                   akinhc(lj,lk) PCE
DCE inhib.  by O2, Fe(III) PCE, TCE
      0.10                                   akinhc(lj,lk) O2
     20.00                                   akinhc(lj,lk) FE3
      0.01                                   akinhc(lj,lk) PCE
      0.01                                   akinhc(lj,lk) TCE
 VC inhib.  by O2, Fe(III) PCE, TCE, DCE
      0.10                                   akinhc(lj,lk) O2
     20.00                                   akinhc(lj,lk) FE3
      0.01                                   akinhc(lj,lk) PCE
      0.01                                   akinhc(lj,lk) TCE
      0.15                                   akinhc(lj,lk) DCE
******** Chlor.  Cpd.  Stoich.  Factors ********
     0.79                                    stoich(1,1) PCE->TCE
     0.25                                    stoich(1,2) PCE->CL-
     0.74                                    stoich(2,1) TCE->DCE
     0.25                                    stoich(2,2) TCE->CL-
     0.64                                    stoich(3,1) DCE->VC
     0.25                                    stoich(3,2) DCE->CL-
      0.0                                    stoich(3,3) DCE->Eth
     0.45                                    stoich(4,1)  VC->Eth
     0.25                                    stoich(4,2)  VC->CL-
EA Half sat.  constants for red.  dechlor.  of PCE, TCE, DCE, VC
      0.41                                   akhalfc(lc)  PCE
      0.01                                   akhalfc(lc)  TCE
      0.07                                   akhalfc(lc)  DCE
      0.02                                   akhalfc(lc)   VC
EA Max.  spec.  util.  rates for red.  dechlor.  of PCE, TCE, DCE, VC
      0.40                                   vspmxa(lc)   PCE 0.05
      0.42                                   vspmxa(lc)   TCE 0.05
      0.05                                   vspmxa(lc)   DCE 0.05
      0.25                                   vspmxa(lc)    VC 0.05
******** death rate ********
     0.00                                    ykd(ic)   PCE/TCE Redu
     0.00                                    ykd(ic)   DCE/ VC Redu
******** Dir.  oxid.  of DCE & VC by Aerobes ********
ED half sat.  constants
      0.0                                    akhalfd(lc) DCE
```

```
      0.0                                    akhalfd(lc)  VC
ED max.  spec.  util.  rates
      0.00                                   vspmxd(lc)   1.00
      0.00                                   vspmxd(lc)   1.00
******** Dir.  oxid.  of DCE & VC by FE Reducers ********
ED half sat.  constants
      0.0                                    akhalfd(lc) DCE
      0.0                                    akhalfd(lc)  VC
ED max.  spec.  util.  rates
      0.0                                    vspmxd(lc)
      0.0                                    vspmxd(lc)
******** Dir.  oxid.  of DCE & VC by Methanogens ********
ED half sat.  constants
      1.0                                    akhalfd(lc) DCE
      1.0                                    akhalfd(lc)  VC
ED max.  spec.  util.  rates
      0.0                                    vspmxd(lc)
      0.0                                    vspmxd(lc)
******** CH4 Gen.  Coefs.  from DCE & VC ********
      0.80                                   endc(lc)     DCE
      0.80                                   endc(lc)      VC
******** EA Use Coefs.  by DCE & VC ********
oxygen
      3.0                                    agamc(lc,li) DCE
      3.0                                    agamc(lc,li)  VC
Fe(III)
     35.0                                    agamc(lc,li) DCE
     35.0                                    agamc(lc,li)  VC
******** Nutrient Use Coefs.  by DCE & VC ********
```

MLS22-Shallow: Input file for reductive dechlorination package

```
 T        2                                  pceopt,ncdis
******** Chlor.  cpd.  minimum concs.  ********
       0.0                                   acmin(1)  PCE
       0.0                                   acmin(2)  TCE
       0.0                                   acmin(3)  DCE
       0.0                                   acmin(4)   VC
       0.0                                   acmin(5)  Eth
       0.0                                   acmin(6)  CL-
******** Microb.  pop.  init.  & min.  concs.  ********
         0     0.250                         ymold(1)
         0     0.030                         ymold(2)
     0.001                                   ymmin
Yield Coefficients
      0.0                                    yield(1) PCE
      0.0                                    yield(2) TCE
      0.65                                   yield(3) DCE
      0.00                                   yield(4)  VC
Inhibition Terms
PCE inhib.  by O2, Fe(III)
      0.10                                   akinhc(lj,lk) O2
     20.00                                   akinhc(lj,lk) FE3
TCE inhib.  by O2, Fe(III) PCE
      0.10                                   akinhc(lj,lk) O2
     20.00                                   akinhc(lj,lk) FE3
      1.90                                   akinhc(lj,lk) PCE
DCE inhib.  by O2, Fe(III) PCE, TCE
      0.10                                   akinhc(lj,lk) O2
     20.00                                   akinhc(lj,lk) FE3
      0.10                                   akinhc(lj,lk) PCE
      0.60                                   akinhc(lj,lk) TCE
 VC inhib.  by O2, Fe(III) PCE, TCE, DCE
      0.10                                   akinhc(lj,lk) O2
     20.00                                   akinhc(lj,lk) FE3
      0.01                                   akinhc(lj,lk) PCE
      0.01                                   akinhc(lj,lk) TCE
      0.00                                   akinhc(lj,lk) DCE
******** Chlor.  Cpd.  Stoich.  Factors ********
     0.79                                    stoich(1,1) PCE->TCE
     0.25                                    stoich(1,2) PCE->CL-
     0.74                                    stoich(2,1) TCE->DCE
     0.25                                    stoich(2,2) TCE->CL-
     0.00                                    stoich(3,1) DCE->VC
     0.25                                    stoich(3,2) DCE->CL-
      0.0                                    stoich(3,3) DCE->Eth
     0.00                                    stoich(4,1)  VC->Eth
     0.25                                    stoich(4,2)  VC->CL-
EA Half sat.  constants for red.  dechlor.  of PCE, TCE, DCE, VC
      0.57                                   akhalfc(lc)  PCE
      0.20                                   akhalfc(lc)  TCE
      1.30                                   akhalfc(lc)  DCE
      0.00                                   akhalfc(lc)   VC
EA Max.  spec.  util.  rates for red.  dechlor.  of PCE, TCE, DCE, VC
      0.40                                   vspmxa(lc)   PCE 0.05
      1.00                                   vspmxa(lc)   TCE 0.05
      0.06                                   vspmxa(lc)   DCE 0.05
      0.00                                   vspmxa(lc)    VC 0.05
******** death rate ********
     0.00                                    ykd(ic)   PCE/TCE Redu
     0.004                                   ykd(ic)   DCE/ VC Redu
******** Dir.  oxid.  of DCE & VC by Aerobes ********
ED half sat.  constants
      0.0                                    akhalfd(lc) DCE
```

```
      0.0                                     akhalfd(lc)  VC
ED max.  spec.  util.  rates
      0.00                                    vspmxd(lc)   1.00
      0.00                                    vspmxd(lc)   1.00
******** Dir.  oxid.  of DCE & VC by FE Reducers ********
ED half sat.  constants
      0.0                                     akhalfd(lc) DCE
      0.0                                     akhalfd(lc)  VC
ED max.  spec.  util.  rates
      0.0                                     vspmxd(lc)
      0.0                                     vspmxd(lc)
******** Dir.  oxid.  of DCE & VC by Methanogens ********
ED half sat.  constants
      1.0                                     akhalfd(lc) DCE
      1.0                                     akhalfd(lc)  VC
ED max.  spec.  util.  rates
      0.0                                     vspmxd(lc)
      0.0                                     vspmxd(lc)
******** CH4 Gen.  Coefs.  from DCE & VC ********
      0.80                                    endc(lc)     DCE
      0.80                                    endc(lc)      VC
******** EA Use Coefs.  by DCE & VC ********oxygen
      3.0                                     agamc(lc,li) DCE
      3.0                                     agamc(lc,li)  VC
Fe(III)
     35.0                                     agamc(lc,li) DCE
     35.0                                     agamc(lc,li)  VC
******** Nutrient Use Coefs.  by DCE & VC ********
```

MLS22-Deep: Input file for reductive dechlorination package

```
 T        2                                  pceopt,ncdis
******** Chlor.  cpd.  minimum concs.  ********
       0.0                                   acmin(1)  PCE
       0.0                                   acmin(2)  TCE
       0.0                                   acmin(3)  DCE
       0.0                                   acmin(4)   VC
       0.0                                   acmin(5)  Eth
       0.0                                   acmin(6)  CL-
******** Microb.  pop.  init.  & min.  concs.  ********
         0     0.250                         ymold(1)
         0     0.020                         ymold(2)
     0.001                                   ymmin
Yield Coefficients
      0.0                                    yield(1) PCE
      0.0                                    yield(2) TCE
      0.75                                   yield(3) DCE
      0.75                                   yield(4)  VC
Inhibition Terms
PCE inhib.  by O2, Fe(III)
      0.10                                   akinhc(lj,lk) O2
     20.00                                   akinhc(lj,lk) FE3
TCE inhib.  by O2, Fe(III) PCE
      0.10                                   akinhc(lj,lk) O2
     20.00                                   akinhc(lj,lk) FE3
      1.90                                   akinhc(lj,lk) PCE
DCE inhib.  by O2, Fe(III) PCE, TCE
      0.10                                   akinhc(lj,lk) O2
     20.00                                   akinhc(lj,lk) FE3
      0.40                                   akinhc(lj,lk) PCE
      0.50                                   akinhc(lj,lk) TCE
 VC inhib.  by O2, Fe(III) PCE, TCE, DCE
      0.10                                   akinhc(lj,lk) O2
     20.00                                   akinhc(lj,lk) FE3
      0.01                                   akinhc(lj,lk) PCE
      0.01                                   akinhc(lj,lk) TCE
      0.00                                   akinhc(lj,lk) DCE
******** Chlor.  Cpd.  Stoich.  Factors ********
     0.79                                    stoich(1,1) PCE->TCE
     0.25                                    stoich(1,2) PCE->CL-
     0.74                                    stoich(2,1) TCE->DCE
     0.25                                    stoich(2,2) TCE->CL-
     0.00                                    stoich(3,1) DCE->VC
     0.25                                    stoich(3,2) DCE->CL-
      0.0                                    stoich(3,3) DCE->Eth
     0.0                                     stoich(4,1)  VC->Eth
     0.25                                    stoich(4,2)  VC->CL-
EA Half sat.  constants for red.  dechlor.  of PCE, TCE, DCE, VC
      1.00                                   akhalfc(lc)  PCE
      0.30                                   akhalfc(lc)  TCE
      2.10                                   akhalfc(lc)  DCE
      0.00                                   akhalfc(lc)   VC
EA Max.  spec.  util.  rates for red.  dechlor.  of PCE, TCE, DCE, VC
      0.40                                   vspmxa(lc)   PCE 0.05
      1.50                                   vspmxa(lc)   TCE 0.05
      0.07                                   vspmxa(lc)   DCE 0.05
      0.00                                   vspmxa(lc)    VC 0.05
******** death rate ********
     0.00                                    ykd(ic)   PCE/TCE Redu
     0.004                                   ykd(ic)   DCE/ VC Redu
******** Dir.  oxid.  of DCE & VC by Aerobes ********
ED half sat.  constants
      0.0                                    akhalfd(lc) DCE
```

```
      0.0                                    akhalfd(lc)  VC
ED max.  spec.  util.  rates
      0.00                                   vspmxd(lc)   1.00
      0.00                                   vspmxd(lc)   1.00
******** Dir.  oxid.  of DCE & VC by FE Reducers ********
ED half sat.  constants
      0.0                                    akhalfd(lc) DCE
      0.0                                    akhalfd(lc)  VC
ED max.  spec.  util.  rates
      0.0                                    vspmxd(lc)
      0.0                                    vspmxd(lc)
******** Dir.  oxid.  of DCE & VC by Methanogens ********
ED half sat.  constants
      1.0                                    akhalfd(lc) DCE
      1.0                                    akhalfd(lc)  VC
ED max.  spec.  util.  rates
      0.0                                    vspmxd(lc)
      0.0                                    vspmxd(lc)
******** CH4 Gen.  Coefs.  from DCE & VC ********
      0.80                                   endc(lc)     DCE
      0.80                                   endc(lc)      VC
******** EA Use Coefs.  by DCE & VC ********
oxygen
      3.0                                    agamc(lc,li) DCE
      3.0                                    agamc(lc,li)  VC
Fe(III)
     35.0                                    agamc(lc,li) DCE
     35.0                                    agamc(lc,li)  VC
******** Nutrient Use Coefs.  by DCE & VC ********
```

vita

Heather Veith Rectanus

Education

Master of Science, Civil Engineering, August 2000
Geoenvironmental Option
Virginia Polytechnic Institute and State University, Blacksburg, VA
Thesis: Assessment of Intrinsic Bioremediation at a PCE Contaminated Site
Co-Advisors: John T. Novak and Mark A. Widdowson

Bachelor of Science, Nuclear Engineering, May 1998
Bachelor of Arts, German, May 1998
Kansas State University, Manhattan, KS

Honors Affiliations

National Science Foundation Fellowship, 1998-2001
Virginia Tech Charles E. Via Fellowship, 1998-1999
Nuclear Engineering Scholar, ORI for Science and Education, 1997
American Nuclear Society Scholar, 1995-1997
National Academy for Nuclear Training Scholar, 1996-1998
Tau Beta Pi
Phi Kappa Phi
Phi Beta Kappa
American Nuclear Society, 1992-present
Alpha Nu Sigma

Research Interests

Groundwater Contaminant Fate and Transport
Nuclear Waste Remediation
Monitored Natural Attenuation

Professional Experience

Research
Masters Research Assistant, Department of Civil and Environmental Engineering, Virginia Tech, August 1998 - August 2000

•Performed groundwater field sampling including dissolved hydrogen
•Conducted microcosm studies on PCE contaminated aquifer sediment
•Modeled PCE degradation via the reductive dechlorination package of SEAM3D

Nuclear
Senior Reactor Operator, Kansas State University TRIGA Mark II Nuclear Reactor Facility, August 1995-May 1998
•Performed mechanical maintenance,
•Conducted public information tours to various audience levels
•Prepared safety analysis reports
•Operated reactor for isotope production.

Language
Study Abroad Scholar, Swiss Federal Institute of Technology (ETH) Zurich, Switzerland, October 1994 - July 1995
•Studied Mechanical Engineering and Nuclear Physics at the ETH

Licensure

Intern Engineer State of Kansas, June 1998
Senior Reactor Operator (SOP-70187), 1 October 1996
Reactor Operator (OP-70105), 4 October 1994

Presentations

D. F. Berry, M.J. Higgins, **H.V. Rectanus**, M. A. Widdowson, and J. T. Novak. *Investigation of Intrinsic Bioremediation at NAB Little Creek, Site 12: Microbiological Assessment.* 1999 International Symposium on Subsurface Microbiology in Vail, CO, August 22-27, 1999.

M. A. Widdowson, J. T. Novak, D. F. Berry, **H. V. Rectanus**, and F. Y. Wang. *Spatial Variation in Reductive Dechlorination of a PCE-Contaminated Aquifer.* Second International Conference on Remediation of Chlorinated and Recalcitrant Compounds in Monterey, CA, May 22-25, 2000.